TUM School of Medicine and Health
Technische Universität München

CRISPR/Cas9 based HLA reduction of T cells for universal T cell therapy

Pascal Maximilian Winterhalter

Vollständiger Abdruck der von der TUM School of Medicine and Health der Technischen Universität München zur Erlangung eines

Doktors der Medizinischen Wissenschaft (Dr. med. sci.)

genehmigten Dissertation.

Vorsitz:

apl. Prof. Dr. Klaus-Peter Janssen

Prüfende der Dissertation:

1. Prof. Dr. Dirk H. Busch
2. Prof. Dr. Gabriele Multhoff
3. Prof. Dr. Florian Bassermann

Die Dissertation wurde am 16.01.2024 bei der Technischen Universität München eingereicht und durch die TUM School of Medicine and Health am 09.10.2024 angenommen.

No sympathy for the devil; keep that in mind.
Buy the ticket, take the ride...
and if it occasionally gets a little heavier
than what you had in mind, well... maybe chalk it off
to forced consciousness expansion:
Tune in, freak out, get beaten.

FEAR AND LOATHING IN LAS VEGAS

Abstract

Adoptive cell therapy (ACT) has recently shown enormous potential in treating cancer and infections. Advances in the field, propelled by the accessibility of genetic engineering tools like clustered regularly interspaced short palindromic repeats (CRISPR)/CRISPR-associated protein 9 (Cas9), have made this technology more available than ever. Specifically, chimeric antigen receptor (CAR) T lymphocyte (T cell) therapy, a subset of adoptive cell therapy, achieved notable success, receiving U.S. Food and Drug Administration (FDA) approval in 2017 for treating relapsed or refractory B lymphocyte (B cell) malignancies. Since then, various forms of CAR T cell therapy have been approved, showing significant clinical success.

Despite this success and the availability of commercial products, the treatment is associated with extremely high costs due to the complex manufacturing and high personalization involved. The standard source for cellular material are patient-derived autologous cells, presenting significant obstacles.

To overcome these limitations the use of allogeneic cell sources is suggested. This would allow the standardization and characterization akin to pharmaceutical products, thereby enabling a certain degree of predictability in clinical outcomes. However, unless there is an exact match in human leukocyte antigen (HLA) between donor and recipient, the transfer of cells may result in rejection, leading to treatment failure and potential severe adverse effects. This challenge has led to the development of HLA knock-out (KO) T cells, theoretically providing a source of universally compatible donor cells. However, it remains unknown whether this editing affects the physiological function of T cells. Moreover, cells missing HLA may elicit "missing-self" recognition through natural killer (NK) cells, impacting effectiveness due to NK cell-mediated rejection. Generation of T cells through engineering of non-canonical HLA class I were then proposed. This would further complicate the manufacturing process and raises serious safety concerns. These cells can now successfully evade, whithout physiological regulation, immunological safety mechanisms.

In this thesis, we answer the question and demonstrate that HLA class I and class II KO cells retain their physiological effector function both *in vitro* and *in vivo*. T cells with a complete loss of HLA avoid allorecognition by foreign T cells but trigger NK cell responses.

We further show, that selective editing of individual canonical HLA class I alleles is possible in a single editing step. This approach reduces canonical HLA class I, enabling the cells to be not universally but multi-donor compatible through a simplified matching process. By reducing HLA class I to one remaining molecule, HLA-matching can be reached for large population shares, considering the relatively frequent occurrence of certain HLA alleles. These HLA-reduced T cells exhibit no alloreactivity of sensitized

T cells and do not elicit an NK cell response *in vitro*. Furthermore, we demonstrate excellent *in vivo* behavior with improved functionality over conventionally HLA-mismatched allogeneic CAR T cells.

By demonstrating the feasibility of generating multi-compatible T cells for adoptive T cells in a single editing step, retaining their physiological function, this approach significantly contributes to enhancing the accessibility and safety of adoptive cell therapy.

Zusammenfassung

Die adoptive Zelltherapie hat in jüngster Zeit ein enormes Potenzial bei der Behandlung von Krebs und Infektionen bewiesen. Die Fortschritte auf diesem Gebiet, die durch das Aufkommen von gentechnischen Werkzeugen wie CRISPR/Cas9 vorangetrieben wurden, haben diese Technologie verfügbarer denn je gemacht. Insbesondere die CAR-T-Zelltherapie, eine Unterform der adoptiven Zelltherapie, erzielte einen bemerkenswerten Erfolg mit der Zulassung 2017 durch die FDA für die Behandlung therapierefraktärer B-Zell-Malignome. Seitdem sind verschiedene Formen der CAR-T-Zelltherapie zugelassen worden, die bemerkenswerte klinische Erfolge feiern.

Trotz dieses Erfolgs und der Verfügbarkeit kommerzieller CAR-T-Zell Produkte ist die Behandlung mit einer komplexen Herstellung, hohen Personalisierung und, dadurch bedingt, sehr hohen Kosten verbunden. Ausgangsmaterial für die Therapie sind in der Regel vom Patienten stammende autologe Zellen, was einige Limitationen mit sich bringt.

Um diese Einschränkungen zu überwinden, wird die Verwendung allogener Quellen für Zellen vorgeschlagen. Dies würde eine Standardisierung und Charakterisierung ähnlich wie bei pharmazeutischen Produkten ermöglichen und damit ein gewisses Maß an Vorhersagbarkeit der klinischen Ergebnisse schaffen. Wenn sich jedoch keine exakte HLA-Übereinstimmung zwischen Spender und Empfänger findet, kann der Zelltransfer zu einer Abstoßung führen, was ein Versagen der Behandlung und potenziell schwerwiegende unerwünschte Nebenwirkungen zur Folge hat. Dieser Umstand hat zur Erforschung von HLA-KO-T-Zellen geführt, die theoretisch eine Quelle universell kompatibler Spenderzellen darstellen. Es ist jedoch noch nicht bekannt, ob dieses Editing die physiologische Funktion der T-Zellen beeinträchtigt. Darüber hinaus können Zellen, durch die Abwesenheit von HLA, die Abstoßung durch NK-Zellen auslösen, was wiederum die Wirksamkeit der Therapie beeinträchtigt. Ein weiterer Ansatz ist es, NK-Zell-resistente T-Zellen durch Engineering von nicht-kanonischen HLA-Klasse-I Molekülen zu erzeugen. Dies würde den Herstellungsprozess weiter erschweren und darüber hinaus ernste Sicherheitsbedenken mit sich bringen. Diese Zellen entziehen sich nun ohne physiologischer Regulierung zu unterliegen, Sicherheitsmechanismen des Immunsystems.

In dieser Arbeit beantworten wir die Frage nach der Funktion von HLA KO Zellen und zeigen, dass HLA-Klasse-I- und -Klasse-II-KO-Zellen ihre physiologische Effektorfunktion sowohl *in vitro* als auch *in vivo* beibehalten. T-Zellen mit einem vollständigen Verlust von HLA entgehen der Erkennung durch allogene T-Zellen, lösen aber NK-Zell-Reaktionen aus.

Wir zeigen außerdem, dass das selektive Editing einzelner kanonischer HLA-Klasse-I-Allele in einem einzigen Bearbeitungsschritt möglich ist. Dieser Ansatz reduziert die kanonische HLA-Klasse I so, dass die Zellen zwar nicht universell, aber durch einen vereinfachten Matching-Prozess mit mehreren Spendern kompatibel sind. Durch die Reduktion

der HLA-Klasse I auf ein verbleibendes Molekül kann angesichts des relativ häufigen Auftretens bestimmter HLA-Allele ein HLA-Matching für große Bevölkerungsanteile erreicht werden. Diese HLA-reduzierten T-Zellen erfahren keine Alloreaktivität durch sensibilisierte T-Zellen und lösen keine NK-Zellreaktion *in vitro* aus. Darüber hinaus können wir ein exzellentes *in-vivo*-Verhalten mit verbesserter Funktionalität im Vergleich zu herkömmlichen HLA-ungematchten allogenen CAR-T-Zellen zeigen.

Durch die hier nachgewiesene Machbarkeit der Produktion multikompatibler T-Zellen für adoptive T-Zelltherapie in einem einzigen Bearbeitungsschritt unter Konservierung der physiologischen Funktion, trägt dieser Ansatz wesentlich zur Verbesserung der Zugänglichkeit und Sicherheit der adoptiven Zelltherapie bei.

Contents

List of Figures

List of Tables

Abbreviations

4-1BBL	4-1BB ligand
aCD19-CAR	anti CD19 chimeric antigen receptor
ACT	adoptive cell therapy
B cell	B lymphocyte
B-LCL	B-cell lymphoblastoid cell line
β2m	β-2-microglobulin
B2M	beta-2-microglobulin gene
CAR	chimeric antigen receptor
Cas9	CRISPR-associated protein 9
CD	cluster of differentiation
CIITA	class II major histocompatibility complex transactivator
CMV	cytomegalovirus
CRISPR	clustered regularly interspaced short palindromic repeats
crRNA	CRISPR RNA
DMEM	Dulbecco's modified eagle medium
DNA	deoxyribonucleic acid
dsDNA	double-stranded DNA
EBV	Epstein-Barr virus
EGFRt	truncated epidermal growth factor receptor
EMA	ethidium monoazide
EURCAU	European Caucasian
FACS	fluorescence activated cell sorting
FCS	fetal calf serum
FDA	U.S. Food and Drug Administration
GM-SCF	granulocyte-macrophage colony-stimulating factor
GMP	Good Manufacturing Practice
gRNA	guide RNA

gRNA	guide RNA
GVHD	graft-versus-host disease
Gy	Gray
HDR	homology-directed repair
HLA	human leukocyte antigen
HSCT	hematopoietic stem cell transplantation
HSPC	haematopoetic stem and progenitor cell
ICCS	intracellular cytokine staining
IFNγ	Interferon-γ
IL-2	interleukin 2
IL-3	Interleukin-3
ILT2	immunoglobulin-like Transcript 2
Iono	ionomycin
iPSC	induced pluripotent stem cell
KI	knock-in
KIR2DL1-4	killer cell immunoglobulin-like receptor 2DL1-4
KO	knock-out
MHC	major histocompatibility class
MLR	mixed lymphocyte reaction assay
NEAA	non essential amino acids
NF-κB	nuclear factor kappa B
NFAT	nuclear factor of activated T cells
NK	natural killer
NKG2A	natural killer group 2A
NSG-SGM3	NOD.Cg-Prkdc^{scid}Il2rg^{tm1Wjl}Tg(CMV-IL3,CSF2, KITLG)1Eav/MloySzJ
NSG/HHD	NOD.Cg-Prkdc^{scid}Il2rg^{tm1Wjl}Tg(HLA-A/H2-D/ B2M)1Dvs/SzJ
OTR	orthotopic TCR replacement
PBMC	peripheral mononuclear blood cell
PBS	phosphat-buffered saline
PCR	polymerase chain reaction
PFU	plaque-forming units
PHA	Phythaemagglutinin
PI	propidium iodide
PMA	phorbol myristate acetate

RFXANK	regulatory factor X-associated ankyrin-containing protein
RNA	ribonucleic acid
RNP	ribonucleoprotein
RNP	ribonucleoprotein
RT	room temperature
SCF	stem cell factor
T cell	T lymphocyte
TCR	T-cell receptor
TIL	tumor-infiltrating lymphocyte
TNFα	tumor necrosis factor alpha
TRAC	T cell receptor alpha constant
tracrRNA	trans-activating crRNA
TRBC	T cell receptor beta constant
UK	United Kingdom

1 Introduction

The human immune system is a highly specialized system that protects the body from external threats through complex cellular and molecular mechanisms. It consists of two major components: the evolutionarily older innate immunity and adaptive immunity. The innate immune system heavily relies on physical and chemical barriers. In the event of a pathogen breaching these barriers, it can be eliminated through direct interactions with antimicrobial proteins or by specialized cells that recognize evolutionarily preserved pathogen patterns.

In contrast, the adaptive immune system distinguishes between self and non-self recognition and complements the innate immune system in protecting against infections by recognizing antigens through lymphocytes. Two major cell types comprise the lymphocytes: B lymphocytes (B cells) and T lymphocytes (T cells). B cells and T cells play distinct roles in antigen recognition and response. Lymphocytes can recognize specific antigens through their membrane-bound receptors.

However, T cells with their T-cell receptors (TCRs) cannot directly recognize foreign proteins. For a protein to be recognized through a T cell receptor, it must be processed in a specific way and presented on major histocompatibility class (MHC) molecules, also known as human leukocyte antigen (HLA) molecules. For example, for antigen presentation on HLA class I molecules, the protein undergoes intracellular degradation in the cytosol. The resulting peptides, 8-10 amino acids in length, are then mounted on MHC molecules in the endoplasmic reticulum. This process enables T cells not only to recognize steric-accessible antigens but also to identify antigens within foreign proteins.

A highly diverse repertoire of T cell receptors is generated during the development of T lymphocytes through somatic recombination. However, to avoid unintentional harm to the host's tissues, they need to distinguish between self and non-self antigens. This distinction is achieved through positive and negative selection. During maturation, T lymphocytes that react positively to self-MHC molecules undergo positive selection and thus survive. It is believed that a weak interaction with self-peptide:MHC molecules is an indicator that the T cell can effectively recognize antigens bound to MHC, ensuring its proper function. [1,2] Highly auto-reactive T cells that could harm the host are removed through negative selection, leading to self-tolerance.

The underlying mechanism of antigen processing and presentation enables the adaptive immune system to recognize any presented antigen, whether it is microbial and internalized through phagocytosis by innate immune cells or an antigen produced by an infected or malignantly transformed cell.

Furthermore, in contrast to the innate immune system, the adaptive immune system is capable of forming immunological memory. Upon response to a specific pathogen, memory cells that are long-term persistent are generated. Should the same pathogen

be reencountered, the adaptive immune system then mounts a rapid response, leading to immunity or rapid clearance of the infection with a lesser burden of symptoms. This principle is used in the concept of immunization through vaccines.

The clinical relevance of understanding the immune system is evident in the field of cancer immunotherapy. Breakthroughs like checkpoint inhibitors, which block proteins that inhibit T-cell responses, have revolutionized cancer treatment. For instance, drugs like pembrolizumab and nivolumab have successfully treated various cancers, improved patient outcomes, and extended survival rates [3, 4].

Recent advancements in genome editing technologies, such as clustered regularly interspaced short palindromic repeats (CRISPR)/CRISPR-associated protein 9 (Cas9), have opened up new possibilities in immunology research and treatment, allowing for a deeper understanding of immune responses and the potential to engineer genes. This holds potential implications for personalized medicine and targeted therapies, such as adoptive cell therapy.

1.1 Adoptive cell therapy

Adoptive transfer is described as the transplantation of immunological tissues to achieve immunity, such as the transfer of lymphocytes [5]. The underlying concept is to obtain an immediate, preformed response from the adaptive immune system without the need for prior immunization. This approach aims to address infections or malignant processes.

One of the earliest forms of adoptive cell therapy implemented was bone marrow transplantation in acute leukemia patients, demonstrating clinical improvements post-transplantation due to an observable anti-leukemic effect of the graft [6]. A common, potentially life-threatening side effect of bone marrow transplantation is graft-versus-host disease (GVHD). Following bone marrow transplantation, it was noted that patients who experienced GVHD had fewer tumor relapses compared to those who did not experience GVHD. However, since GVHD is a life-threatening side effect, only patients with a mild form of GVHD had a survival advantage [7].

T cells were successfully identified as responsible for both GVHD and the graft-versus-leukemia effect [8,9]. Allografts that were T-cell depleted in bone marrow transplantation resulted in fewer and less severe cases of GVHD. However, patients who received T-cell-depleted allografts also had a higher probability of relapse [9].

From this point on, T cells rapidly became the research subject and were employed in clinically deployed adoptive cell therapy, including early unedited transfers of T cells e.g., in the form of donor leukocyte infusion [10].

Despite the adoptive transfer of unedited T cells, such as donor leukocyte infusion [10], the transfer of virus-specific T cells [11], and tumor-infiltrating lymphocytes [12] demonstrating significant therapeutic value; the advent of gene editing technologies signifies a substantial leap toward targeted and personalized therapies, expanding the pharmaceutical arsenal for combating infections and cancer.

Currently, three types of adoptive T-cell therapies are striving for regulatory approval. In addition to the previously mentioned tumor-infiltrating lymphocytes, chimeric anti-

gen receptor (CAR) and TCR engineered T-cells have also emerged. With the U.S. Food and Drug Administration (FDA) approval of CAR T-cell therapy tisagenlecleucel (KYMRIAH®, Novartis Pharmaceuticals Corporation) in 2017, a significant milestone in medicine was achieved. It marked the first instance of a gene-modified cell therapy gaining regulatory approval [13].

1.1.1 Adoptive Transfer of unedited T cells

The underlying concept behind adoptive transfer is to achieve immediate immunity and effector function. Adoptive transfer offers an onset of action as rapid as that of chemotherapy, in contrast to vaccination, other forms of immunization, or immune checkpoint inhibitors. To accomplish this, it is necessary to transfer antigen-experienced T cells. Whether the target is a viral infection or a solid tumor, these T cells have to be identified and isolated.

It was discovered that T cells infiltrating solid tumors are capable of lysing autologous tumor cells ex vivo after expansion. However, they do not exhibit the same effect on allogeneic tumors or autologous normal cells [12]. Tumor-infiltrating lymphocytes (TILs), specifically T cells, exhibit a strong association with tumorous antigens. These findings suggest a potential clinical application for the treatment of solid tumors in the form of adoptive cell therapy.

TILs can be prepared for adoptive cell therapy by excising the tumorous mass, extracting the lymphocytes, expanding them *in vitro*, and subsequently reintroducing them into the patient. This groundbreaking approach was pioneered by Rosenberg et al. in 1988 in the treatment of patients with metastatic melanoma [12]. Adopting T-cell therapy using TILs has proven to be highly effective in tumors characterized by high somatic mutation rates, such as those found in lung cancer, melanoma, and bladder cancer [14]. It was later discovered, through next-generation sequencing, that TILs recognize neo-epitopes derived from the somatic mutations occurring in the patient's tumor [15]. Additionally, T cells capable of targeting a common driver mutation present in many human tumors have been identified. This discovery paves the way for further refinement and development of this therapeutic method for targeted treatments.

Using somatic-mutation-specific TILs combined with interleukin 2 (IL-2) supplementation and checkpoint inhibitors have demonstrated the potential to initiate sustained regression in cases of metastatic breast cancer [14]. The adoptive transfer of TILs shows promise as an innovative approach for treating therapy-refractory patients.

The use of unedited T cells is by far not limited to TILs. Adoptive T-cell transfer can be a valuable solution in various situations where there is a lack of an existing immune response that is urgently needed. One illustrative example is allogeneic hematopoietic stem cell transplantation (HSCT), a procedure that essentially eliminates an individual's adaptive immune system and replaces it with the transplanted graft. In these situations, reactivation of cytomegalovirus (CMV) or Epstein-Barr virus (EBV) infections can occur, leading to a highly severe and potentially life-threatening complication. In healthy individuals, latent herpes virus infections such as CMV or EBV are typically kept in check by life-long-persisting virus-specific T cells. Thus, CMV seropositive patients

face the highest risk when receiving a graft from a seronegative donor during allogeneic HSCT [16]. Since the host's bone marrow and, thus, the immune system are depleted prior to transplantation, virus-specific T cells are no longer present, and the graft inherently lacks them. Infusions of donor-derived lymphocytes, specific for CMV antigens, have been identified as conferring immunity [17] until, eventually, a new population of autologous virus-specific T cells is formed. It has been shown that lymphocytes from HLA matched third-party donors can also be used for treatment [18].

This, in essence, highlights the significant potential of adoptive T-cell therapy in combating both cancer and infections.

1.1.2 Adoptive Transfer of TCR engineered T cells

After the remarkable success achieved through the adoptive transfer of T cells, TCR engineering has emerged as a solution to address the limitations associated with adoptive cell therapy. Using TILs for adoptive transfer requires the presence of a solid tumor that can be surgically removed to harvest TILs. In the case of virus-specific T cells, an HLA-matched donor is required because virus-specific T cells from third-party donors are commonly rejected [19].

However, in both scenarios, unless antigen-specific selection methods are used, the T cell receptor repertoire composition remains highly heterogeneous. Even with such selection methods, while antigen specificity may be consistent, receptor binding affinity and the composition of T cell phenotypes still vary significantly.

Consequently, the efficacy of therapy is neither standardized nor guaranteed. It could even be argued that, for example, TILs might be less effective because they often fail to completely eradicate the tumor and can be influenced by the tumor's microenvironment and immunological escape mechanisms.

TCR-engineered T cells aim to overcome these limitations by using TCRs with well-established and tested antigen specificity and affinity. This approach also enhances the standardization of this highly personalized form of treatment by using the same TCR for a group of patients with the same tumor entity. Gene editing technologies further enable the efficient and rapid production of patient-specific cell products by, e.g., introducing the engineered TCR into easily obtainable peripheral T cells. However, the use of genetic editing to enhance therapeutic value requires a critical evaluation of the product's safety.

1.1.3 Adoptive Transfer of CAR T cells

The T-cell response can also be redirected and engineered through the use of a CAR. These CARs feature an antibody-binding domain, enabling them to recognize almost any surface antigen independently of HLA. In general, a CAR consists of an antigen-binding domain, usually a single-chain derived from the variable part of an antibody (scFv), a hinge region that links the two extracellular parts, a transmembrane domain, and intracellular signaling domains that control T-cell activation [20].

First-generation CARs relied solely on cluster of differentiation (CD)3-ζ as a signaling domain [21]. While the activation achieved through CD3-ζ is sufficient to induce

cytolytic activity as a T-cell effector function, first-generation CARs lacked a robust cytokine response [22]. Physiological T-cell stimulation typically requires a co-stimulatory receptor, such as CD28 [23]. Subsequently, new generations of CARs were developed to include one or more co-stimulatory domains, such as CD28, enhancing their potency [20]. Second-generation CARs (CD3-ζ and CD28 co-stimulatory domain) were compared with first-generation CARs (only CD3-ζ activating domain), both targeting the CD19 antigen in patients. Second-generation CARs showed significantly better expansion and persistence than first-generation CARs [24].

A clinically relevant feature of CAR T cells is their ability to recognize surface antigens directly, akin to antibodies. This overcomes the limitation of T-cell receptors (TCRs), which rely on HLA-restricted antigen presentation but can additionally recognize intracellular proteins. However, a common mechanism in malignant cells is the loss or downregulation of HLA molecules, rendering the TCR useless [25], unlike CAR T cells.

One of the most successful examples to date is anti CD19 chimeric antigen receptor (aCD19-CAR) therapy targeting B-cell malignancies. CD19 is an ideal target because it is highly expressed on B-cells, is not present in other tissues, and is not shed as a soluble antigen. CAR T cells targeting CD19 have shown remarkable results, leading to FDA approval for this novel therapy [13]. Cross-targeting of non-malignant B cells does not affect the therapy; it may be beneficial in preventing the formation of anti-CAR antibodies. However, despite CD19 being the ideal target antigen for CAR T cell therapy, antigen loss is a common cause of therapy failure.

While CAR T cells demonstrate remarkable success rates in patients, they come with serious adverse events such as cytokine release syndrome and neurotoxicity. Cytokine release syndrome, especially, correlates with CAR T cell activation and is influenced by factors like tumor burden, CAR T cell dosage, and prior lymphodepletion [26–28]. Therefore, refining CAR T cell activation to balance its effects and adverse effects is essential in CAR T cell engineering.

However, B-cell malignancies have a distinct conformation from solid tumors, which are less accessible for CAR T cells, primarily due to the tumor microenvironment. CAR T cells face numerous challenges when adapting for solid tumors, including identifying the right tumor-associated antigen and overcoming the poor trafficking of CAR T cells due to impaired chemokine-mediated recruitment [29].

CARs are typically introduced into the cell through retroviral transduction, which results in random integration. This may lead to varying expression levels, clonal expansion, or malignant transformation [30]. With the emergence of advanced gene editing tools like CRISPR/Cas9, there is potential to address some of the limitations of CAR T cell therapy. One can edit the TCR locus directly, leading to a more defined CAR T cell generation and, ultimately, a more efficient and safer cellular product.

1.2 Limitations of adoptive cell therapy

One of the predominant challenges lies in the highly personalized nature of adoptive cell therapy. And highly personalized medicine is often characterized by its com-

plexity and high costs. Adoptive cell therapy with the antiCD19-CARs tisagenlecleucel (KYMRIAH®, Novartis Pharmaceuticals Corporation) and axicabtagene ciloleucel (YESCARTA®, Kite Pharma) has prices for the drug alone at $ 475,000 respectively $ 373,000 [31]. However, this still does not include costs for apheresis, lymphodepletion or treatment of occurring adverse effects. In 2017, mean total costs for a case treated with tisagenlecleucel were reported to be $ 510,963 and with axicabtagene ciloleucel $ 402,647 [31]. These high costs can prohibit individuals from benefiting from this kind of therapy.

Moreover, manufacturing has to be done under Good Manufacturing Practice (GMP) guidelines. Since very few hospitals can comply with the GMP standards, it is usually done offsite, increasing complexity. Moreover, this type of treatment can only be provided at select specialized tertiary care centers [3]. This especially restricts patient access to this form of treatment. Additionally, the absence of standardized procedures and significant variability in CAR T cell production can impact the heterogeneity in clinical results [3, 32].

Both the circumstances and the manufacturing process itself impose additional limitations. The source of cell material for adoptive cell therapy is almost always autologous, primarily due to the challenges presented by HLA. This means that the cells are derived from the patients themselves. The manufacturing process, while it may be standardized, does not inherently guarantee a consistent source material. This is especially relevant because adoptive cell therapy is not typically the first-line treatment but rather a choice for refractory situations or relapses. Consequently, there is a high likelihood that the patient has already experienced one of the numerous immune defects associated with cancer treatment [33].

When it comes to efficacy, factors such as killing capacity, cytokine release, phenotype, expansion, and persistence exhibit a considerable degree of unpredictability when using an autologous source of cells.

In conclusion, the high costs, manufacturing complexities, and limited availability of adoptive cell therapy, coupled with the unpredictable nature of using autologous cells, pose significant challenges for patients seeking this highly personalized form of treatment. These challenges emphasize the need for continued research and advancements in the field to potentially make this currently personalized treatment less personalized, more accessible, and reliable.

1.3 Ideal cell product

As for every pharmaceutical, the ideal product should be safe, effective, and demonstrate consistent quality while also being readily accessible to patients. For T cells involved in adoptive cell therapy, it is vital that the product demonstrates robust antigen recognition and cytotoxicity against target cells. Minimal off-target effects, optimal expansion capabilities, and prolonged *in vivo* persistence are also essential features. To ensure easy patient access, cells are ideally readily available in an off-the-shelf-like manner.

The T-cell effector function is a crucial feature of the ideal cellular product. The engineered cells should not be impaired in their effector function and exhibit the same levels of cytokine release and the same efficacy and efficiency of cytotoxicity as physiological T cells. Therefore, antigen recognition should be robust and lead to the same kind of activation as physiological T cells.

Prolonged *in vivo* persistence is another key feature of the ideal cell product. The transferred cells should remain active and efficiently kill their target cells, whether tumorous or virally infected. Ideally, the transferred product complements the adaptive immune system, providing long-lasting protection, supporting complete remission, and reducing the severity of symptoms upon re-infection.

The ability to persist within the host for an extended period makes it even more crucial for the product to be safe. The product should not harm the host by minimizing off-target effects. In addition, the product itself should avoid generating immunogenicity, increasing the likelihood of genetic aberrations and malignant transformation. It should be capable of presenting self-antigens in the rare event of malignant transformation.

The ideal choice is autologous cells to reduce immunogenicity and enable safe self-antigen presentation. However, autologous cells may be compromised or exhausted due to prolonged cancer disease [34] or prior treatments [35]. In contrast, allogeneic cells, derived from healthy donors, offer the advantages of being assessable and enabling standardization of composition, efficacy, and dosage [36]. Unfortunately, allogeneic cell sources are limited by the complexities of the HLA system [37]. Therefore, the preferred solution would involve a matched HLA-identical allogeneic donor.

In conclusion, the ideal cellular product for adoptive cell therapy should exhibit features like robust antigen recognition, cytotoxicity, and prolonged *in vivo* persistence while maintaining safety. T-cell effector function should mirror physiological T cells. Autologous cells are preferred for safety, but their individual variance in function due to cancer or treatments is a concern. Allogeneic cells, while offering standardization and accessibility, face limitations due to the HLA system, making matched HLA-identical allogeneic donors the preferred source.

1.4 Methods to overcome limitations

The use of autologous cells comes with numerous disadvantages, including numbers and quality of harvested cells and prolonged vein-to-vein time compared with the use of an off-the-shelf product [37]. Thus, one method to overcome the limitation of autologous cells is the use of allogeneic cells from healthy donors. These can be manufactured in advance, stored, and delivered as an off-the-shelf product. The use of allogeneic cells raises other kinds of problems, such as alloreactivity and rejection by the host's immune system. There are currently two approaches to overcome this limitation. Either through the use of genetic engineering or selecting different subpopulations e.g. such as $\gamma\delta$-T cells [36].

The use of genetic engineering to create universal cells derived from healthy donors for adoptive cell therapy is very promising. Perhaps the most significant barrier hindering

allogeneic cell use is HLA matching. It is nearly impossible to have an HLA-identical donor on hand, nor their cells in a large library in an off-the-shelf manner. Efforts are underway to develop universal cells that avoid graft-vs-host disease, demonstrate optimal cytotoxic effector function, and ideally evade rejection while persisting.

Several strategies involve knocking out HLA by targeting β-2-microglobulin (β2m) and class II major histocompatibility complex transactivator (*CIITA*) to overcome the HLA matching barrier [38–40]. Nevertheless, this approach is reported to result in limited engraftment due to natural killer (NK) cell activation through a missing self-response [41–43]. To address this challenge, investigations into strategies such as introducing CD47 [44, 45] as a "don't-eat-me" signal, HLA-E [46, 47], and HLA-G [45, 48] have been conducted. Due to HLA-E exclusively inhibiting natural killer group 2A $(NKG2A)^+$ NK cells, there is a suggestion to overexpress HLA-G to additionally affect killer cell immunoglobulin-like receptor 2DL1-4 $(KIR2DL1\text{-}4)^+$ and immunoglobulin-like Transcript 2 $(ILT2)^+$ NK cells [49].

Another intriguing approach involves introducing an artificial receptor into the cell, enabling it to directly evade rejection, as proposed with an alloimmune defense receptor comprising a 4-1BB ligand (4-1BBL) domain [50]. However, such editing strategies deviate further from physiological expression profiles and behavior. Additionally, a thorough investigation of potential risks associated with these engineered cells is needed.

In essence, all of the aforementioned methods to overcome HLA incompatibility either render the product prone to rejection through NK cells or further enhance the complexity of product generation and alter the cell's physiology.

A very promising approach, however, is not to eliminate HLA compatibility completely from the equation but to minimize HLA diversity. The requirement to match only a few alleles instead of a full set of HLA does not create universally compatible donor cells but rather multi-compatible ones. This may, in fact, be a sweet spot that meets all the requirements and successfully overcomes limitations while maintaining cell physiology as closely as possible.

Editing of individual alleles in primary human T cells has already been successfully demonstrated for HLA-A [51]. This approach selectively modifies specific alleles, leaving the remaining HLA alleles and their expression unaffected. In contrast, a knock-out of beta-2-microglobulin gene (*B2M*) eliminates the entire HLA class I, including non-canonical HLA molecules. The residual expression of HLA class I molecules serves as a potential safety mechanism, preserving the cells' capability for antigen presentation. This safeguards against malignant transformation or infection.

Additional studies have demonstrated the feasibility of generating multi-compatible donor cells through CRISPR/Cas9 targeting individual HLA alleles in induced pluripotent stem cells (iPSCs) [45, 52]. Despite iPSCs being a rich source of cell material, their use in adoptive T-cell therapy requires labor-intensive differentiation and maturation processes. Furthermore, reported challenges include low editing efficacies and the time-consuming selection of clones [52]. As a result, it remains uncertain whether this approach can be effectively applied to primary human T cells.

1.5 Human Leukocyte Antigen

The human leukocyte antigen (HLA) system plays a crucial role in enabling the immune system to distinguish between self and non-self [53]. This is necessary for protecting the human body against infection but raises severe problems for transplantation or adoptive cell therapy.

HLA refers to genes encoded on the human MHC, a roughly 3.6 megabase long gene cluster on chromosome 6. It is found very early in vertebrates and is structurally well-preserved despite being highly polymorphic [54]. The high polymorphism earned it the name major histocompatibility complex since it is the major obstacle for tissue transplantation.

The antigen-presenting molecules of the HLA system exist in two variants, namely class I and class II. HLA class I and class II molecules have a very similar three-dimensional structure and function [55].

HLA class I molecules are expressed in almost all nucleated cells and are responsible for antigen presentation of peptides derived from the cytoplasm. Antigen presentation is usually directed toward $CD8^+$ T cells [54, 56]. class I molecules also serve as self-recognition molecules for NK cells [43,54]. HLA class I commonly refers to the canonical HLA class I molecules (HLA-A, -B, C), also known as HLA class Ia, and the rest of the HLA class I molecules as non-canonical ones (HLA class Ib) [57]. The initial definition of non-canonical class Ib HLA molecules was established based on their low polymorphism, restricted distribution, and the unclear function [54]. Subsequent research has unveiled a shift in this definition, revealing that HLA class Ib molecules exhibit considerable polymorphism (e.g., MICA, Qua1), engage in antigen presentation (e.g., Qua2, HLA-G), and demonstrate ubiquitous expression (e.g., M3) [54, 58]. However, HLA class Ia molecules can be found on virtually every human nucleated cell except for the trophoblast, which does express classical HLA-C and nonclassical HLA-E and HLA-G [59].

HLA class II molecules (e.g., HLA-DR, HLA-DQ, and HLA-DP) are typically found on the surface of antigen-presenting cells, such as B cells, macrophages, and dendritic cells. Class II molecules present antigens originating from endosomal processing of exogenous peptides, primarily to $CD4^+$ T cells. Interestingly, the crystallographic structure of HLA class I and class II is very similar in overall structure but differs in subunit composition [1]. A complete HLA molecule consists of four domains; in the case of class I, an MHC-encoded α-chain contributes three domains, along with β2m. A class II molecule consists of two MHC-encoded non-covalently bound chains, each with two domains. The peptide-binding groove of HLA class II is formed by two domains, one from each chain [1]. Similar to class I molecules, the peptide-binding groove is the site of major polymorphisms in HLA molecules [1]. HLA molecules can bind and subsequently present a diverse range of peptides. It is important to note that peptides in the binding groove are integral components of the HLA molecules, necessary for stabilizing the HLA molecule on the cell surface [1].

The diversity and polymorphism of HLA molecules are responsible for a unique antigen-binding capability, presenting a wide array of pathogens. This diversity influences both

self-tolerance and the body's ability to recognize foreign antigens, contributing to the individualized nature of immune responses.

The clinical significance of HLA becomes apparent in transplantation, where it plays a crucial role in distinguishing self from non-self. Any deviant HLA antigen can trigger an immune response. The success of allograft transplantation was initially observed to be higher in identical twins [60]. Subsequently, graft losses were associated with HLA disparity [61]. Mismatches in HLA between the donor and recipient can be classified by examining individual alleles. Retrospective studies indicate that the HLA mismatch at different HLA loci varies in potency. In the first year after transplantation, the class II HLA-DR locus has a more pronounced impact on rejection than HLA-A and HLA-B. However, in subsequent years, all three loci demonstrate an equivalent and additive influence on graft survival [62].

Therefore, ensuring that all the available alleles match appears to be beneficial. In short, matching reduces the chances of short-term rejection, lowers the need for immunosuppression, and decreases the risk of immediate failure, especially in sensitized patients. Every reported study of organ and bone marrow transplants so far has demonstrated a benefit from HLA matching [61].

1.6 Variability and Probability of Matching

To identify a fully HLA-matched allogeneic donor, allele compatibility for the HLA loci A/B/C/DRB1/B3/B5/DQB1 is assessed, following a widely used standard [63]. However, full compatibility (four-digit typing) at the A/B/C/DRB1/B3/B5/DQB1 loci is defined as a "10/10" match, taking into account the second DRB locus in the DR-matching scheme [63].

In theory, the extensive polymorphism of HLA leads to countless HLA phenotypes, which would make the search for an unrelated HLA-identical individual seemingly impossible. Fortunately, HLA is inherited in sets of alleles known as haplotypes, resulting in a one in four chance for an individual to be HLA identical to a sibling [61, 64]. This ensures that HLA matching of unrelated individuals can be achieved at a much higher proportion than might otherwise be possible.

Transplantation or graft donors usually are not unrelated. In these cases, there is less compatibility in the HLA system tolerated since siblings usually share not only HLA but also at least 50 % of their non-HLA histocompatibility antigens, which should not be neglected.

Theoretically, HLA polymorphism results in an immense variety of HLA phenotypes, making the quest for an unrelated HLA-identical individual seem futile. Fortunately, HLA is inherited in sets of alleles known as haplotypes, creating a one in four chance for an individual to be HLA identical to their sibling [61, 64]. This genetic inheritance mechanism significantly increases the likelihood of achieving HLA matching between unrelated individuals.

Typically, transplant or graft donors are not unrelated. In such cases, there is more tolerance for incompatibility in the HLA system, as siblings do not only share HLA but also, at a minimum, 50 % of their non-HLA histocompatibility antigens [61].

However, when patients lack an HLA-identical sibling donor, the search for an unrelated allogeneic donor can begin through various donor registries. Establishing a bank with enough cell products for adoptive cell therapy would require including thousands of random donors. This process appears to be time-consuming, costly, and almost impractical.

A current approach involves creating a bank of HLA-homozygous donors, effectively halving the number of alleles that require matching. Calculations based on data from the WHO nomenclature report suggest a theoretical total of 13,860 HLA-A, -B, and -DR combinations, each representing a potential homozygous HLA-typed donor [65].

Covering the first 150 of these theoretical homozygous combinations for HLA-A, -B, and -DR would result in a match for 94 % of the United Kingdom (UK) population [65]. This underscores the potential of genetic engineering to enhance the compatibility of unrelated allogeneic donor sources.

2 Aim of this thesis

Adoptive cell therapy has the potential to revolutionize the treatment of cancers and infectious diseases. Currently, several limitations exist that restrict the application of adoptive cell therapy in routine clinical treatments.

One of the many limitations is the high degree of personalization required for this kind of treatment and the inevitable use of patient-derived cells to manufacture adoptive cell products. The use of allogeneic donor cells may overcome several limitations of autologous therapy. However, the diversity and complexity of HLA polymorphism significantly limit the pool of available donor cells for adoptive cell therapy.

This thesis aims to investigate current approaches to overcome donor incompatibility and enable HLA knocked-out cells for use in adoptive cell therapy and to analyze their influence on T cell functionality. Many authors have suggested the elimination of HLA class I and II to generate universally compatible donor cells. However, less is understood about whether this would affect intrinsic T-cell functionality.

Our second objective is to investigate how we can enhance donor compatibility using the gene-editing system CRISPR/Cas9. Specifically, our strategy involves targeting individual HLA class I alleles to create a reduced set with fewer molecules that need to be matched. Through this approach, we aim to address challenges such as rejection dependent on T cells and NK cells. We plan to develop a proof-of-concept for engineering multi-compatible CAR T cells and test their adoptive transfer in a humanized mouse model to bridge the gap between theory and practice. This will allow for thorough observation and study of their behavior and impact.

In conclusion, this thesis explores the field of adoptive cell therapy, addressing donor compatibility challenges with the potential to reconsider strategies for treating cancer and infectious diseases.

3 Material and methods

3.1 Material

3.1.1 Commodities

Item	Supplier
0.22 µm sterile filter	Kisker, Steinfurt, Germany
0.45 µm sterile filter	Kisker, Steinfurt, Germany
1.0 ml Sub-Q	BD Biosciences, Franklin Lakes, USA
1.0 ml, 1.5 ml 2.0 ml reagent tubes	Kuhnle, Karlsruhe, Germany
1.2 ml, 2.0 ml Cryo-vial	Th. Geyer, Renningen, Germany
1.5 ml LoBind-DNA reaction tube	Eppendorf, Hamburg, Germany
15 ml, 50 ml Falcon Cell Star	Greiner bio-one, Heidelberg, Germany
384-well plates medium binding	Greiner bio-one, Heidelberg, Germany
5 ml Polypropylen round-bottom tube	Greiner Corning, Durham, USA
5 ml Polystyrene round-bottom tube	Greiner Corning, Durham, USA
500 ml filtration system stericup (0.22 µm)	Kisker, Steinfurt, Germany
70 µm, 100 µm cell strainer	STARLAB, Hamburg, Germany
96-well plates U-bottoms	Kisker, Steinfurt, Germany
96-well plates V-bottoms	Kuhnle, Karlsruhe, Germany
C-Slide cell counting chamber slide	NanoEnTek, Seoul, South Korea
Cover Plate	Greiner bio-one, Heidelberg, Germany
Culture flask 25 cm^2, 75 cm^2, 150 cm^2	Th. Geyer, Renningen, Germany
E-Plate 96	OLS, Bremen, Germany
Leukosep™ centrifuge tubes	Greiner bio-one, Heidelberg, Germany
Parafilm	Merck, Darmstadt, Germany

PCR reaction tubes	Brand, Werthelm, Germany
Pipette filter tips (1µl, 10/20µl, 200µl, 1 ml)	STARLAB, Hamburg, Germany
Serological pipettes (5 ml, 10 ml, 25 ml)	Greiner bio-one, Heidelberg, Germany
Syringe (1 ml, 3 ml, 5 ml, 50 ml)	Braun, Melsungen, Germany
Tissue culture treated plates (6-, 12-, 24-, 96-Well)	Omnilab, München, Germany

3.1.2 Chemicals and reagents

Compound	**Supplier**
aCD3/aCD28 Expamer	Juno Therapeutics, München, Germany
β-Mercaptoethanol	Roth, Karlsruhe, Germany
2-Propanol	Roth, Karlsruhe, Germany
6x loading dye	Thermo Fisher Scientific, Ulm, Germany
Acetic Acid	Roth, Karlsruhe, Germany
Agarose	Roth, Karlsruhe, Germany
Alt-R® Cas9 Electroporation Enhancer	IDT DNA, Coralville, USA
Alt-R® CRISPR-Cas9 tracrRNA	IDT DNA, Coralville, USA
Alt-R® S.p. HiFi Cas9 Nuclease V3	IDT DNA, Coralville, USA
Ampicillin	Roth, Karlsruhe, Germany
Bicoll Separating Solution	Merck, Darmstadt, Germany
Bovine Serum Albumin	Sigma, Taufkirchen, Germany
$CaCl_2$	Merck, Darmstadt, Germany
CD28-Fab	Juno Therapeutics, München, Germany
Collagen R (0,2%)	Serva, Heidelberg, Germany
D-Biotin	Sigma, Taufkirchen, Germany
DMEM, NEAA, high glucose, no glutamine	Thermo Fisher Scientific, Ulm, Germany
DMSO	Sigma, Taufkirchen, Germany

dNTPs	Roche, Penzberg, Germany
Dulbeccos Phosphate Buffered Saline	Merck, Darmstadt, Germany
Ethanol	Roth, Karlsruhe, Germany
Ethidium Monoazide	Molecular Probes, Leiden, Netherlands
Fetal Calf Serum	GE Healthcare, Chalfont St. Giles, UK
Gentamicin	Thermo Fisher Scientific, Ulm, Germany
Golgi-Plug	BD Biosciences, Franklin Lakes, USA
Golgi-Stop	BD Biosciences, Franklin Lakes, USA
HCl	Roth, Karlsruhe, Germany
Heparin-Natrium-25000	Ratiopharm, Ulm, Germany
HEPES	Roth, Karlsruhe, Germany
human Interferon-γ	Biolegend, San Diego, USA
Human serum	in-house production
Interleukin-15	Peprotech, Hamburg, Germany
Interleukin-2	Peprotech, Hamburg, Germany
Interleukin-7	Peprotech, Hamburg, Germany
Ionomycin	Sigma, Taufkirchen, Germany
Isopropanol	Roth, Karlsruhe, Germany
Kanamycin	Roth, Karlsruhe, Germany
L-Glutamine	Sigma, Taufkirchen, Germany
LB agar	in-house
LB medium	in-house
Lentiboost A	UNKNOWN
MgCl2	Merck, Darmstadt, Germany
Na_2HPO_4	Roth, Karlsruhe, Germany
NaCl	Roth, Karlsruhe, Germany
NaOH	Roth, Karlsruhe, Germany
NH_4Cl	Sigma, Taufkirchen, Germany
Penicillin/Streptomycin	Thermo Fisher Scientific, Ulm, Germany

Percoll	GE Healthcare, Uppsala, Sweden
Phorbol myristate acetate	Sigma, Taufkirchen, Germany
Phytohaemagglutinin	Thermo Fisher Scientific, Ulm, Germany
Propidium Iodide	Merck, Darmstadt, Germany
Retronectin	Takara Bio, Shiga, Japan
Rotisafe Gel Stain	Roth, Karlsruhe, Germany
RPMI 1640	Thermo Fisher Scientific, Ulm, Germany
SAM2	Juno Therapeutics, München, Germany
Tris-HCl	Roth, Karlsruhe, Germany
Triton-X 100	Roth, Karlsruhe, Germany
Trypan blue	Roth, Karlsruhe, Germany
Trypsin-EDTA (0.25 %)	Thermo Fisher Scientific, Ulm, Germany

3.1.3 Buffers and media

Solution	**Composition**
Antibiotics supplement (add 5 %)	20 ml Gentamicin; 200 ml Penicillin/Streptomycin; 780 ml RPMI 1640
Complete freezing medium	1x FCS; 10 % (v/v) DMSO
FACS buffer	1x PBS; 0.5 % (w/v) BSA; pH 7.45
FACS-EDTA buffer	1x PBS; 0.5 % (w/v) BSA; 2 mM EDTA; pH 7.45
Complete medium	500 ml RPMI 1640; 50 ml FCS; 25 ml SC^{+}

RPMI SC $^-$	500 ml RPMI 1640; 50 ml FCS; 25 ml SC^-
Complete DMEM	500 ml DMEM; 50 ml FCS; 25 ml SC^+
SC^+ (supplement complete, in 1 l medium)	1 ml β-mercaptoethanol; 20 ml Gentamicin; 23.83 g HEPES; 4 g L-Glutamine; 200 ml Penicillin/Streptomycin
SC^- (supplement complete, in 1 l medium)	1 ml β-mercaptoethanol; 23.83 g HEPES; 4 g L-Glutamine
Trypan blue solution	1x PBS; 0.15 % (v/v) trypan blue
1M electroporation buffer [66]	5 mM KCl; 15 mM $MgCl_2$; 120 mM Na_2HPO_4/NaH_2PO_4 pH 7.2; 50 mM Manitol
Ammonium chloride-Tris (ACT)	10 % (v/v) 0.17 M Tris-HCl pH 7.5; 90 % (v/v) 0.17 M NH_4Cl
50× TAE buffer	2 M Tris-HCl; 2 M CH_3COOH; 50 mM EDTA; pH 8.0

3.1.4 Peptides

Peptide	Sequence	HLA haplotype	Supplier
$pp65_{495\text{-}503}$	NLVPMVATV	A*02:01	Peptides & elephants, Potsdam, Germany
$IE1_{88\text{-}96}$	QIKVRVDMV	B*08:01	Peptides & elephants, Potsdam, Germany

3.1.5 Antibodies

Human Antigen	Fluorophore	Clone	Supplier*
CD69	PE	FN50	BioLegend
CD107a	PE	H4A3	BioLegend
CD11c	PE	S-HCL-3	BioLegend
CD137	FITC	4B4	eBioscience
CD137	PE-Cyanine7	4B4	Invitrogen
CD14	PE	61D3	eBioscience
CD154	PE	24-31	BioLegend
CD154	APC	24-31	BioLegend
CD19	eFlour 450	HIB19	Life Technologies
CD19	ECD	J3-119	Beckman Coulter
CD20	APC-eFlour 780	2H7	Invitrogen
CD28	purified	37.51	BioLegend
CD3	PC7	UCHT1	Beckman Coulter
CD3	Pacific Blue	UCHT1	BD
CD3	APC	UCHT1	Life Technologies
CD3	BV 421	SK7	BD Biosciences
CD33	BV 421	WM53	BioLegend
CD33	APC	UCHT1	Life Technologies
CD33	BV 421	WM53	BioLegend
CD34	FITC	4H11	Life Technologies
CD34	PE	4H11	Life Technologies

CD366 (TIM3)	Pacific Blue	F38-2E2	BioLegend
CD3e	purified	145-2C11	BioLegend
CD4	PE	RPA-T4	Life Technologies
CD45	PE-Cyanine7	2D1	eBioscience
CD45	Krome Orange	J33	Beckman Coulter
CD45	Pacific Orange	HI30	Exbio
CD45	Pacific Blue	T29/33	DAKO
CD45	ECD	J33	Beckman Coulter
CD56	FITC	TULY56	Life Technologies
CD69	PE-Cyanine7	FN50	eBioscience
CD8	PE	3B5	Invitrogen
CD8α	APC	RPA-T8	BioLegend
CD8α	FITC	B9.11	Beckman Coulter
CD8α	eFlour 450	OKT8	eBioscience
CD8α	APC-eFlour 780	OKT8	eBioscience
CD8α	PE-Cyanine7	OKT8	eBioscience
EGFR	PE	AY13	BioLegend
EGFR	BV 421	AY13	BioLegend
HLA A2	FITC	BB7.2	BD Pharmingen
HLA A3	PE	REA950	Miltenyi
HLA ABC	APC	W6/32	BioLegend
HLA ABC	Pacific Blue	W6/32	BioLegend
HLA B7	PE	BB7.1	BioLegend
HLA B8	APC-Vio770	REA145	Miltenyi
HLA BC	APC	B1.23.2	Invitrogen
HLA DR	PE	TÜ36	BD Pharmingen
HLA DR	Pacific Blue	L243	BioLegend
HLA DR	Pacific Orange	L243	Exbio
HLA E	PE/Cyanine7	3D12	BioLegend
HLA-DR,DP,DQ	FITC	TÜ39	BD Pharmingen
hTCR α/β	FITC	IP26	BioLegend
hTCR α/β	PE	IP26	BioLegend
IFNγ	FITC	25723.11	BD Pharmingen

IFNγ	PE	45.15	Beckman Coulter
IL-2	APC	5344111	BD Pharmingen
murine β2m	PE	A16041A	BioLegend
murine CD45.1	APC-Cy7	A20	BioLegend
murine CD45.1	PE	A20	BioLegend
murine CD45.1	PE/Cy7	A20	BioLegend
murine TCRβ	APC/Fire750	H57-597	BioLegend
murine TCRβ	APC	H57-597	BioLegend
PD-1	APC	eBioJ105	Invitrogen
Streptavidin	FITC	n/a	BD Pharmingen
Streptavidin	eFlour 450	n/a	Life Technologies
TNFα	PE-Cyanine7	MAb11	eBioscience

*BD Biosciences, Franklin Lakes, USA
Beckman Coulter, Beckman Coulter, Brea, USA
Biolegend, San Diego, USA
eBioscience now Thermo Fisher Scientific, Ulm, Germany

3.1.6 CRISPR guides

Name	**Target**	**Sequence**	**Supplier**
β2m gRNA1	1st exon *B2M*	CGCGAGCACAGCTAAGGCCA [40]	IDT*
β2m gRNA2	1st exon *B2M*	GGCCACGGAGCGAGACATCT [30]	IDT*
β2m gRNA3	1st exon *B2M*	ACTCACGCTGGATAGCCTCC	IDT*
CIITA gRNA1	1st exon *CIITA*	CTGACAGGTAGGACCCAGCA	IDT*
CIITA gRNA2	2nd exon *CIITA*	AGAAGTGGTAGAGGCACAGG	IDT*
CIITA gRNA3	2nd exon *CIITA*	CATCGCTGTTAAGAAGCTCC	IDT*
CIITA gRNA4	2nd exon *CIITA*	GGTCCATCTGGTCATAGAAG [45]	IDT*

CIITA gRNA5	2nd exon *CIITA*	GGAAGGTGATGAAGAGACCA [38]	IDT*
TRAC guide6	1st exon TRAC	AGAGTCTCTCAGCTGGTACA	IDT*
TRBC guide3	1st exon TRBC	GGAGAATGACGAGTGGACCC	IDT*
Xu1	A*24:02	AAACATGAAGAAAGCAGATG [52]	IDT*
Xu2	A*01:01	CTGAGCTGCCATGTCCGCCG [52]	IDT*
Xu3	B*15:01	AAATGTCCTGTGAGGGGACT [52]	IDT*
Xu4	B*08:01	GCGCCGTGGATAGAGCAGGA [52]	IDT*
Xu5	C*03:03	AACACGGGGAAAGCAGCTGT [52]	IDT*
Xu6	C*07:01	GGATGGGGAGGACCAGACCC [52]	IDT*
Xu7	A*02:01	ACCCAGTTCTCACTCCCATC [52]	IDT*
Xu9	A*03:01	ACCCTGAGATGGGATAAGGA [52]	IDT*
Xu11	B*44:03	ACTCCACGCACAGACCCTCC [52]	IDT*
Xu13	B*51:01	ACGCTGCAGCGCGCGGGTAC [52]	IDT*
Xu15	C*15:02	AAAGTCACCAGTCACCCACC [52]	IDT*
Xu17	C*16:01	CACACCCTCCAGTGGATGTA [52]	IDT*

Supplier*: IDT DNA, Coralville, USA

3.1.7 Plasmids

Epitope	**Vector**	**Resistance**	**Molecular details**
a-human CD 19 JCAR017	p15A	Ampicillin	3xSTII hinge +/- EGFRt*
a-human CD 19 JCAR021	p15A	Ampicillin	3xSTII hinge +/- EGFRt*
CMV B8–IE1$_{88–96}$ TRAC KI TCR 3-2	pMK	Kanamycin	murine constant region w/ additional cysteine bridge
CMV A2/pp65$_{495–503}$ TRAC KI TCR 6-2	pMK-RQ	Kanamycin	murine constant region w/ additional cysteine bridge
HLA E dimer	p15A	Ampicillin	*
HLA E trimer	p15A	Ampicillin	*

Molecular details*: kindly provided by Juno Therapeutics - a BMS company

3.1.8 PCR Primers

Primer	Sequence	Supplier
β2m exon 1 fwd	GCCTCCAGCCTGAAGTCCTA	Sigma, Taufkirchen, Germany
β2m exon 1 rev	CTCTGACGCTTATCGACGCC	Sigma, Taufkirchen, Germany
CIITA exon 2 fwd	ATCCACACTTTCCAGTTCCC	Sigma, Taufkirchen, Germany
CIITA exon 2 rev	ATCCACACTTTCCAGTTCCC	Sigma, Taufkirchen, Germany
HLA E HDR genomic fwd	ACAGCAAACTCACCCAGTCT	Sigma, Taufkirchen, Germany
HLA E HDR genomic rev	AAAGAGCGGAAGAGAAACCC	Sigma, Taufkirchen, Germany
hTRAC HDR genomic fwd	CTGCCTTTACTCTGCCAGAG	Sigma, Taufkirchen, Germany
hTRAC HDR genomic rev	CATCATTGACCAGAGCTCTG	Sigma, Taufkirchen, Germany

3.1.9 Molecular kits and standards

Kit / Standard	Supplier
BD Cytofix/Cytoperm	BD Biosciences, Franklin Lakes, USA
CFSE Cell Division Tracker Kit	Biolegend, San Diego, USA
123count eBeads® Counting Beads	Thermo Fisher, Ulm, Germany
Agencout AMPure XP	Beckman Coulter, Brea, USA
DNeasy Blood & Tissue Kit	QIAGEN, Venlo, Netherlands
eBioscience™ Cell Proliferation Dye eFluor™ 450	Thermo Fisher, Ulm, Germany
GeneRuler 1 kb DNA ladder	Thermo Fisher, Ulm, Germany
GoTaq® G2 Flexi DNA Polymerase	Promega, Madison, USA
Herculase II Fusion Enzyme with dNTPs Combo	Agilent, Santa Clara, USA
P3 Primary Cell 96-well Nucleofector™ Kit	Lonza, Basel, Switzerland
SE Cell Line 4D-Nucleofector™	Lonza, Basel, Switzerland

SV Miniprep DNA Purification System	Promega, Madison, USA
SV Wizard® Gel and PCR Clean-Up System	Promega, Madison, USA
Wizard® Genomic DNA Purification Kit	Promega, Madison, USA

3.1.10 Vectors and organisms

Vector/ Organism	Purpose	Supplier
E. coli Stbl3	bacteria for plasmid amplification	Thermo Fisher Scientific, Ulm, Germany
HepG2	target cell line	kind gift by Prof. Dr. Ulrike Protzer
K562	target cell line	ATCC, Teddington, UK
K562 A*02:01^{+}	target cell line	in-house
K562 B*08:01^{+}	target cell line	in-house
mCMV-NLV	virus strain	kind gift by Luka Cicin-Sain
NSG-SGM3 Strain #013062	mouse line	Jackson Laboratories
NSG/HHD HLA-A*02:01 Strain #014570	mouse line	Jackson Laboratories
RD114	packaging cell line	ATCC, Teddington, UK

3.1.11 Equipment

Equipment	Model	Supplier
Balance	ACS/ ACJ 320-4M	Kern & Sohn, Balingen, Germany
Automated Cell Counter	EVE™ PLUS	NanoEnTek, Seoul, South Korea
Balance	EG 2200-2NM	Kern & Sohn, Balingen, Germany
Centrifuges	Biofuge fresco	Heraeus, Hanau, Germany
Centrifuges	Biofuge stratos	Heraeus, Hanau, Germany
Centrifuges	Multifuge 3 S-R	Heraeus, Hanau, Germany
Centrifuges	Sorvall RC6+	Thermo scientific, Ulm, Germany

Centrifuges	Varifuge 3.0RS	Heraeus, Hanau, Germany
Cryo container	Nalgene® Mr.Frosty™	Thermo scientific, Ulm, Germany
Electrophoresis chamber	PerfectBlue™ Gel System Mini L	Peqlab, Erlangen, Germany
Electrophoresis power supply	EPS 600	Pharmacia Biotech, Uppsala, Sweden
Flow Cytometer	Cytoflex S	Beckman Coulter, Brea, USA
Flow Cytometer	Cytoflex LX	Beckman Coulter, Brea, USA
Flow Cytometer	Cytoflex	Beckman Coulter, Brea, USA
Flow Cytometer	MoFlo XDP Cell Sorter	Beckman Coulter, Brea, USA
Flow Cytometer	MoFlo Astrios EQ	Beckman Coulter, Brea, USA
Flow Cytometer	BD FACSAria™ III Cell Sorter	BD Biosciences, Franklin Lakes, USA
Gel imaging system	Molecular Imager® Gel Doc™ XR+	BioRad, München, Germany
Heat block	Thermomixer compact	Eppendorf, Hamburg, Germany
Ice maker	ZBE 30-10	Ziegra Eismaschinen, Isernhagen, Germany
Incubator	HERAcell 240	Heraeus, Hanau, Germany
Laminar flow hood	HERAsafe	Heraeus, Hanau, Germany
Magnet stand	DynaMag™-2	Thermo scientific, Ulm, Germany
Microscope	Axiovert S100	Carl Zeiss, Jena, Germany
Nanodrop device	ND-1000	Kisker, Steinfurt, Germany
Neubauer chamber	Neubauer improved	Schubert, München, Germany
PCR Cycler	T3000 Thermocycler	Biometra, Göttingen, Germany
pH-Meter	MultiCal pH 526	WTW, Weilheim, Germany
RTCA analyzer	xCELLigence® RTCA MP	Agilent, Santa Clara, USA
Tissue Grinder	Dounce Tissue Grinder A	Sigma, Taufkirchen, Germany
Transfection device	4D-Nucleofector™ Core Unit	Lonza, Basel, Switzerland
Transfection device	4D-Nucleofector™ X-Unit	Lonza, Basel, Switzerland
Transfection device	96-well Shuttle™ Add-on	Lonza, Basel, Switzerland

Water bath	Type 1002	GFL, Burgwedel, Germany

3.1.12 Software

Software	Version	Supplier
Affinity Designer	1.9	Serif Ltd.
CytExpert Acquisition and Analysis Software	2.4	Beckman Coulter, Brea, USA
FlowJo 10	10.6.1	FlowJo LLC
ICE	2.0	Synthego Corporation
Prism 9	9.5.0	GraphPad Software
TIDE	2.0.1	Desktop Genetics
xCELLigence RTCA Software Pro	1.0.1.	ACEA Biosciences

3.2 Methods

3.2.1 Cell culture

3.2.1.1 Isolation of peripheral mononuclear blood cells (PBMCs)

PBMCs were isolated from either fresh blood of healthy donors or commercially available buffy coats. Written informed consent from the donors was obtained and use was approved according to national law by the Institutional Review Board (Ethikkomission der Medizinischen Fakultät der Technischen Universität München; vote 34/20 S). Bicoll Separating Solution (Merck) was used to isolate PBMCs using density gradient centrifugation. Fresh whole blood was diluted 1:1 or buffy coats 1:2 with sterile phosphat-buffered saline (PBS). In a 50 ml Leucosep™ tube 15 ml of Bicoll was placed and the tube was centrifuged for 1 min at room temperature (RT) in order to place the Bicoll right beneath the porous membrane. 35 ml of blood-PBS mixture was added on top and centrifuged for 15 min at RT. The forming ring of PBMCs was transferred and washed twice with 50 ml of sterile PBS. A pellet was formed via centrifugation for 8 min and 1500 rpm at RT. Cells were counted with a Neubauer-improved cell counting chamber using Trypan blue solution for live/dead discrimination.

3.2.1.2 Cell culture of T cells

Cells were cultured in complete RPMI (supplemented with FCS and SC^+) at 37 °C and 5 % CO_2 unless indicated otherwise. For resting of cells, medium was supplemented with 50 IU/ml IL-2. For feeder-free expansion of cells, medium was supplemented with 180 IU/ml IL-2. If the medium turned acidic, cell density was adjusted to 1×10^6 /ml by adding fresh complete medium containing IL-2.

3.2.1.3 Cell culture of NK cells

For short-term culture of NK cells, cells were cultured in complete medium supplemented with 100 IU/ml IL-2 at a density of 1×10^6 /ml at 37 °C and 5 % CO_2.

3.2.1.4 Feeder cell culture

For feeder-cell based rapid expansion, allogeneic PBMCs were mitotically inactivated by irradiation with 35 Gy. Cells were washed twice with complete medium. Target to feeder cell ratio was adjusted to 1:5 and a total cell density of 1×10^6 /ml. Medium was supplemented with 180 IU/ml IL-2 and 1 µg/ml Phythaemagglutinin (PHA). If the medium turned acidic, fresh complete medium containing 50 IU/ml IL-2 was added. Weekly, feeder-cell culture was renewed with fresh irradiated allogeneic feeder cells.

3.2.1.5 Freezing of cells

Cells were pelleted and resuspended in complete freezing medium (FCS containing 10 % DMSO) at a cell density of 2×10^7 /ml. Cell suspension was distributed in cryo vials and

carefully brought to -80 °C by using a Mr.Frosty™ cryo container filled with Isopropyl alcohol. For longterm storage, cryo vials were transferred into liquid nitrogen after 2 days.

3.2.1.6 Thawing of cells

Cryo vials were taken out of the freezer and put into a water bath at 37 °C to start thawing. Cell solution was then quickly transferred into pre-warmed complete medium in order to dilute the DMSO at least to a 10-fold dilution. Cells were washed once in complete medium and re-suspended at a calculated cell density of 2×10^6 /ml in completed medium containing 50 IU/ml IL-2 and incubated overnight at 37 °C and 5 % CO_2.

3.2.1.7 Transformation into bacteria and plasmid preparation

Commercially ordered (Twist Bioscience) deoxyribonucleic acid (DNA) plasmids were transformed into Stbl3™ chemically competent *E. coli* via heat shock (42 °C). Bacteria were then plated onto antibiotic enriched (100 µg/ml Ampicillin or Kanamycin) LB agar plates and incubated overnight at 37 °C. 3 ml of LB medium containing 100 µg/ml Ampicillin or Kanamycin was inoculated with a carefully picked single colony and cultured overnight at 37 °C. Plasmid purification was done using PureYield™ Plasmid Miniprep System (Promega) according to manufacturer's protocol. DNA was eluted with H_2O and concentration was determined via Nanodrop.

3.2.2 Genome engineering

Genome engineering for CRISPR/Cas9 knock-out (KO) and homology-directed repair (HDR)-mediated TCR knock-in (KI) was described in previous publications [67, 68]. It is depicted in this thesis specifically to the experiments performed.

3.2.2.1 Ribonucleoproteins (RNPs) production

For delivering up to three guides simultaneously, 80 µM crRNA (see 3.1.6 for guide sequences) and 80 µM Trans-activating crRNA (tracrRNA) were mixed 1:1 and incubated at 95 °C for 5 min, then cooled on benchtop to room temperature. 6 µM high fidelity Cas9 (IDT DNA) was added slowly to gRNA solution to yield 3 µl of RNPs with 3 µM Cas9, 20 µM tracRNA, 20 µM crRNA and 20 µM electroporation enhancer (IDT DNA). RNPs were incubated for 15 min at room temperature. 3 µl of RNPs were used per 1×10^6 cells.

3.2.2.2 RNP production for administration of multiple guides

For delivering multiple guides simultaneously, RNPs with a smaller volume were needed. 80 µM crRNA (see 3.1.6 for guide sequences) and 80 µM trans-activating crRNA (tracrRNA) were mixed 1:1 and incubated at 95 °C for 5 min, then cooled on the benchtop

to room temperature. 20 µM high fidelity Cas9 (IDT DNA) was added slowly to gRNA solution to yield RNPs with 10 µM Cas9, 20 µM tracRNA, 20 µM crRNA and 20 µM electroporation enhancer (IDT DNA). RNPs were incubated for 15 min at room temperature. 1 µl of RNPs were used per 1×10^6 cells.

3.2.2.3 HDR DNA template design

DNA templates for TCRs 6-2 and 3-2 for orthotopic TCR replacement via CRISPR/Cas9-mediated HDR KI were kindly provided by Kilian Schober [68]. Templates had the following structure: 5' homology arm (300–400 base pairs (bp)), P2A, TCR-β (including mTRBC with additional cysteine bridge [69]), T2A, TCR-α (including mTRBC with additional cysteine bridge [69]), bovine growth hormone polyA signal (bGHpA) tail, 3' homology arm (300–400 bp); synthesized by either GeneArt (Thermo Fisher Scientific) or Twist Bioscience and cloned into a vector with either Ampicillin or Kanamycin resistance for bacterial amplification.

DNA templates of different anti-human CD19 targeting CAR clones (JCAR017, JCAR021) for CRISPR/Cas9-mediated HDR KI were designed *in silico*, synthesized by GeneArt (Thermo Fisher Scientific) or Twist Bioscience and cloned into a vector with Ampicillin resistance for bacterial amplification. scFv sequences of JCAR017 (clone: FMC63) and JCAR021 were kindly provided by Juno Therapeutics – a Bristol Myers Squibb Company. The extracellular binding domain of the CAR construct was linked to a spacer domain consisting out of a triple repetitive sequence of Strep-tag II (STII) [70,71] and parts of the IgG4-Fc molecule; followed by a trans-membrane region originated from the CD28 chain; followed by intracellular signaling domains, CD3-ζ and 4-1BB. As a transduction marker, a truncated version of EGFR (EGFRt) could be linked by a viral T2A peptide to the aforementioned CAR construct [72, 73]. CAR construct HDR templates had the following structure: 5' homology arm (300–400 base pairs (bp)), P2A, CAR construct, TGA Stop codon, bGHpA tail, 3' homology arm (300–400 bp).

DNA templates of single-chain HLA-E for CRISPR/Cas9-mediated HDR KI were kindly provided by Juno Therapeutics – a Bristol Myers Squibb company. The single-chain dimer and trimer sequences were obtained from U.S. Patent No. US 2004/0225112 A1 [74]. HLA E single-chain HDR templates had the following structure: 5' homology arm, T2A, B2M targeting signal, HLA-G peptide (only for trimer form), G4Sx3 flexible linker (only for trimer form), B2M protein, G4Sx4 flexible linker, HLA-E heavy chain, bGHpA, 3' homology arm.

3.2.2.4 HDR DNA template production

Linearized double-stranded DNA (dsDNA) polymerase chain reaction (PCR) products were used for electroporation, unless indicated otherwise. PCR was performed using the Herculase II Fusion Enzyme (Agilent). Template amplification was done for 8×100 µl. PCR mix composition and thermocycler settings are depicted in table 3.1. Confirmation of successful amplification was done by running a gel-electrophoresis on a 1.5 % agarose gel for 40 min at 115 V. PCR product was purified using Ampure XP bead purification

according to the manufacturer's protocol. dsDNA was eluted in 10 mM Tris buffer pH 8.5; concentration was measured using Nanodrop and set to 1 µg/µl.

Table 3.1: PCR for generation of dsDNA HDR template

Mastermix composition (800 µl)	**Thermocycler settings**	
8 µl DNA template	95 °C 5 min	
16 µl forward primer	95 °C 30 s	×40
16 µl reverse primer	62 °C 30 s	
8 µl Herculase II	72 °C 30 s	
16 µl 100 mM dNTPs	72 °C 5 min	
80 µl 5 × Herculase buffer	hold at 4 °C	
400 µl PCR grade water		

3.2.2.5 CRISPR/Cas9-mediated KO and KI of T cells

Cells were activated two days prior to electroporation using 4.8 µl/ml aCD3/aCD28 Expamer (Juno Therapeutics), 300 IU/ml IL-2, 50 IU/ml IL-7 and 50 IU/ml IL-15 for 1×10^6 cells. By incubating in 1 mM D-Biotin (Sigma Aldrich) for 20 min at room temperature, expamer-stimulus was removed. Cells were then electroporated (pulse code EH-100) with Cas9 ribonucleoprotein (RNP) and 1 µg DNA template (see 3.2.2.4) in either P3 (Lonza) or 1M electroporation buffer [66] (20 µl per 1×10^6 T cells) with either a 4D Nucleofector X-unit or 96-well Shuttle Add-on (Lonza), unless indicated otherwise. After electroporation, cells were cultured in RPMI SC^- with 180 IU/ml IL-2 added. After 12 hours, 5 % of antibiotics supplement was added.

3.2.2.6 CRISPR/Cas9-mediated KO of B-LCLs

B-LCLs were harvested and counted. 5×10^5 cells were resuspended in 17 µl supplemented SF buffer (Lonza). 3 µl of RNP mixture (as described in 3.2.2.1) were added directly into the resuspended cells. For electroporation, Lonza Nucleofector 4D X-unit was used with pulse code DN-100. Electroporated cells were rested for 5 min at room temperature. Cells were transferred into 250 µl warm complete medium and cultured at 37 °C and 5 % CO_2.

3.2.2.7 Sequencing for KO confirmation

Genomic DNA was extracted using the DNeasy Blood & Tissue Kit (QIAGEN) three days after electroporation. PCR for amplification of the targeted locus was performed, using the GoTaq® G2 Flexi DNA Polymerase (Promega). PCR mix composition and thermocycler settings as in table 3.2 below. Confirmation of successful amplification was done by gel-electrophoresis for 40 min at 115 V on a 1.5 % agarose gel. PCR Product was then purified using SV Wizard® Gel and PCR Clean-Up System (Promega); and sent

for Sanger sequencing (Eurofins). Data were analyzed and KO scores were determined using TIDE (Desktop Genetics) [75] or ICE (Synthego) [76].

Table 3.2: PCR for KO confirmation via sequencing

Mastermix composition (50 µl)	**Thermocycler settings**	
10 µl 5 × Flexi buffer	95 °C 2 min	
2 µl forward primer 10 mM	95 °C 30 s	×30
2 µl reverse primer 10 mM	60 °C 30 s	
0.25 µl GoTaq	72 °C 1 min	
10 µl 100 mM dNTPs	72 °C 5 min	
4 µl $MgCl_2$ 25 mM	hold at 4 °C	
20.75 µl H_2O		
+ 1 µl DNA template		

3.2.3 Functional assays

3.2.3.1 FACS acquisition and sorting

Acquisition of flow cytometry data was performed on Cytoflex, Cytoflex S or Cytoflex LX machines (Beckman Coulter). Sorting was done on MoFlo XDP (Beckman Coulter), MoFlo Astrios EQ (Beckman Coulter or BD FACSAria™ III (BD Biosciences) machines. Data were analyzed using FlowJo10 (FlowJo LLC).

3.2.3.2 Antibody staining

Samples were washed twice prior to antibody staining in cold FACS buffer. If absolute cell numbers were needed for analysis, 10 µl of 123count™ eBeads counting beads (invitrogen) were added to the sample prior to the washing steps. Cells were resuspended in FACS buffer containing antibodies and incubated for 20 min on ice in the dark. For live/dead discrimination, cells were washed in FACS buffer supplemented with 1:100 of an 0.2 mg/ml propidium iodide (PI) solution and incubated for another 3 minutes on ice in the dark. Samples were then washed twice in cold FACS buffer, filtered through a nylon mesh, and analyzed on a flow cytometer.

3.2.3.3 Flow cytometric cell sorting

For fluorescence activated cell sorting (FACS), staining was performed as described in 3.2.3.2 under sterile conditions. Cells were sorted in 1 ml of sterile FCS. Finally, cells were pelleted and resuspended in complete medium as in 3.2.1.2 with or without feeder cells depending on cell numbers and the following experiment.

3.2.3.4 NK cell assay

One day prior to the assay, NK cells were acquired by isolating PBMCs from fresh blood; sorting for $CD3^{-}CD8^{-}CD56^{+}$ cells. Sorted cells were held in culture overnight in complete medium supplemented with 100 IU/ml IL-2. The next day, NK cells and target cells were washed, counted and cell density was adjusted to 6×10^5 /ml. 3×10^4 NK cells (50 µl) were added to 3×10^4 (50 µl) target cells for a 1:1 effector to target ratio, respectively to 6×10^4 (100 µl) for a 1:2 ratio, in a 96-well plate with round bottoms. Wells were filled up with complete medium to a total volume of 200 µl. Cells were co-incubated for 5 h in the presence of a fluorophore-conjugated aCD107a antibody (1:100). After one hour GolgiStop (BD Biosciences) was added to each well at a final concentration of 6 µg/ml. Positive controls were K562 cells as targets and a sole stimulation with phorbol myristate acetate (PMA) (25 ng/ml) and ionomycin (Iono) (1 µg/ml). As negative control served NK cells alone. Cells were then washed and additional antibody staining for flow cytometry was performed as described in 3.2.3.2.

3.2.3.5 Intracellular cytokine staining

To investigate response upon antigen-TCR interaction, we performed an intracellular cytokine staining (ICCS) assay. K562 target cells (retrovirally transduced with HLA-A*02:01) were irradiated with 80 Gy, washed twice, counted and resuspended in complete medium at a density of 3×10^6 /ml. Peptide pulsing was done by adding different concentrations (10^{-4} M, 10^{-6} M, 10^{-7} M, 10^{-8} M, 10^{-9} M, 10^{-10} M, 10^{-12} M) of peptide as a dilution series to seeded K562 and incubating overnight at 37 °C and 5 % CO_2. T cells were rested one day prior in complete medium without any supplemented IL-2 overnight. Target cells were harvested, washed three times in complete medium, counted and adjusted to a density of 6×10^5 /ml; and seeded into a 96-well plate with round bottoms (3×10^4/well). Effector $CD8^{+}$ transgenic-TCR^{+}T cells were collected, washed three times and added in a 1:1 ratio to target cells. Cells were co-incubated in a total volume of 200 µl of complete medium supplemented with 2 µl/ml GolgiPlug (BD Biosciences) for four hours at 37 °C and 5 % CO_2.

As positive control, effector T cells were incubated without target cells and stimulated with PMA (25 ng/ml) and Iono (1 µg/ml). As negative control, effector T cells were co-incubated with non-peptide-pulsed K562 target cells. All conditions were performed in technical triplicates.

After co-incubation, cells were washed in cold FACS buffer. For live/dead discrimination, cells were resuspended in 50 µl cold FACS buffer containing 2 µg/ml ethidium monoazide (EMA), and incubated for 15 min on ice in exposure to bright light. Cells were then washed twice and surface staining was performed as described in 3.2.3.2 for 20 min on ice in the dark. For permeabilization and fixation, cells were washed in cold FACS buffer and incubated in 100 µl Cytofix solution (BD Biosciences) for 20 min on ice in the dark. From now on cells were pelleted using 1700 rpm instead of 1500 rpm. Samples were washed twice in cold Permwash (BD Biosciences). For intracellular staining, cells were incubated with antibodies for cytokines (IL-2, tumor necrosis factor alpha

(TNFα) and Interferon-γ (IFNγ))in cold Permwash for 30 min on ice in the dark. Samples were washed twice in cold Permwash and one last time in cold FACS buffer. Cells were resuspended in 100 µl of cold FACS buffer and filtered through a nylon mesh before sample acquisition on a flow cytometer.

3.2.3.6 xCELLigence killing assay

To assess the real-time killing capacity of HLA KO cells we performed a killing assay using the xCELLigence® RTCA System (ACEA Bio). For peptide pulsing, HepG2 cells were harvested, washed 1.5 times with DMEM and counted. Cells were resuspended in DMEM containing the peptide (10^{-6} M) at a density of 5×10^6 /ml and incubated on a vial roller for two hours.

Meanwhile, sample wells of a 96-well E-Plate (OLS) were filled with 100 µl complete DMEM and background was measured by placing it in the xCELLigence® RTCA System.

HepG2 cells were washed 2.5 times with DMEM and resuspended in complete DMEM. 8×10^4 (100 µl) HepG2 cells were seeded per well and growth was measured for at least 24 h. T cells were added when the growth curve hit saturation. 100 µl were carefully removed from each sample well. Overnight rested T cells were harvested, washed in complete medium and counted. 100 µl complete medium supplemented with 100 IU/ml containing different numbers of effector T cells for different effector to target ratios (1:1, 1:3) were added. As a positive control of target cell growth, complete medium containing 100 IU/ml IL-2 was added. As a positive control of target cell lysis, 100 µl of complete medium containing 2 % Triton-X were added. xCELLigence® RTCA Software Pro (ACEA) and Prism9 (GraphPad) were used to analyze the data.

E-plates were re-used up to five times. For regeneration, all wells were trypsinized overnight in the fridge. Plates were thoroughly washed with sterile PBS and finally with H_2O. Washed plates were left to dry with an open lid under the sterile hood.

3.2.4 Mixed lymphocyte reaction assay

An integral aspect of this thesis involved establishing a mixed lymphocyte reaction assay (MLR) to investigate the alloreactive potential of allogeneic HLA-engineered T cells. Various approaches were systematically tested and refined. As an approach to demonstrate alloreactivity, PBMCs were co-incubated with allogeneic cells, followed by intracellular cytokine staining. Furthermore, co-culturing PBMCs over different durations was attempted to drive alloreactivity; along with subsequent re-challenges of selected alloreactive cells after 7 days of co-culture, either with or without adjuvants such as PHA. Throughout these investigations, it became apparent that the most promising outcomes were achieved by promoting the growth of alloreactive cells while minimizing non-alloreactive proliferation stimuli. These cells were either isolated via cell sorting to enhance their frequency or utilized without prior selection to maintain cell fitness.

3.2.4.1 MLR as 2 d co-culture with primed effector cells

To promote the growth of alloreactive cells, the effector cells were primed by co-culturing them with wild-type HLA target cells (obtained from both autologous and allogeneic donors) in complete medium with minimum concentrations of IL-2 (10 IU/ml) for 7 days. The resulting subsets of effector cells, namely allogeneic primed and autologous primed effector cells, were subsequently utilized in the assay to investigate the alloreactive potential of given samples.

Fresh blood was collected from a healthy donor, and PBMCs were isolated as described in 3.2.1.1. Cells were split in halves, one serving consecutively as effector cells and one as target cells for autologous priming. Target cells were collected and mitotically inactivated through irradiation (35 Gy). Cells were washed twice, counted and resuspended in complete medium supplemented with 10 IU/ml IL-2 at a density of 1×10^6 cells/ml. Effector and target cells were co-cultured in a 1:1 ratio for 7 days at 37 °C and 5 % CO_2.

After 7 days, effector cells were harvested and labeled with the eBioscience™ Cell Proliferation Dye eFluor™ 450 Kit (Thermo Fisher) according to the manufacturer's protocol. Desired target cells for the MLR were collected, irradiated at 35 Gy and labeled with the CFSE Cell Division Tracker Kit (Biolegend) according to the manufacturer's protocol. Both target and effector cells were resuspended in complete medium containing 10 IU/ml IL-2 and cell density was adjusted to 1×10^6 /ml. The target cells were seeded at a density of 1×10^5 cells/well (100 µl) in a 96-well plate with flat bottoms and allowed to rest for 1 h at 37 °C and 5 % CO_2. Subsequently, 1×10^5 (100 µl) effector cells were added to each well, and the cells were co-cultured together for 2 d at 37 °C and 5 % CO_2. As a positive control, the effector cells were stimulated with 1.5 µl/ml aCD3/aCD28 expamer reagent (Juno Therapeutics). Autologous target/effector pairs (HLA-matched) and effector cells alone served as negative controls. All conditions were performed in technical triplicates. After 44 hours of co-culture, staining was perfomed with aCD8, aCD137 and aCD154 antibodies as described in 3.2.3.2.

3.2.4.2 MLR as 2 d co-culture with sorted effector cells

To promote the growth of alloreactive cells, effector cells were co-cultured with wild-type HLA target cells obtained from both autologous and allogeneic donors. Fresh blood was collected from each donor, and PBMCs were isolated as described in 3.2.1.1. The cells were divided into halves, with one undergoing irradiation at a dose of 35 Gy to serve as target cells, while the other half was labeled with the eBioscience™ Cell Proliferation Dye eFluor™ 450 Kit (Thermo Fisher) according to the manufacturer's protocol, representing the effector cells.

Effector and target cells were then co-cultured at a density of 1×10^6 cells/ml in complete medium supplemented with IL-2 at a concentration of 10 IU/ml. The co-culture was maintained at 37 °C and 5 % CO_2 for 7 days. After this period, the effector cells were harvested, and CD8 staining was performed as previously (3.2.3.2) described. Subsequently, the $CD8^+eF450^{low}$ population was sorted, expanded using feeder cells and

PHA, as described in 3.2.1.4. Upon sufficient expansion, the effector cells were harvested again and labeled with eFluor™ 450 proliferation dye.

Desired target cells for the MLR were collected, irradiated at 35 Gy and labeled with the CFSE Cell Division Tracker Kit (Biolegend) according to the manufacturer's protocol. Both target and effector cells were resuspended in complete medium containing 10 IU/ml IL-2 and cell density was adjusted to 1×10^6 /ml. The target cells were seeded at a density of 1×10^5 cells/well (100 µl) in a 96-well plate with flat bottoms and allowed to rest for 1 h at 37 °C and 5 % CO_2. Subsequently, 1×10^5 (100 µl) effector cells were added to each well, and the cells were co-cultured together for 2 d at 37 °C and 5 % CO_2. As a positive control, the effector cells were stimulated with 1.5 µl/ml aCD3/aCD28 expamer reagent (Juno Therapeutics). Autologous target/effector pairs (HLA-matched) and effector cells alone served as negative controls. All conditions were performed in technical triplicates. After 44 hours of co-culture, staining was performed with aCD8, aCD137 and aCD154 antibodies as described in 3.2.3.2.

3.2.5 *in vivo* methods

3.2.5.1 *in vivo* transfer in humanized mouse model

Female 4-week-old NSG-SGM3 mice (Jackson Laboratories) were humanized through *i.v.* administration of human $CD34^+$ cells ($3 - 7.5 \times 10^4$ cells/mouse) isolated from umbilical cord blood; following irradiation 24 h prior with 1 Gy. An HLA-A*02:01 positive donor for umbilical cord blood was selected. Human immune system reconstitution took place over 12 weeks. Peripheral blood was then analyzed via flow cytometry to identify different immune cell populations. PBMCs used as effector cells all received an aCD19-CAR (JCAR 21) knock-in into the endogenous *TRAC* gene locus and were (in the case of HLA reduction) simultaneously edited for all HLA class I alleles except for HLA-A*02:01. Finally, cells were administered directly after electroporation without prior sorting or further *in vitro* culturing via the intravenous route into recipient mice. After administration, peripheral blood was analyzed using flow cytometry as described in 3.2.5.4 every four days. Endpoint analysis of peripheral blood (3.2.5.4), bone marrow (3.2.5.6) and spleen (3.2.5.5) was done on day 15 *post injectionem* or when the experiment reached termination criteria.

3.2.5.2 *in vivo* transfer in syngeneic infection mouse model

Before T cell transfer, NSG/HHD HLA-A*02:01 mice (Jackson Laboratorie) were irradiated with 2 Gy to create a niche for the transferred cells. $CD8^+$ TCR-transgenic T cells with and without *B2M* KO were then injected intraperitoneally, resuspended in 200 µl FCS supplemented with 200 IU IL-2. The endogenous TCR was orthotopically replaced with a CMV-specific TCR (TCR 6-2). The next day, mice were infected intraperitoneally with 5×10^3 plaque-forming units (PFU) mCMV-NLV (virus provided by Luka Cicin-Sain). On day 7 after infection, the mice were sacrificed and the liver was processed for flow cytometry analysis (see 3.2.5.3).

3.2.5.3 Flow cytometric analysis of lymphocytes in liver tissue

Mice were sacrificed and the liver was weighed and processed with tissue grinder dounce "A" along with 2 ml PBS. Mixture was placed in 15 ml falcon tubes and centrifuged for 6 min at 1500 rpm and RT. The supernatant was discarded and the pellet was resuspended with 6 ml of 40 % Percoll (diluted with PBS). Density gradient centrifugation was then performed for 20 min at 2600 rpm and RT with brakes disabled and acceleration set to 5. The supernatant was carefully discarded. Cells were resuspended in 5 ml ACT buffer and incubated for 5 min at RT to perform red blood cell lysis. Lysis was stopped by addition of 5 ml complete DMEM and cells were pelleted by centrifugation for 6 min at 1500 rpm. Cells were resuspended in 200 µl FACS buffer and rested on ice. From this point on, cells were stained as described in 3.2.3.2.

3.2.5.4 Flow cytometric analysis of lymphocytes in peripheral blood

50 µl blood were drawn from the tail vein and directly diluted with 50 µl of heparinized PBS (5000 IE/ml Heparin). The sample was transferred in a 15 ml falcon tube filled with 10 ml ACT buffer. Incubated for 10 min at RT, then lysis was stopped by adding 5 ml of complete medium. Tubes were centrifuged for 7 min at 1500 rpm and RT; supernatant was discarded. The pellet was resuspended in 5 ml ACT buffer for a second red blood cell lysis. Lysis was stopped after 5 min by adding 5 ml complete medium. Cells were pelleted by centrifugation for 7 min at 1500 rpm and RT. If the pellet still appeared red, an optional third red blood cell lysis was performed, otherwise cells were resuspended in 100 µl cold FACS buffer and staining was continued as described in 3.2.3.2.

3.2.5.5 Flow cytometric analysis of lymphocytes in spleen tissue

Mice were sacrificed and the spleen was placed in a 70 µm cell strainer inside a 6 cm petri dish filled with 10 ml of complete medium. Spleen was mashed through cell strainer using the piston of a 2 ml syringe. Cell strainer was rinsed and medium was transferred into a 15 ml falcon tube. Samples were then centrifuged for 5 min at 1500 rpm at 4 °C and supernatant was discarded. Red blood cell lysis was performed at RT using 5 ml ACT buffer. After 5 min lysis was stopped by adding 5 ml of cold complete medium. Samples were centrifuged for 5 min at 1500 rpm at 4 °C, supernatant was discarded and cells were resuspended in 200 µl cold FACS buffer. Cells were counted and a maximum of 1×10^7 cells were seeded in one well of a 96-well plate with V-bottoms. Staining was performed as in 3.2.3.2.

3.2.5.6 Flow cytometric analysis of lymphocytes in bone marrow

Mice were sacrificed and femur and tibia of one hind leg were harvested. The epiphyses were cut off and the bone marrow was flushed with complete DMEM, using a 1.0 ml Sub-Q syringe (BD Biosciences) into a 15 ml falcon tube filled with 10 ml of complete DMEM. See Liu and Quan, 2015 [77] for further technical explanations of hind leg dissection. Samples were centrifuged for 5 min at 1500 rpm at 4 °C and supernatant was discarded.

Red blood cell lysis was performed at RT using 3 ml ACT buffer. After 3 min lysis was stopped by adding 3 ml of cold complete DMEM. Samples were centrifuged for 5 min at 1500 rpm at 4 °C, supernatant was discarded and cells were resuspended in 200 µl cold FACS buffer. Cells were counted and a maximum of 1×10^7 cells were seeded in one well of a 96-well plate with V-bottoms. Staining was performed as in 3.2.3.2.

4 Results

4.1 Establishment of HLA class I and class II KO

To investigate the functional implications of HLA-deficient T cells, it was necessary for us to develop a strategy for generating T cells that lack entirely either HLA class I, class II, or both. CRISPR/Cas9-mediated knock-out (KO) was the undeniably clear approach to generate HLA-deficient T cells due to its exceptional precision and efficiency in selectively targeting specific genes. Primary human T cells, much like nearly all nucleated human cells, express HLA class I and class II molecules on their cell surfaces. HLA class I molecules are surface-bound through the shared subunit β-2-microglobulin (β2m) (Fig. 4.1.a). Targeting the *B2M* gene has previously been suggested to completely disrupt HLA class I. To replicate this strategy, we disrupted the *B2M* gene in primary human T cells with specific CRISPR/Cas9 guide RNAs (gRNAs) (Fig. 4.1.b-d). Successful editing was confirmed at the protein level by flow-cytometric assessment and at the DNA level by Sanger sequencing, followed by ICE analysis (see 3.2). In essence, we successfully achieved HLA class I-deficient T cells via CRISPR/Cas9-mediated knock-out, as flow cytometry and ICE analysis confirm.

In contrast to HLA class I molecules, class II molecules lack a common transmembrane domain for cell-surface anchoring. Instead, they consist of distinct α and β-chains. To achieve HLA class II-deficiency with a single edit, targeting a separate gene is necessary. Various transcription factors regulating HLA class II genes have been identified as potential candidates for this purpose (Fig. 4.1.e). We focused on attempting to disrupt the regulatory factor X-associated ankyrin-containing protein (*RFXANK*) and class II major histocompatibility complex transactivator (*CIITA*) genes to potentially generate HLA class II-deficient T cells. For this purpose, we identified three potential gRNA candidates for each gene. Subsequently, we performed CRISPR/Cas9-mediated knock-out using the chosen guides and then examined HLA DR expression levels through flow-cytometric analysis (Fig. 4.1.f). A more in-depth investigation of the most promising candidate targeting the *CIITA* gene was done (Fig. 4.1.g,h). Given that T cells typically express HLA class II only upon activation, flow-cytometric analysis of HLA DR expression provides a directional rather than an accurate KO score. However, sequencing data unveiled a robust knock-out of approximately 12 percent. In order to explore the impact of simultaneously delivering two CRISPR/Cas9 gRNA ribonucleoproteins (RNPs) on editing efficacy, we performed single and double knock-outs of both target genes. We assessed the editing efficacy for both genes by employing Sanger sequencing, followed by ICE analysis (Fig. 4.1.i). This data indicates that there is no difference in

their individual editing efficacy when performing either a single or dual knock-out for each gene.

In summary, we established a robust method for generating HLA class I, class II, or dual deficient T cells using CRISPR/Cas9-mediated knock-out targeting the *B2M* and *CIITA* genes.

4.2 Mixed Lymphocytes Reaction Assays

4.2.1 Establishment

In order to test the alloreactive response towards HLA-edited targets and determine their compatibility and immunogenicity, it was necessary to develop a protocol for a mixed lymphocyte reaction assay (MLR). In principle, this is typically achieved through co-culturing peripheral mononuclear blood cells (PBMCs) from two distinct individuals and evaluating the response using various indicators, such as cytokine production, cell division, and changes in cell surface markers. PBMCs were co-cultured, and effector cells were labeled with eFluor 450 proliferation dye from Thermo Fisher. Dilution of the proliferation dye indicates cell growth, and individual generations can be identified through levels of fluorescence by flow cytometry. Specific gating was established to identify proliferated and highly proliferated cells, as depicted in Fig. 4.2.a. In our initial approach, PBMCs from three distinct donors were co-cultured. These co-cultures comprised either no target cells or irradiated PBMCs from each donor at a 1:1 ratio. After eight days, a second round of stimulation was performed by renewing target cells with freshly irradiated PBMCs sourced from the respective donors. Phythaemagglutinin (PHA) was tested as an adjuvant during culture. Flow-cytometric analysis took place at two different time points (7 days or 2 days after re-challenging). Using PHA as an adjuvant generated overall stimulation so that no proliferation difference could be detected (Fig. 4.2.b). Without an adjuvant, 7 days after re-challenge, a significant difference in proliferation could be detected in three out of six conditions, compared to the autologous HLA match (same donor used for both effector and target cells) (Fig. 4.2.c). A shorter period of re-challenge (2 days instead of 7 days) produced a greater difference in proliferation between the HLA mismatched (two different donors for target and effector cells), and the autologous HLA-matched conditions (Fig. 4.2.d). Whereas only including cells with lesser fluorescence (highly proliferated, see Fig. 4.2.a) in the analysis did not drive results to a more significant difference between conditions (Fig. 4.2.e). During the establishment of this assay, we encountered a major challenge due to significant donor variability in proliferation (data not shown). Consequently, we tested various alternatives in the experimental procedure (data not shown). However, establishment was not as straightforward as the data may suggest.

In essence, the addition of an adjuvant turned out to be counterproductive, and the analysis saw improved discrimination through a shortened re-challenge period.

The impact of IL-2 presence was examined in a separate co-culture experiment to drive discrimination even further and achieve robust outcomes. Co-culturing of effector cells for 4 days after re-challenge with 50 IU/ml IL-2 led to no notable differences in

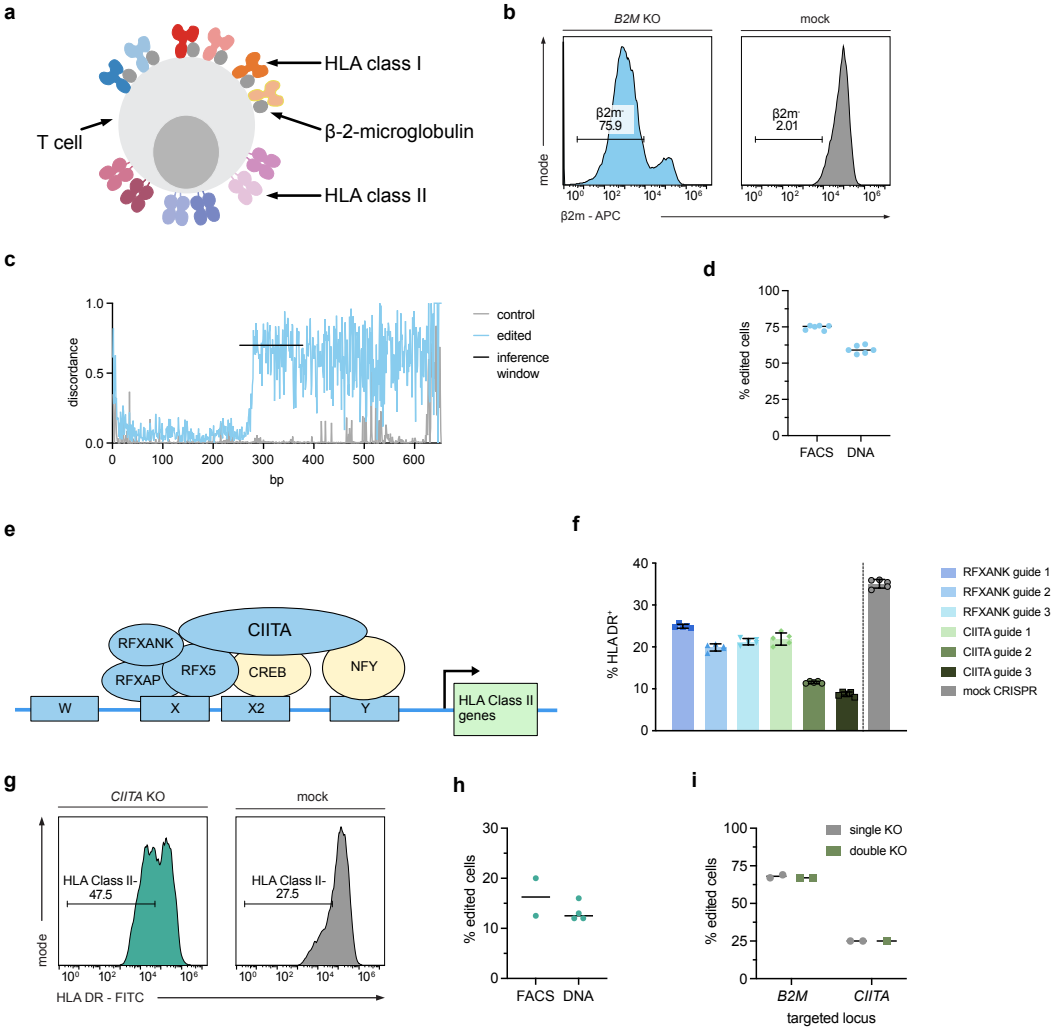

Figure 4.1: HLA class I and II knock-out (KO) Establishments. **a**, Visualization of HLA-bearing T cell. **b**, Flow-cytometric analysis of $\beta 2m^{-}$-T cells (gated on living lymphocytes) isolated from peripheral blood mononuclear cells of a healthy donor, one set of cells was edited using *B2M* gRNA (left), while the other set remained unedited (right) [78]. **c**, Discordance plot as generated by ICE analysis of a β2m-edited sample (blue) in comparison to mock edited cells (grey, control). Discordance, represented by the black line, measures the level of disagreement between the wild type and edited sample at each base within a defined inference window [78]. **d**, Frequency of successful HLA class I knock-out determined using flow cytometry (FACS) and ICE analysis after DNA sequencing (n=6 technical replicates) [78]. **e**, Transcriptional Promoters of HLA class II genes as identified possible CRISPR/Cas9-targets for HLA class II KO. **f**, Flow-cytometric analysis of primary human T cells (gated on living lymphocytes) for HLA DR after CRISPR/Cas9-mediated targeting of indicated HLA class II transcriptional factors with indicated guides (n=5 technical replicates, bar height indicates mean, error bars indicate SD). **g**, Flow-cytometric analysis of *CIITA* KO T cells (gated on living CD8+ lymphocytes) from peripheral blood mononuclear cells of a healthy donor, one set of cells was edited using *CIITA* gRNA (left), while the other set remained unedited (right) [78]. **h**, Frequency of successful HLA class II knock-out determined using flow cytometry (FACS) and ICE analysis after DNA sequencing (n=2 or 4 technical replicates, respectively) [78]. **i**, Analysis of KO efficacy as determined using ICE analysis achieved either through a single or double guide editing.
Parts of the figure were reprinted with permission from [78].

proliferation. This was consistent across both HLA match and mismatch conditions, as well as in comparison to T-cell receptor (TCR) KO effector T cells (Fig. 4.2.f). Nevertheless, when IL-2 was absent during the re-challenge phase, distinct proliferation differences re-emerged (Fig. 4.2.g). In conclusion, leveraging the immunogenicity of target cells as a proliferation and activation stimulus through minimal cytokine supplementation enhances robust and reliable outcomes.

To combine previous findings, freshly isolated PBMCs from diverse donors were co-cultured with freshly irradiated PBMCs sourced from allogeneic donors. This co-culture lasted 7 days, with only 10 IU/ml of supplemented IL-2 (allo priming). The primed effector cells were re-challenged for two days with fresh irradiated PBMCs derived from the same donor against which the effector cells were initially primed. Flow-cytometric analysis of activation markers showed greater expression of CD137 on $CD8^+$ effector T cells when they were re-challenged with HLA-mismatched allogeneic targets (Fig. 4.2.h). In our observations, the most robust results in mixed lymphocyte reactions were obtained through the upregulation of CD137 on effector T cells or the survival of target cells, rather than through proliferation, CD69 upregulation, or target cell survival alone (data not shown). As a result, we have chosen to focus on these readouts. However, the data is still subject to significant variability depending on the donor. Nonetheless, cumulative analysis proved these findings to be significant across all conditions (Fig. 4.2.i).

In summary, our results suggest the adoption of an MLR protocol that involves priming effectors with minimal cytokine supplementation against unedited wild-type (WT) PBMCs from donors. This protocol consists of seven days of co-culture, followed by re-challenging the expanded alloreactive cells and assessing activation and proliferation on the second-day post-re-challenge.

4.2.2 Alloreactivity of HLA class I deficient T cells

The established MLR protocol (Fig. 4.3.a) should not only demonstrate immunogenicity between two HLA non-identical donors but also evaluate the immunogenicity and compatibility of allogeneic HLA-edited cell products. To test this, PBMCs from donor A were allo primed using PBMCs from donor B. It is important to note that donor B does not share any HLA alleles with donor A. PBMCs from donor B were HLA edited and sorted for successful editing and $CD3^+$ T cells (no HLA I). Unedited $CD3^+$ T cell-sorted PBMCs from donor A (HLA I match) and donor B (HLA I mismatch) were used as target cells. In addition, HLA-edited and sorted cells from donor B that are lacking HLA class I (no HLA I) were also used as targets for re-challenging the primed effector cells (Fig. 4.3.c,d). This led to preferential activation of effectors challenged with HLA mismatched target cells (Fig. 4.3.b). However, missing HLA class I on allogeneic target cells only induced activation to the same extent as autologous HLA-matched T cells. These findings support the assay's objective of distinguishing varying levels of immunogenicity and confirming the reduced immunogenicity of HLA class I KO cells.

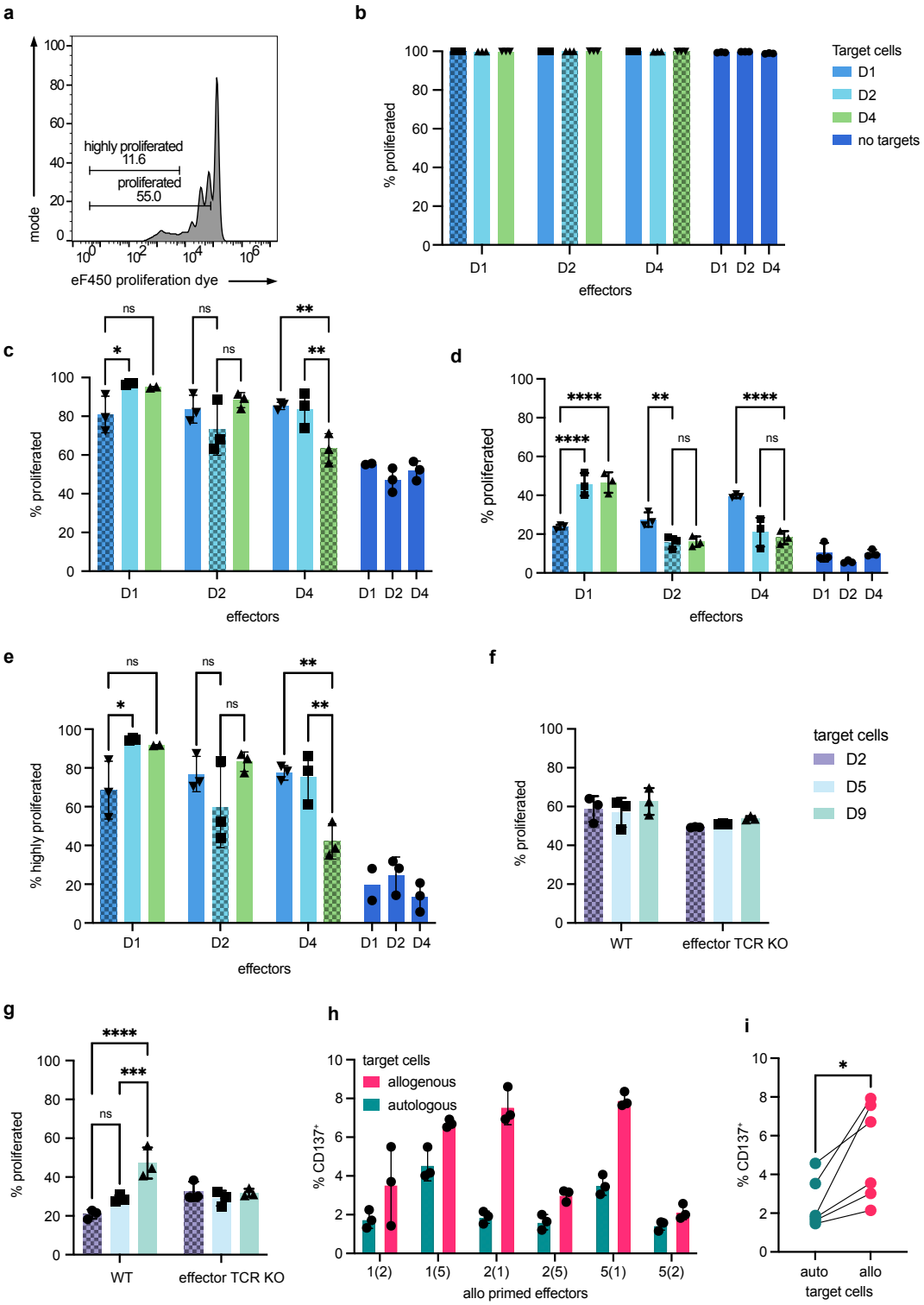
a
highly proliferated
11.6
proliferated
55.0
mode
eF450 proliferation dye
b
% proliferated
Target cells
D1
D2
D4
no targets
effectors
c
% proliferated
effectors
d
% proliferated
effectors
e
% highly proliferated
effectors
f
% proliferated
target cells
D2
D5
D9
WT
effector TCR KO
g
% proliferated
WT
effector TCR KO
h
% CD137+
target cells
allogenous
autologous
allo primed effectors
i
% CD137+
auto
allo
target cells

Figure 4.2 *(preceding page)*: Mixed Lymphocytes Reaction Assay Establishments. **a**, FACS plot showing definition of gates used in proliferation dye dilution analysis in b,c,d,e,f,g , y-axis normalized to mode. **b**, Frequency of proliferated effector cells after co-culture of indicated effector:target combination for 8 days, restimulation with indicated fresh target cells and readout after 7 days, added PHA as adjuvant; effector cells derived from donors as indicated on x-axis, target cell donors indicated by color coding, checkered bar indicates autologous HLA match; n=3 technical replicates, mean with SD. **c**, Frequency of proliferated effector cells after co-culture of indicated effector:target combination for 8 days, restimulation with indicated fresh target cells and readout after 7 days, no added adjuvant; effector cells derived from donors as indicated on x-axis, target cell donors indicated by color coding, checkered bar indicates autologous HLA match; statistical testing by ordinary two-way ANOVA and Tukey's multiple comparisons test, results are only shown for selected comparisons, n=3 technical replicates, mean with SD. **d**, Frequency of proliferated effector cells after co-culture of indicated effector:target combination for 8 days, restimulation with indicated fresh target cells and readout after 2 days, no added adjuvant; effector cells derived from donors as indicated on x-axis, target cell donors indicated by color coding, checkered bar indicates autologous HLA match; statistical testing by ordinary two-way ANOVA and Tukey's multiple comparisons test, results are only shown for selected comparisons, n=3 technical replicates, mean with SD. **e**, Frequency of highly proliferated effector cells after co-culture of indicated effector:target combination for 8 days, restimulation with indicated fresh target cells and readout after 7 days, no added adjuvant; effector cells derived from donors as indicated on x-axis, target cell donors indicated by color coding, checkered bar indicates autologous HLA match; statistical testing by ordinary two-way ANOVA and Tukey's multiple comparisons test, results are only shown for selected comparisons, n=3 technical replicates, mean with SD. **f**, Frequency of proliferated effector cells after 4 days of co-culture with unedited PBMCs from three different indicated donors, effector cells were PBMCs from a single donor either unedited (WT) or with CRISPR/Cas9-mediated TCR KO, co-cultured with unedited PBMCs from three different indicated donors for 7 days, 50 IU/ml IL-2 was used throughout co-culture; checkered bar indicates autologous HLA match; n=3 technical replicates, mean with SD. **g**, Frequency of proliferated effector cells after 4 days of co-culture with unedited PBMCs from three different indicated donors, effector cells were PBMCs from a single donor either unedited (WT) or with CRISPR/Cas9-mediated TCR KO, co-cultured with unedited PBMCs from three different indicated donors for 7 days, no IL-2 was used throughout co-culture; checkered bar indicates autologous HLA match; statistical testing by ordinary two-way ANOVA and Tukey's multiple comparisons test, results are only shown for selected comparisons, n=3 technical replicates, mean with SD. **h**, Frequency of $CD137^+$ $CD8^+$ effector cells; effector cells were PBMCs from indicated donors co-cultured for 7 days with allogeneic PBMCs (allo priming) and then restimulated for 44 hours with fresh irradiated PBMCs as target cells, either autologous or allogeneic from the same donor used in the priming process; donor combination used for priming effector cells is displayed on the x-axis, with the number in parentheses indicating the donor used as allogeneic target; checkered bar indicates autologous HLA match; n=3 technical replicates, mean with SD. **i**, Cumulative analysis of data shown in h; statistical testing by paired two-tailed t-test;n=6 biological replicates consisting out of 3 technical replicates each. ns, not significant; *, $P \leq 0.05$; **, $P \leq 0.01$; ***, $P \leq 0.001$; ****, $P \leq 0.0001$

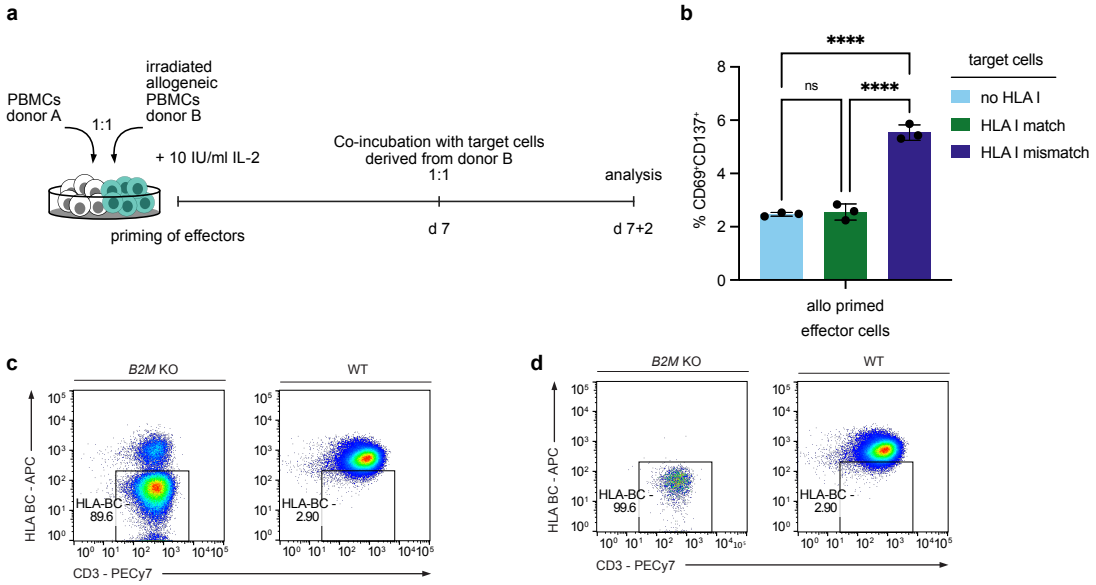

Figure 4.3: Alloreactivity of HLA class I edited targets. **a**, Experimental setup for Mixed Lymphocytes Reaction Assay. **b**, Frequency of $CD69^{+}CD137^{+}$ $CD8^{+}$ effector cells after 48 h of co-culture with indicated target cells; effector cells were peripheral mononuclear blood cells from donor A, co-cultured for 7 days together with PBMCs from donor A (allo priming). Target cells were autologous unedited cells from donor B (HLA I match), allogeneic *B2M* KO cells (no HLA I), and allogeneic unedited cells (HLA I mismatch). Target cells were sorted for $CD3^{+}$ and successful KO if applicable; statistical testing by ordinary two-way ANOVA and Tukey's multiple comparisons test, n=3 technical replicates, mean with SD; ns, not significant; ****, $P \leq 0.0001$ [78]. **c**, Flow-cytometric analysis of *B2M* KO targets for mixed lymphocyte reaction (MLR) assay (gated on living lymphocytes) after electroporation with indicated gRNAs prior to cell sorting [78]. **d**, as in c, now after cell sorting prior to MLR assay in case of B2M KO cells (WT cells were not sorted) [78]. Parts of the figure were reprinted with permission from [78].

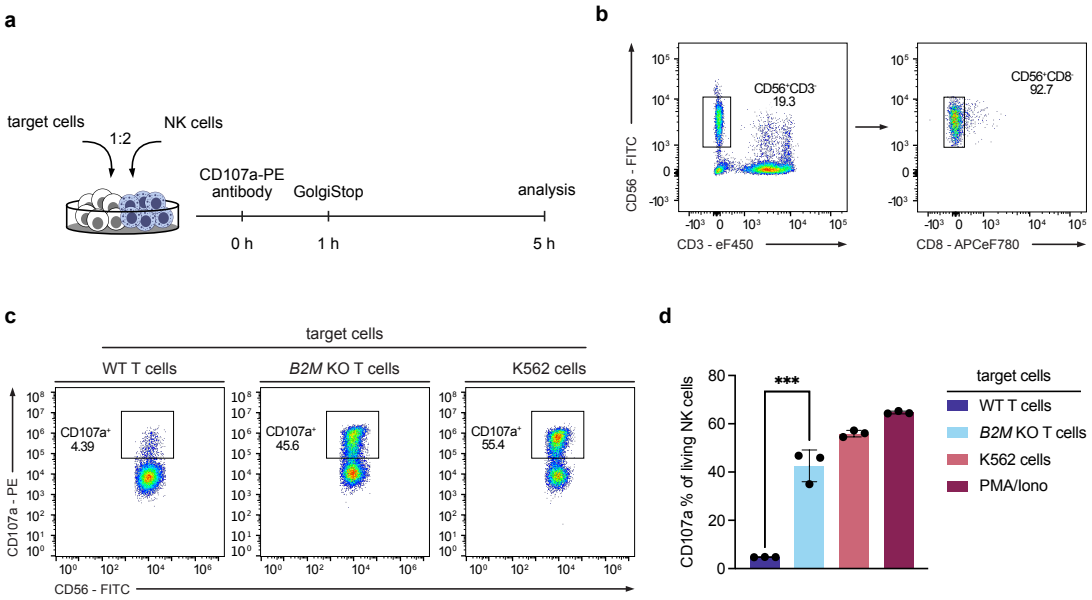

Figure 4.4: Recognition through NK cells. **a**, Experimental setup for NK cell recognition assay [78]. **b**, Representative FACS-plots showing gating strategy for isolating $CD56^+CD3^-CD8^-$ NK cells from fresh PBMCs (pregated on living lymphocytes). **c**, Representative flow cytometric analysis of $CD107a^+$ NK cells (percentage of living $CD56^+$ $CD8^-$ lymphocytes) after 5 h of co-incubation with indicated target T cells, K562 cells or PMA/Iono; cells were sorted for successful editing [78]. **d**, Quantification of data shown in c; n=3 technical replicates; statistical testing was done using an unpaired two-tailed t-test, and results are only shown for comparison of WT and *B2M* KO T cells; mean with SD; ***, $P \leq 0.001$ [78].
Parts of the figure were reprinted with permission from [78].

4.3 Recognition through NK cells

HLA editing holds the potential to protect cells from rejection by alloreactive T cells, yet it might inadvertently trigger NK cells through a mechanism known as "missing-self" activation. To thoroughly explore this potential concern, we conducted a co-incubation experiment involving NK cells and distinct target cells (*B2M* KO or unedited T cells). Positive controls were established through stimulation with K562 cells or PMA/Ionomycin. This co-incubation was performed in the presence of an anti-CD107a antibody and GolgiStop (BD Biosciences) (Fig. 4.4.a). The NK cells were obtained through sorting $CD56^+CD3^-CD8^-$ NK cells from freshly isolated PBMCs (Fig. 4.4.b). The sort-purified *B2M* KO T cells induced greater degranulation in NK cells compared to unedited (WT) T cells, almost to the same degree as positive controls did (Fig. 4.4.c,d).

In essence, these findings confirmed that *B2M* KO T cells are prone to rejection through NK cells, highlighting a potential consideration in HLA editing strategies.

4.4 Functionality of HLA KO T cells

4.4.1 Generation of HLA KO T cells with orthotopic T cell receptor replacement for subsequent functionality testing

Much remains to be understood about whether the loss of HLA expression leads to changes in intrinsic T-cell functionality. To investigate this matter, we generated HLA class I and II-deficient T cells and simultaneously replaced the native T-cell receptor with a transgenic one during the same editing step. Orthotopic TCR replacement (OTR) ensures that the T cells demonstrate physiological behavior, as the specific antigen recognition and activation mechanism closely mimics the natural immune response, enhancing the authenticity and reliability of the functional assays [68, 79]. Furthermore, through the introduction of a TCR possessing known antigen specificity and affinity, we gain the ability to finely regulate the extent of T-cell stimulation, in contrast to unspecific stimulation approaches. We introduced either HLA-A*02-restricted TCR 6-2 specific for the cytomegalovirus (CMV)-epitope $pp65_{495\text{-}503}$, or HLA-B*08-restricted TCR 3-2 specific for the CMV-epitope $IE1_{88\text{-}96}$. Although the investigation initially focused on TCR 3-2 transgenic cells, most of the experiments were conducted using TCR 6-2 due to the greater availability of HLA-A*02^+ target cells. In parallel, the cells underwent additional editing steps: either *B2M* KO, *CIITA* KO, or no further editing ("TCR KI only"). Edited cells were then sort purified for $CD8^+$ $hTCR^-$ $mTRBC^+$ and if relevant were further sorted to be $\beta 2m^-$ ("*B2M* KO") or HLA DR^- ("*CIITA* KO") (Fig. 4.5). In essence, these data demonstrate the feasibility of generating adoptive-transfer ready $CD8^+$ T cells with additional HLA engineering for subsequent functionality testing.

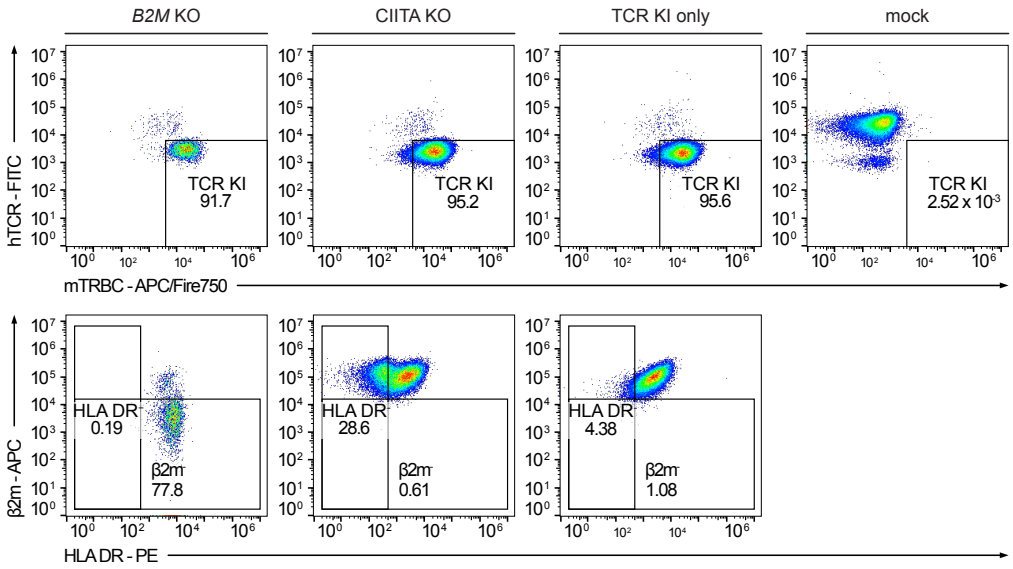

Figure 4.5: Generation of HLA KO T cells with orthotopic T cell receptor replacement for subsequent functionality testing. Flow-cytometric analysis of primary human T cells after CRISPR/Cas9-editing and cell sorting for $CD8^+$ $hTCR^-$ $mTRBC^+$ pregated on living $CD8^+$ (first row) and $CD8^+$ $hTCR^-$ $mTRBC^+$ (second row) cells; all conditions received orthotopic T-cell receptor replacement with TCR 6-2 and either no additional editing ("TCR KI only") or knocked out endogenous *B2M* ("*B2M* KO") or *CIITA* ("*CIITA* KO"), unedited cells shown for comparison ("mock"). This figure was adapted and reprinted with permission from [78].

4.4.2 Intrinsic functionality of HLA KO T cells *in vitro* and *in vivo*

T-cell functionality is characterized by a spectrum of cellular behaviors integral to the immune response. Target cell recognition, cytokine production, and cytotoxicity are commonly measured as indicators of T-cell functionality in response to specific antigen stimuli. To assess the cytokine release capability of HLA-edited cells, edited cells were co-incubated with peptide-pulsed K562, transgenic for HLA-A*02 or HLA-B*08, and stained for intracellular cytokines Interferon-γ (IFNγ) and tumor necrosis factor alpha (TNFα) (Fig. 4.6.a). HLA class I and class II-deficient cells showed no alteration in target-cell recognition and cytokine-release sensitivity compared to TCR-transgenic cells with no further editing (Fig. 4.6.b,c). In order to assess *in vitro* killing capacity as another evidence of T-cell functionality, we performed an xCELLigence® real-time cell analysis of peptide-pulsed HepG2 target cells held in co-culture with the HLA-edited T cells. TCR-transgenic T cells with additional *B2M* KO demonstrated target cell elimination kinetics and efficacy equivalent to that of HLA-unedited T cells (Fig. 4.6.d). The same trend appears to hold true for TCR-transgenic cells with additional *CIITA* KO (Fig. 4.6.e). In essence, this data demonstrates that HLA class I or class II-deficient T cells maintain their capacity for target cell recognition, cytokine production, and cytotoxicity – preserving T-cell functionality akin to physiological T cells.

To investigate the behavior of HLA-edited T cells in response to authentic antigen presentation within a syngeneic infection model, as opposed to constant stimulation in an artificial *in vitro* antigen-presentation context, we generated TCR 6-2 transgenic T cells with or without an additional *B2M* KO. These cells were subsequently transferred into NOD.Cg-Prkdc^{scid}Il2rg^{tm1Wjl}Tg(HLA-A/H2-D/B2M)1Dvs/SzJ (NSG/HHD) HLA-A*02:01-transgenic mice one day after irradiation. The mice were infected with murine CMV (mCMV), expressing the human CMV epitope pp65$_{495\text{-}503}$ (Fig. 4.7.a). Murine CMV infects mice syngeneically, and due to the HLA-A*02 transgeneicity, adoptively transferred human T cells can recognize infected target cells. Transferred TCR-transgenic CD8$^+$ T cells with and without additional *B2M* KO could be both recovered in infected livers on day 8 after transfer (Fig. 4.7.b). Moreover, the percentage of β2m$^-$ cells of transferred *B2M* KO cells was entirely maintained throughout the *in vivo* experiment (Fig. 4.7.c).

In conclusion, this data suggests that HLA class I-deficient T cells are neither positively nor negatively selected *in vivo*, which is consistent with our earlier findings that *B2M* knock-out does not impact T-cell functionality.

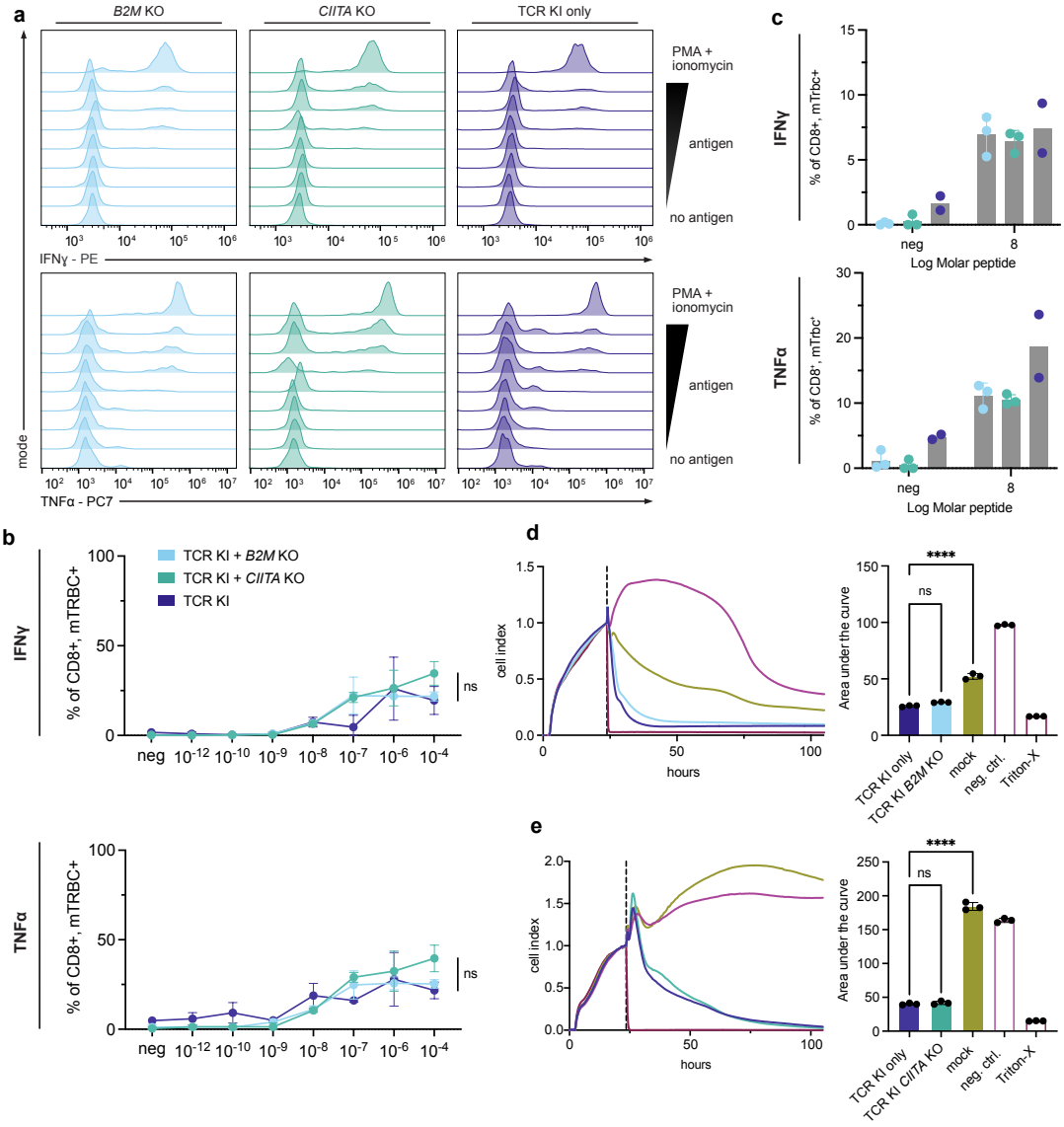
a
B2M KO
CIITA KO
TCR KI only
PMA + ionomycin
antigen
no antigen
IFNγ - PE
TNFα - PC7
mode
c
IFNγ
% of CD8+, mTrbc+
Log Molar peptide
TNFα
% of CD8+, mTrbc+
b
TCR KI + B2M KO
TCR KI + CIITA KO
TCR KI
% of CD8+, mTRBC+
ns
neg
d
cell index
hours
Area under the curve
****
TCR KI only
TCR KI B2M KO
mock
neg. ctrl.
Triton-X
e
TCR KI CIITA KO

Figure 4.6 *(preceding page)*: Functionality of HLA KO T cells. **a**, Representative flow-cytometric intracellular cytokine staining of IFNγ and TNFα in response to no antigen, increasing amounts of antigen or phorbol 12-myristate 13-acetate (PMA) and ionomycin; PBMCs as effector cells underwent orthotopic TCR replacement with CMV NLV-specific TCR 6-2 (TCR KI) and were simultaneously edited with *B2M* gRNA (*B2M* KO) or *CIITA* gRNA (*CIITA* KO); K562 cells loaded with NLV-peptide $pp65_{495\text{-}503}$ as antigen were used for stimulation [78]. **b**, Quantification of data from a (n=2-3 technical replicates, mean with SD), x-axis indicating logarithmic molar peptide concentration; neg, negative control [78]. **c**, Excerpt of data from b (n=2-3 technical replicates, mean with SD), x-axis indicating logarithmic molar peptide concentration; neg, negative control. **d**, Killing of target cells (HepG2 cells pulsed with NLV-peptide $pp65_{495\text{-}503}$) by HLA class II KO T cells as assessed by xCELLigence assay (measured through changes in cell index over time, left panel) and quantified as area under the curve (right panel) calculated over the entire time period shown; addition of effector cells indicated by dashed line; positive control of target cell lysis achieved through addition of detergent Triton-X; negative control (neg. ctrl.) shows uninhibited target cell growth through absence of effector cells; mock edited effector cells were used as control to show non-specific effect on target cell growth through displacement; $CD8^+$ T cells from a, b and c were used as effector cells and sorted for successful editing ($CD8^+$ $hTCR^-$ $mTRBC^+$ $b2m^-$ /$CIITA^-$); statistical testing by ordinary one-way ANOVA and Tukey's multiple comparisons test), results are only shown for selected comparisons, n=3 technical replicates, mean with SD; ns, not significant; ****, $P \leq 0.0001$. **e**, As in d with HLA class I KO cells as subject of investigation [78]. Parts of this figure were reprinted with permission from [78].

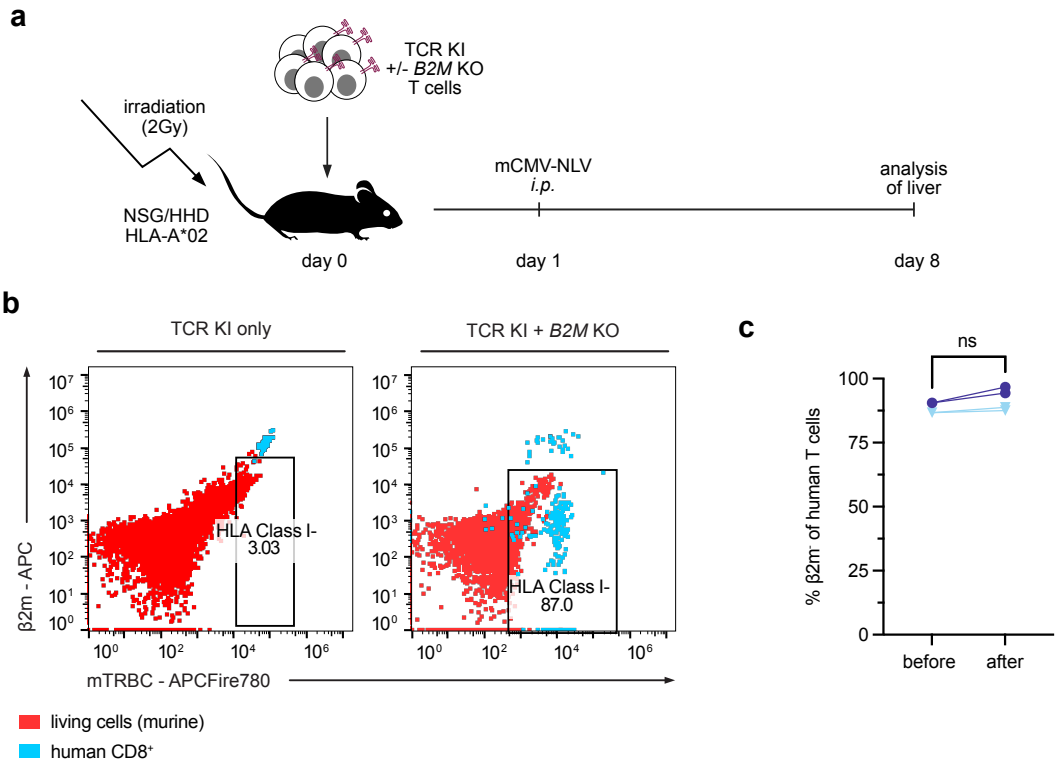

Figure 4.7: Intrinsic *in vivo* functionality of HLA class I deficient primary human T cells. a, Experimental setup for *in vivo* transfer of antigen-specific HLA-edited primary human T cells; effector cells were administered *i.p.* into NSG/HHD HLA-A*02 mice after irradiation with 2 Gy; the next day the mice were infected *i.p.* with mCMV-NLV; $CD8^+$ T cells used as effector cells all underwent orthotopic TCR replacement with TCR 6-2 (TCR KI) and were simultaneously edited with *B2M* gRNA (*B2M* KO) and sorted for successful editing. **b**, Representative flow cytometric analysis of β2m and transgenic TCR (mTRBC) expression (as percentage of $hCD8^+$) of primary human $CD45^+$ T cells (blue) recovered in the liver seven days after in vivo transfer of TCR KI cells into mice. All living murine cells (red) are included for comparison. **c**, Frequency of HLA class I deficient primary human T cells before *in vivo* transfer and after recovery in the liver; pooled data from two independent experiments (light blue or purple color barcode) with n=2 mice each; statistical testing by paired two-tailed t-test; ns, not significant. This figure was reprinted with permission from [78].

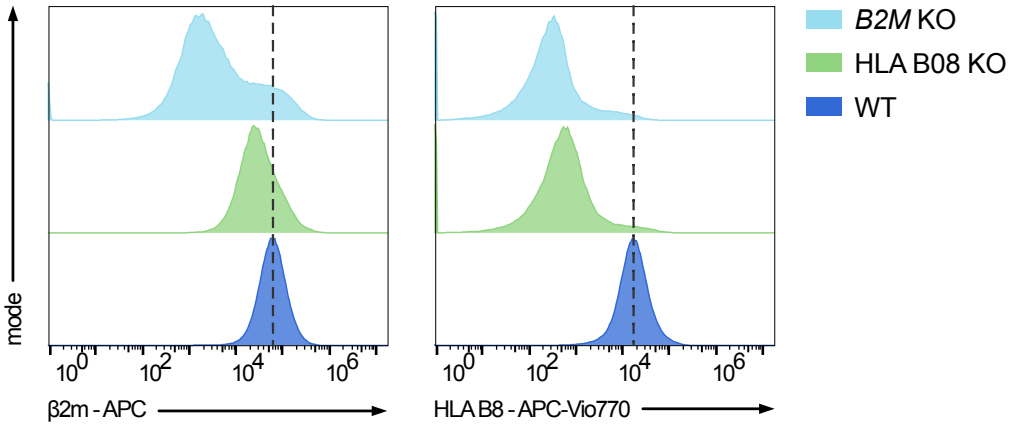

Figure 4.8: Allele-specific targeting of HLA molecules. Flow-cytometric histograms showing expression of β2m and HLA B08 of PBMCs edited with *B2M* gRNA ("*B2M* KO"), HLA B*08-specific gRNA ("HLA B8 KO") or no editing ("WT").

4.5 HLA reduction rather than HLA disruption

4.5.1 Generation of HLA-reduced T cells through single allele targeting

A library of supposedly HLA allele-selective guides has already been published [52]. To test whether we could edit all HLA-A,B, and C alleles simultaneously, we identified corresponding guides from this library for one of our donor's HLA type. Delivering a single HLA-B*08:01-selective guide that is not selective for the other HLA alleles the donor has led to a lesser expression of β2m and a near complete loss of HLA-B*08 expression as assessed by flow cytometry (Fig. 4.8). This confirms the selectivity of the proposed gRNA for HLA-B*08:01 and serves as a proof of principle that the library can be employed to create cells with reduced HLA expression by individually targeting specific HLA alleles.

In order to distinguish between successful and unsuccessful editing in a convenient manner and ideally enable the selection of successfully edited cells through fluorescence activated cell sorting (FACS), we opted for another donor for our HLA reduction experiments. Commercially available antibodies exist for HLA-A*02, HLA-A*03, and HLA BC (cells expressing any HLA-B or -C molecules). Consequently, we selected an HLA-A*02:01$^+$ A*03:01$^+$ B*44:03$^+$ B*51:01$^+$ C*15:02$^+$ C*16:01$^+$ donor. We obtained cells from this donor and performed editing for a single HLA allele (e.g. "A02 KO" in case of HLA-A*02), individually edited simultaneously all six HLA class I alleles except for one (e.g. "6-1 (A02) KO" for all HLA class I alleles, except for HLA-A*02), or left unedited ("WT" or "mock") (Fig. 4.9.a). Further, we knocked out *B2M* ("*B2M* KO") and all six HLA class I alleles separately ("6x KO") as controls. After editing, we performed a flow-cytometric analysis with respective antibodies (Fig. 4.9.b-d). A complete loss of

β2m could only be observed in the *B2M* KO sample, but not in samples where HLA alleles were targeted individually. A loss of HLA BC-expression could be observed in case of *B2M* KO, 6x KO, and in those conditions, only the guides for HLA-A alleles were left out of the editing cocktail (6-1 (A02) KO, 6-1 (A03) KO). HLA-A*02^{-} and HLA-A*03^{-} cells were observed when HLA-A-selective guides were present in the editing cocktail.

Using a combination of individual guides for each canonical HLA class I allele, excluding HLA-A*02, led to a very distinct HLA expression profile (Fig. 4.10). This generated distinct populations lacking HLA BC expression but retained residual expression for HLA-A*02, HLA-A*03, or neither of these alleles. Consequently, the number of individual HLA alleles expressed, led to distinct β2m protein expression levels (Fig. 4.10).

In conclusion, this data demonstrates the feasibility of generating HLA-reduced cells with distinct expression profiles of desired HLA alleles by targeting individual HLA alleles.

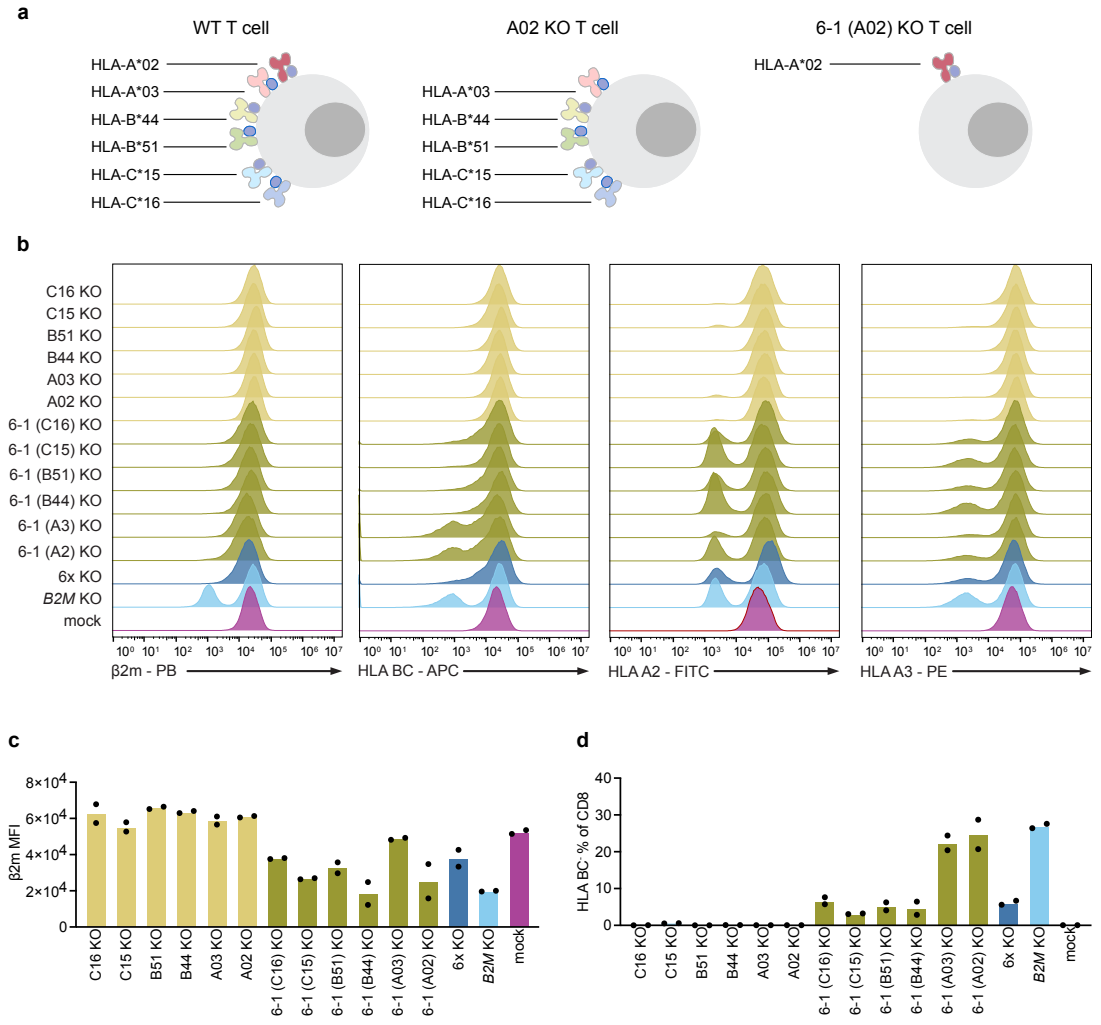

Figure 4.9: Generation of HLA-reduced T cells. **a**, Experimental scheme showing the HLA class I reduction concept through single HLA allele targeting. **b**, Flow-cytometric histograms showing expression of β2m, HLA BC, HLA A2 and HLA A3 of primary human CD8$^+$ T cells of an HLA A*02$^+$ A*03$^+$ B*41$^+$ B*55$^+$ C*15$^+$ C*16$^+$ donor edited with HLA allele-specific gRNAs; editing was performed for individual HLA alleles (e.g. for HLA-A*03 in case of "A03 KO"), for all HLA alleles except one (e.g. for all except HLA-A*03 in case of "6-1 (A03) KO"), for all six alleles ("6x KO"), for *B2M* ("*B2M* KO") or for no target ("mock"). **c**,**d**, Quantification of β2m geometric mean fluorescence intensity (MFI; c) or percentage of HLA BC$^-$ CD8 T cells (d) for data from b;n=2 technical replicates, bar height indicates mean. This figure was adapted and reprinted with permission from [78].

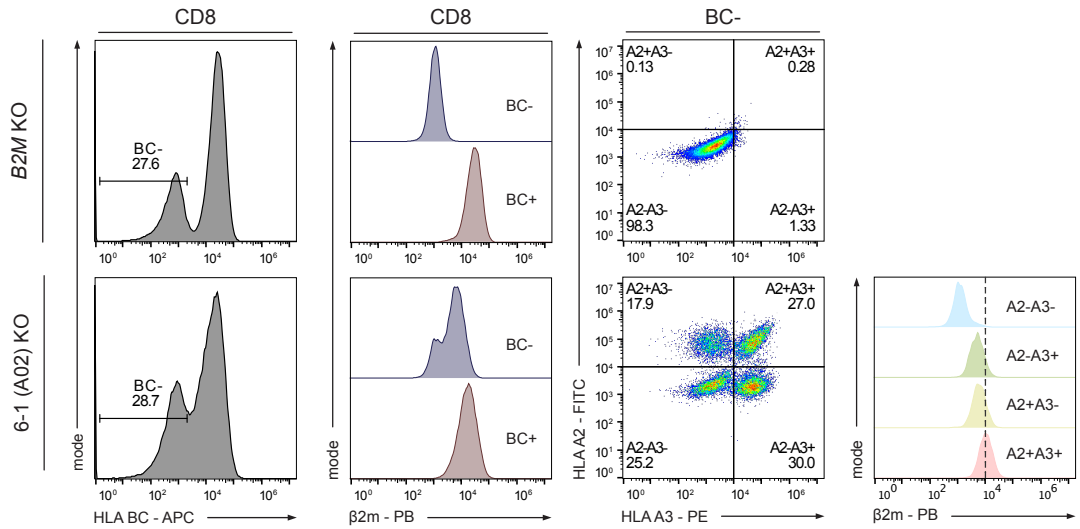

Figure 4.10: Characterization and definition of subsets of HLA-reduced T cells. Flow-cytometric characterization of 6-1 (A2) KO T cells (in which all HLA class I molecules were targeted except for HLA A2) compared to *B2M* KO T cells; left: HLA BC$^-$ population pre-gated on living CD8$^+$ T cells, second from left: β2m expression of HLA BC$^-$ and HLA BC$^+$ populations pregated on living CD8$^+$ T cells; second from right: HLA A2 and HLA A3 expression pregated on HLA BC$^-$ CD8$^+$ living T cells; right: β2m expression of HLA BC$^-$ subsets as defined in dot plots second from right. This figure was adapted and reprinted with permission from [78].

4.5.2 Alloreactive and NK cell-mediated recognition of HLA reduced targets

The objective of generating HLA-reduced cells was to avoid provoking alloreactive recognition. To examine this, we replicated the MLR experiment using these HLA-reduced target cells. PBMCs from three healthy donors were primed with PBMCs from the same donor, which was previously used to generate HLA-reduced cells (allo primed). Effector cells shared only the HLA-A*02:01 or HLA-A*03:01 allele with the donor of the target cells. HLA-reduced cells were sorted for successful editing prior to the re-challenge of primed effector cells.

HLA-reduced cells that are HLA-A2$^+$ HLA-A3$^-$ elicit alloreactive recognition by a HLA-A2$^-$ HLA-A3$^+$ donor, while such recognition is not observed from both HLA-A2$^+$ HLA-A3$^-$ donors (Fig. 4.11.a). However, an alloreactive response cannot be observed in the latter donors for HLA-A2$^-$ HLA-A3$^+$ target cells. It is important to note that alloreactivity may not be consistently observed across all individual HLA molecules in every donor within this group.

In brief, this is consistent with our aim to generate HLA-reduced cells as a strategy to evade alloreactive response.

Alloreactive rejection is not the only mechanism why adoptive cell transplantation could fail. The absence of HLA class I is known to induce NK-cell activation through "missing-self" recognition. Specific HLA types, such as HLA-C, play a role in suppressing NK-cell responses. However, in our scenario, HLA-C is absent. Therefore, it has to be investigated whether HLA-reduced cells are prone to NK cell-mediated rejection. For this, sort-purified cells lacking all canonical HLA class I molecules (A2$^-$A3$^-$BC$^-$), only expressing HLA-A*02:01 (A2$^+$A3$^-$BC$^-$) or HLA-A*03:01 (A2$^-$A3$^+$BC$^-$), HLA class I-deficient cells (*B2M* KO), HLA-E knock-in T cells (HLA E KI) and unedited cells (WT) were used in an NK cell assay (Fig. 4.11.b).

T cells expressing only HLA-A*02:01 or HLA-A*03:01 did not induce activation of NK cells. Interestingly, also A2$^-$A3$^-$BC$^-$-cells failed to induce NK-cell activation despite the absence of all canonical HLA class I molecules. This resulted in a level of protection against "missing self"-recognition that was comparable to that achieved by T cells incorporating an HLA-E knock-in. Moreover, A2$^-$A3$^-$BC$^-$ cells could be stained for HLA-E (Fig. 4.11.c), which is consistent with the preserved expression of β2m observed in the "6x KO" configuration (Fig. 4.9.b,c).

In summary, this data confirms that HLA-reduced T cells evade alloreactive T cells and NK cell-mediated rejection.

4.6 *in vivo* functionality of HLA reduced T cells

4.6.1 Humanized mouse model for *in vivo* investigation

We used a humanized mouse model to investigate the functionality and behavior of HLA-reduced T cells within a human immune system in an *in vivo* context. In this investigation, the subject under scrutiny is typically co-transferred with a mixture of diverse immune cells, often obtained from PBMCs. However, this approach limits the duration of

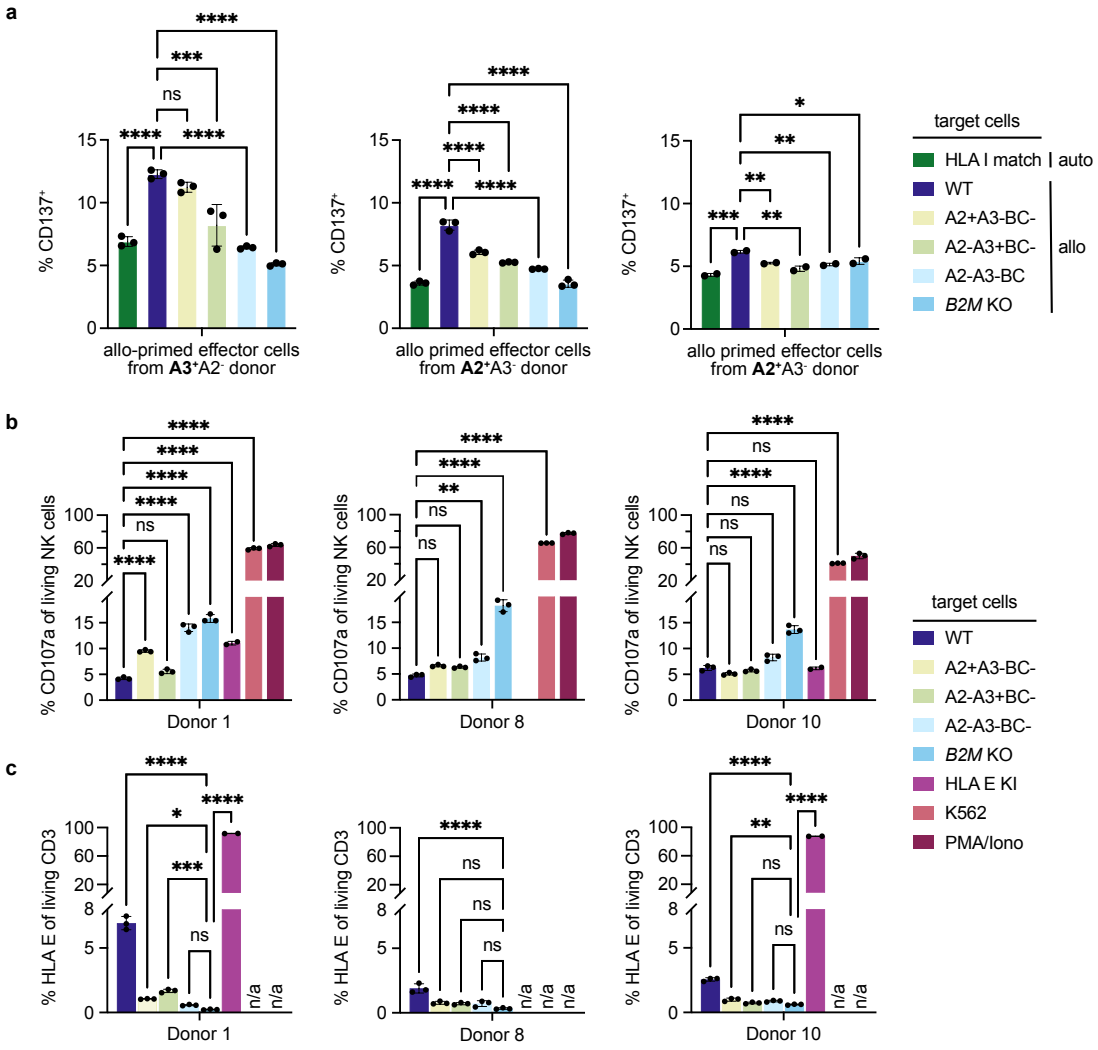

Figure 4.11: Alloreactive and NK cell-mediated recognition of HLA reduced targets. **a**, Percentage of $CD137^+CD8^+$ effector cells after 48 h of co-culture with pretreated indicated T cell effectors; effector cells were peripheral mononuclear blood cells from indicated donors co-cultured for 7 days together with PBMCs from donor B (allo priming); donors only share an allele for HLA A2 or HLA A3 as indicated; target cells were T cells from donor B without (WT) or with HLA class I reduction, sorted for $CD8^+$ and HLA BC^- and $A2^-$ $A3^-$, $A2^+$ $A3^-$ or $A2^-$ $A3^+$; HLA-reduced target cells with HLA $BC^-A2^-A3^+$ (left) or HLA $BC^-A2^+A3^-$ phenotype respectively signify a synthesized HLA match; statistical testing was done using an ordinary one-way ANOVA and Tukey's multiple comparisons test and results are only shown for selected comparisons; n=2-3 technical replicates. **b**, Quantification of $CD107a^+$ NK cells (percentage of living $CD56^+$ $CD8^-$ lymphocytes) from three different indicated donors after 5 h of co-incubation with indicated target cells; n/a, not performed experimental conditions; statistical testing was done using an ordinary two-way ANOVA and Tukey's multiple comparisons test and results are only shown for selected comparisons; n=2-3 technical replicates. **c**, Expression of HLA E for target populations in b as assessed by flow cytometry; n/a, not performed experimental conditions; statistical testing was done using an ordinary two-way ANOVA and Tukey's multiple comparisons test and results are only shown for selected comparisons; n=2-3 technical replicates. ns, not significant; *, $P \leq 0.05$; **, $P \leq 0.01$; ***, $P \leq 0.001$; ****, $P \leq 0.0001$. This figure presents data collected by Linda Warmuth during the revision of [78].

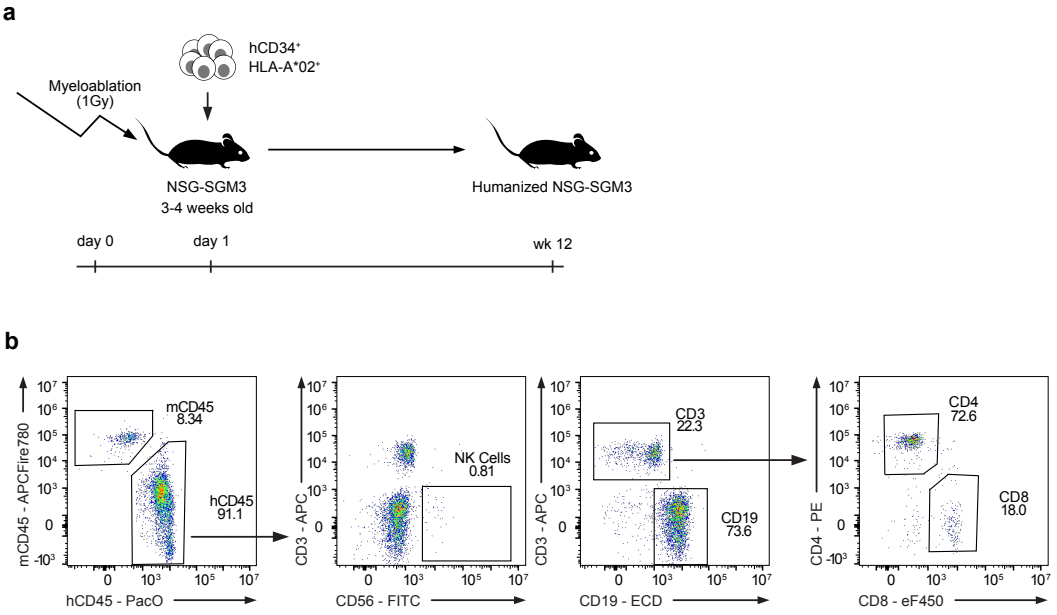

Figure 4.12: Humanized mouse model for *in vivo* investigation. a, Experimental setup for humanization of hu-CD34 NSG-SGM3 mice; humanization was performed with cord blood derived hCD34$^+$ cells from a HLA-A*02$^+$ donor, myeloablation was performed with 1 Gy one day prior to *i.v.* administration of hCD34$^+$ in order to create a niche for transferred cells. **b**, Reconstituted populations from humanized mice one day prior to injection as determined by flow cytometry; mCD45, murine CD45; hCD45, human CD45. This figure was adapted and reprinted with permission from [78].

follow-up due to compromised persistence and the potential initiation of notable xenoreactivity. In our model, not only all human immune cells are present, but they are also generated endogenously through differentiation from human CD34$^+$ haematopoetic stem and progenitor cells (HSPCs) over a 12-week period on a NOD.Cg-Prkdc^{scid}Il2rg^{tm1Wjl} Tg(CMV-IL3,CSF2,KITLG)1Eav/MloySzJ (NSG-SGM3) background. This framework facilitates, due to the expression of Interleukin-3 (IL-3), granulocyte-macrophage colony-stimulating factor (GM-SCF) and stem cell factor (SCF) a more intricate and accelerated reconstitution of human immune cell lineages.

Following myeloablation with 1 Gy irradiation, which was done to establish a niche for the transplanted cells, HLA-A*02$^+$ human CD34 HSPCs were transferred via the *intravenous* route one day later (Fig. 4.12.a). After a twelve-week period, the degree of humanization was evaluated through flow-cytometric analysis of collected blood samples. Humanization is measured as the chimera between murine CD45$^+$ and human CD45$^+$.

This assessment confirmed successful humanization of at least 25 % human CD45$^+$ and the presence of human CD56$^+$ NK cells, CD19$^+$ B cells, and CD4$^+$ and CD8$^+$ T cells (Fig. 4.12.b).

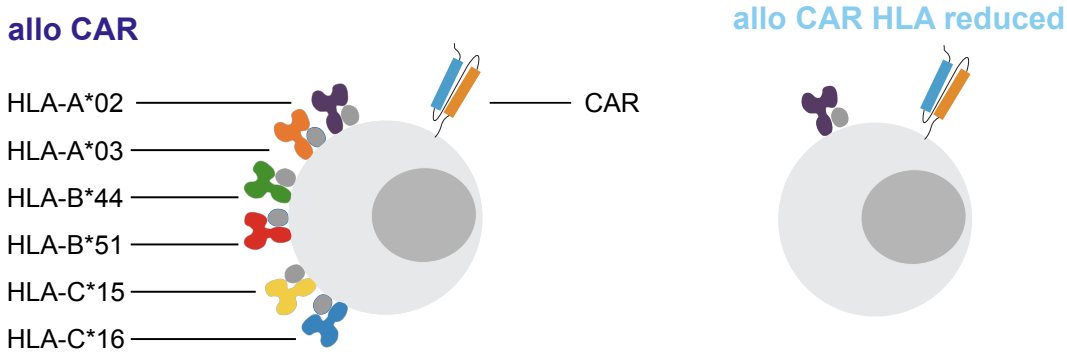

Figure 4.13: aCD19-CAR T cell +/- HLA reduction. Experimental setup for aCD19-CAR T cell, simultaneously edited for all HLA class I alleles except for HLA-A*02. This figure was adapted and reprinted with permission from [78].

4.6.2 Adoptive *in vivo* transfer of aCD19-CAR T cells in humanized mice

To investigate the functionality and potential rejection of HLA-reduced T cells further, we needed to mimic conditions equivalent to those in clinical adoptive cell transfer. This involved ensuring both HLA-compatibility and antigen recognition, achieved through the HLA reduction to retain only compatible alleles and the introduction of either a specific TCR or chimeric antigen receptor (CAR). By reducing HLA to only compatible alleles, we can achieve the same level of compatibility as HLA-matched allogeneic donor cells. Introducing TCR or CAR follows the same approach as in clinical settings.

We knocked out individual HLA alleles from the same donor as previously used, in order to generate only HLA-A*02:01 expressing HLA-reduced T cells. This approach retained the sole matching molecule corresponding to the donor used for humanization. In the same editing step, we introduced an anti CD19 chimeric antigen receptor (aCD19-CAR) via orthotopic TCR replacement in the T cell receptor alpha constant (*TRAC*) locus of the T cell receptor α-chain and parallel KO of the T cell receptor beta constant (*TRBC*) gene (Fig 4.13). Differing from our earlier *in vivo* analysis (Fig. 4.7), we opted for an anti-CD19 CAR as an antigen-specific receptor in this instance. This choice was motivated by the CAR's ability to consistently identify the reconstituted human B cells, thereby allowing the transgenic T cells to be available to allogeneic recognition through both reconstituted T cells and NK cells for a duration of at least one to two weeks. To optimize the engraftment of HLA-reduced T cells, we minimized handling and pre-*in vitro* expansion to the lowest extent feasible. Consequently, we directly transferred these cells into mice after editing, without preceding purification sorting. Flow-cytometric analysis was performed every three days on collected blood samples. On the 14th day after transfer, the mice were sacrificed, and further analysis was carried out on bone marrow and spleen samples (Fig. 4.14.a). As a control served allogeneic aCD19-CAR knock-in (KI) T cells without HLA reduction or no cells.

On the seventh day after the transfer, we noticed a mild decrease in $CD19^+$ B cells when allogeneic aCD19-CAR T cells were transferred. This reduction was even more pronounced when CAR T cells also underwent HLA reduction (Fig. 4.14.b,c). To exclude the possibility that the observed effect in collected blood samples solely resulted from T cell homing into different compartments, we additionally examined bone marrow and spleen samples, which represent hematopoietic and lymphatic tissues, respectively (Fig. 4.14.d). Remarkably, we noted the same pattern: $CD19^+$ B cells were eradicated upon administration of allogeneic aCD19-CAR T cells. The effect was intensified when the transferred T cells underwent HLA reduction. This effect was confirmed through a second independent experiment, with data pooled from both experiments shown in Fig. 4.14.e.

The effect of the aCD19-CAR T cells is clearly noticeable; however, it remains to be investigated if they can also be recovered in collected samples. Introducing a CAR into the endogenous *TRAC* locus renders the CAR susceptible to downregulation upon activation, leading to unsuccessful flow-cytometric antigen staining (data not shown). Nonetheless, while attempting to recover human $CD8^+$ T cells from collected blood samples, a variation in T cell count was noticeable between WT and HLA-deficient/reduced conditions. However, it did not reach statistical significance (Fig. 4.14.f). This data suggests that both HLA-reduced and HLA class I-deficient T cells show higher engraftment rates compared to unmatched allogeneic wild-type T cells. However, in subsequent investigations, it is essential to confirm the successful recovery of CAR T cells through flow-cytometric antibody staining (as suggested in 4.7.3). This will enable a more in-depth exploration into whether the observed enhanced functionality is due to improved T-cell maintenance and whether such enhanced maintenance is connected to evading T or NK cell-mediated rejection.

In summary, our findings indicate that HLA-reduced T cells show improved engraftment and enhanced target-cell elimination when introduced into an unmatched human immune system through adoptive transfer.

4.7 Further engineering of adoptive transfer products

For clinical use as an adoptive transfer product, cells must be extensively characterized and manufactured to yield precise outcomes. Since pharmaceutical products must be free of impurities, it is essential that the product is not only thoroughly understood and characterized but also easily identifiable as the intended successfully edited product.

4.7.1 Off-target editing in complex multisite editing

The challenge with HLA editing arises from its high degree of polymorphism, leading to several complexities in the context of CRISPR/Cas9-editing. In fact, we observed that T cells lacking HLA-A*02:01 were more robustly generated by the “6-1 (A02) KO” guide mix, which contained the supposedly HLA-A*03:01-specific gRNA but not the HLA-A*02:01-specific gRNA (Fig. 4.9). A closer examination of this phenomenon uncovered

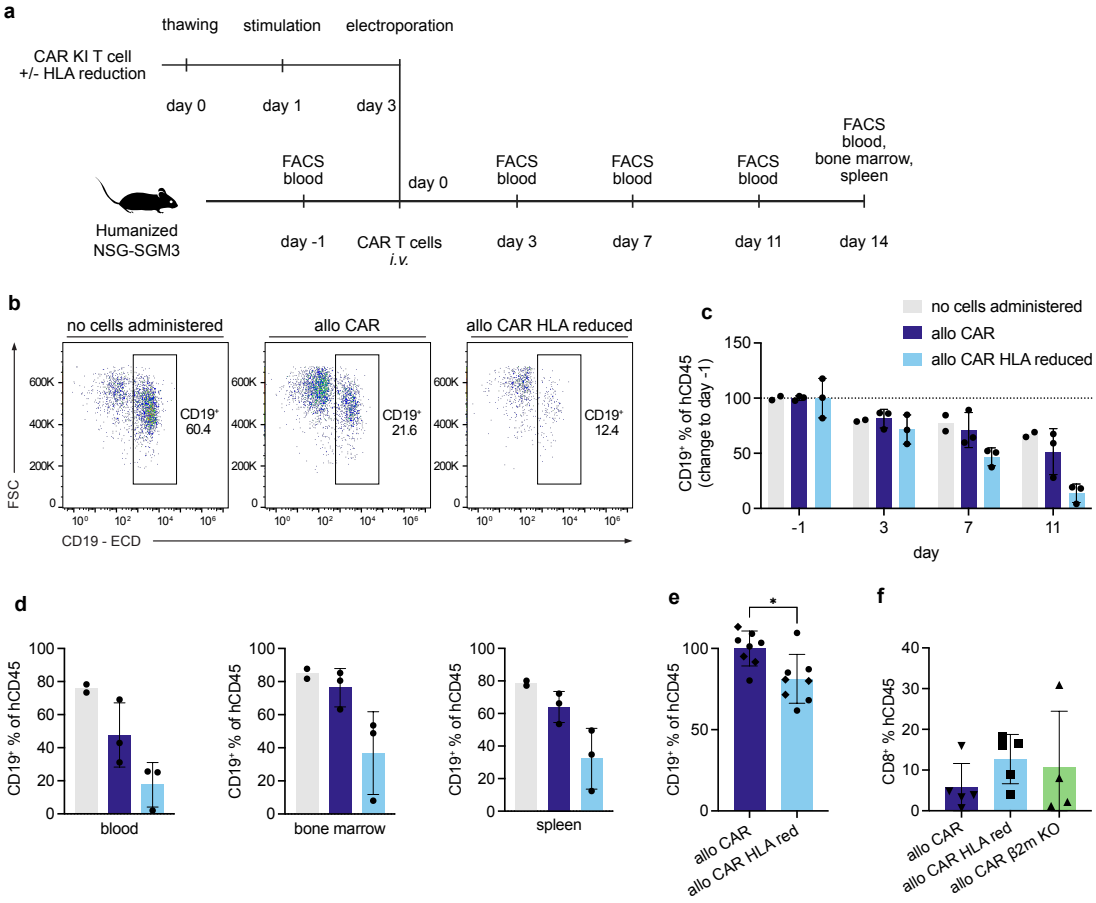

Figure 4.14: *in vivo* functionality of HLA reduced cells in humanized mice. **a**, Experimental setup for *in vivo* transfer of HLA reduced aCD19-CAR T cells; effector cells from HLA-A*02$^+$ donor 2 (same donor as in Fig. 4.10) were administered *i.v.* one day after assessment of humanization of hu-CD34 NSG-SGM3 mice; humanization was performed with cord blood-derived hCD34$^+$ cells from donor C, which were different from cells of donor 2 for every HLA class I allele except for HLA-A*02; every three days, blood samples were drawn and analyzed via flow cytometry; CAR T cells used as effector cells all received an aCD19-CAR knock-in into the endogenous *TRAC* gene locus and were simultaneously edited for all HLA class I alleles except for HLA*02, and were administered directly after electroporation without prior sorting [78]. **b**, Representative FACS-plots showing CD19$^+$ B cells recovered in blood (percentage of living hCD45$^+$ lymphocytes) on day 11 after administration of no cells or aCD19 CAR T cells with unedited or reduced HLA alleles into humanized mice [78]. **c**, Percentage of CD19$^+$ B cells recovered in blood shown as change relative to one day prior to administration of no cells or aCD19 CAR T cells with unedited or reduced HLA alleles into humanized mice. **d**, CD19$^+$ B cells (percentage of hCD45$^+$ living lymphocytes) recovered in indicated organs on day 14 after aCD19 CAR T cell administration with unedited or reduced HLA alleles into humanized mice; n=2-3 mice [78]. **e**, Numbers of CD19$^+$ B cells recovered in blood of humanized mice on day 7 after aCD19 CAR T cell administration with unedited or reduced HLA alleles, pooled data from two independent experiments (dot or diamond symbol barcode), normalized to mean of allo CAR in both experiments; statistical testing was done using an unpaired t-test; n=8 mice; *, P$\leq$0.05 [78]. **f**, CD8$^+$ T cells (percentage of hCD45$^+$ living lymphocytes) recovered in blood on day 7 after aCD19 CAR T cell administration with unedited, reduced HLA alleles or *B2M* KO into humanized mice; n=4-5 mice. Bar height indicates mean; error bars indicate SD (c-f).
Parts of this figure were adapted and reprinted with permission from [78].

that the supposedly HLA-A*03:01-specific gRNA was more effective in editing HLA-A*02:01 than HLA-A*03:01; while conversely, the supposedly HLA-A*02:01-targeting gRNA was more effective in editing HLA-A*03:01 than HLA-A*02:01 (Fig. 4.15.a,b). This indicates some degree of cross-reactivity despite the *in silico* predicted specificity of the proposed CRISPR guides.

4.7.2 Engineering challenges in achieving all desired features while maintaining proximity to physiology

Interestingly, our findings from the NK-cell assay using HLA-reduced targets reveal that T cells lacking the complete canonical HLA class I, achieved through targeting each individual HLA A, B, and C molecule, fail to induce NK-cell activation (Fig. 4.10.c). It is well-established that the absence of self-HLA molecules ("missing-self") triggers NK cell activation. In contrast, molecules such as HLA-C, HLA-E, HLA-G, and HLA-F are believed to be responsible for inhibiting NK cell activation. All the mentioned HLA molecules are disrupted by editing the *B2M* gene. Only HLA ABC molecules are eliminated when HLA reduction is made through individual HLA allele targeting, leaving non-canonical HLA molecules like HLA-E intact (Fig. 4.15.c).

A more complex editing process is required to achieve the desired outcome of preserving HLA-E expression, which allows cells to evade NK-cell recognition otherwise. This involves introducing a single-chain HLA-E construct linked to mature β2m. The re-introduction of mature β2m is essential, as the absence of β2m is responsible for HLA class I knock-out due to the targeting of the *B2M* gene. This construct needs to be incorporated into the genome, either after an initial round of editing or within the same editing step. A single-chain trimer and dimer form of HLA-E has been suggested in prior research [74]. However, our findings indicate that this approach does not only result in low editing efficiencies but also leads to the overexpression of HLA-E beyond physiological levels (Fig. 4.15.d).

4.7.3 Monitoring successful editing and identifying the correct product for purification

Recovering aCD19-CAR T cells in our *in vivo* experiments has posed a challenge. This difficulty arises from our editing process, wherein we insert the CAR construct into the endogenous *TRAC* locus. As a result, the CAR construct becomes subject to the same regulatory principles as the endogenous TCR, leading to downregulation upon T cell activation. Therefore, staining the CAR using flow cytometry becomes challenging due to this downregulation. JCAR17 has a higher affinity for the target than JCAR21, making it more susceptible to activation and downregulation when integrated into the endogenous *TRAC* locus. Even during *in vitro* flow-cytometric analysis of CAR KI T cells, direct staining of the CAR via Streptavidin—a binder to the StrepTag within the CAR construct—shows minimal to no signal (Fig. 4.15.e). To minimize potential activation due to the presence of $CD19^+$ B cells, we utilized cells obtained through $CD3^+$ apheresis.

We incorporated truncated epidermal growth factor receptor (EGFRt) as a transgenic marker linked to the CAR construct to address these issues. This addition enables the identification of successfully edited CAR KI T cells (Fig. 4.15.e). In addition, staining for EGFRt expression is advantageous as it provides strong evidence of successful insertion of the aCD19-CAR construct into the endogenous *TRAC* locus. Moreover, the potential observation of B-cell depletion due to admixture further supports this conclusion.

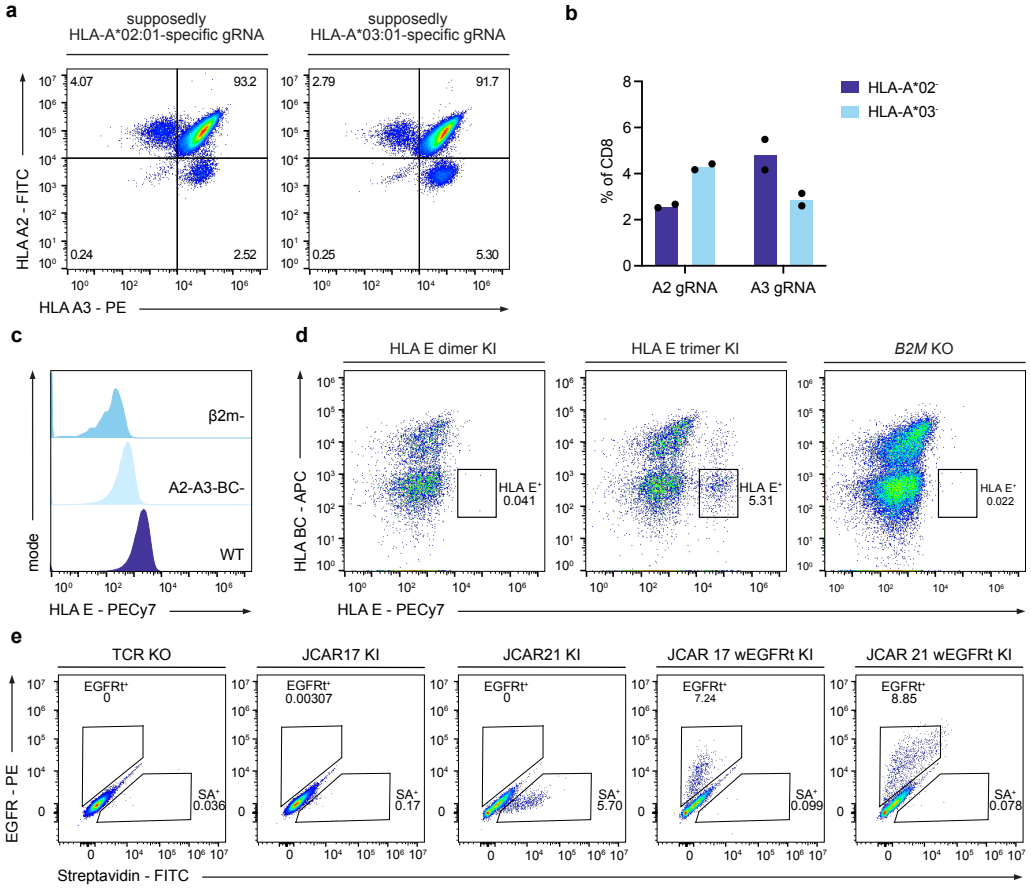

Figure 4.15: Further engineering of adoptive transfer products. **a**, Flow-cytometric analysis showing HLA A2 and HLA A3 expression of $CD8^+$ living T cells edited with indicated supposedly allele-specific guides [78]. **b**, Bar graph showing quantification of data shown in a, n=2 technical replicates [78]. **c**, Expression of HLA E and β2m for target populations in a as assessed by flow cytometry [78]. **d**, Expression of canonical HLA class I and HLA E of CRIPR/Cas9-edited primary human PBMCs as assessed by flow cytometry (pregated on living lymphocytes), cells were all targeted with *B2M* gRNA and received either HLA E dimer HDR DNA template ("HLA E dimer KI"), HLA E trimer HDR DNA template ("HLA E trimer KI") or no template ("*B2M* KO") upon electroporation. **e**, Flow-cytometric analysis of primary human T cells after CRISPR/Cas9-editing, all conditions received orthotopic T cell receptor replacement with the indicated CAR constructs (pregated on $hTCR^-$ living lymphocytes), TCR KO cells shown for comparison ("TCR KO"). Parts of this figure were reprinted with permission from [78].

5 Discussion

5.1 HLA class I and II KO

HLA class I and II knock-outs are not new to science. However, the advent of CRISPR/-Cas9 technology has greatly facilitated such knock-outs, particularly for generating HLA-deficient cells, often termed "universal cells," intended for adoptive cell therapies. This technology's potential impact prompted many authors to edit human stem cells. Induced pluripotent stem cells (iPSCs) have been shown to hold the promise of differentiating into any required cell type. Clonal selection and *in vitro* expansion are also very feasible. Still, using primary human T cells instead of stem cells for adoptive T cell transfer offers numerous advantages. Primary T cells, isolated from PBMCs, exhibit a diverse composition encompassing cytotoxic T cells, helper T cells, central memory T cells, naïve T cells, and antigen-experienced T cells. Therefore, opting for primary T cells over clonal selection and differentiation into cytotoxic T lymphocytes is the superior choice.

Notably, HLA class I's role in antigen recognition and HLA class II's function in guiding helper T cells, cytokine release, and self-upregulation are vital. Surprisingly, little is understood about how the absence of HLA class I and/or II influences T-cell functionality.

The knock-out of β2m has been suggested to eliminate HLA class I. Our findings show that by knocking out *B2M*, one can successfully generate HLA class I deficient T cells. The generated T cells lack not only the canonically highly polymorphic HLA A, B, and C molecules but also non-canonical HLA molecules, e.g., HLA-E. The knock-out of HLA class I is highly robust, as demonstrated not only on the protein level but also through Sanger-Sequencing and frameshift-inducing insertion-deletion analysis (ICE analysis). KO Scores from both approaches indicate effective targeting of both alleles.

In contrast, achieving HLA class II knock-out posed challenges. Unlike class I, class II lacks a common sub-unit anchoring molecules on cell surfaces. RFXANK and *CIITA* were identified as promising candidates, with *CIITA* linked to "bare lymphocyte syndrome". Earlier studies demonstrated successful HLA class II knock-out via *CIITA* targeting. Our CRISPR screening from self-selected guides for RFXANK and CIITA showed a higher potential for achieving HLA class II knock-out through targeting of CIITA, aligning with previous findings.

Nonetheless, an already-published guide provided much better editing efficacy than our self-selected guides. Yet, these editing efficacies were only around 10-20 % leaving us to enrich successfully edited cells through FACS for functional assays. Addressing low editing efficacies was not the only challenge we encountered with *CIITA* KO. Since T cells typically downregulate HLA class II, distinguishing edited cells from those with downregulated HLA class II posed a difficulty. Cytokines like IFNγ induce HLA class II

upregulation and $CD8^+$ T cell death. Sorting HLA class II-low cells via FACS was attempted to enrich HLA-class II-deficient T cells, but total purity remained a challenge. On the other hand, activating T cells so HLA class II would, if intact, get upregulated would downregulate the expression of antigen-specific receptors, which was also targeted for enrichment. Adoptive T cells are typically equipped with a TCR or CAR against the intended target. Combining HLA class II editing with TCR engineering presents challenges for clinical adoptive T cell use. This may be one of the major hurdles for the proposed approach of editing primary human T cells. Although the use of primary T cells in contrast to iPSCs is generally beneficial, editing and sorting for HLA class II deficient cells can be a tedious process and may not always be achievable. It is important to investigate the extent to which impaired purity affects the compatibility and engraftment of a clinical product.

While pure HLA class II-deficient cells are not achieved, we demonstrate robust and reliable *CIITA* KO unaffected by efficacy, even in complex multi-sided CRISPR editing scenarios.

5.2 Alloreactivity

Graft rejection is a grave concern following various types of transplantation. To counter the risk of rejection posed by both the innate and adaptive immune systems, organ transplant recipients typically receive life-long immunosuppressive drugs. However, in the context of adoptive cell therapy, administering immunosuppressive drugs is not feasible, as it contradicts the purpose of transferring immune cells to combat cancer or infections.

Rejection mediated by T cells primarily happens due to HLA mismatch. During T cell differentiation in the thymus, self-HLA recognizing T cells undergo negative selection, leaving naïve T cells capable of reacting to a wide range of foreign antigens. Reportedly, alloreactive T cells, which recognize foreign HLA types, constitute only a small fraction—typically single-digit percentages—of circulating T cells. Transforming these naïve alloreactive T cells into effector T cells in order to generate a measurable result is essential. Given the circumstances that in collected peripheral blood, only a few alloreactive T cells can probably be found, this response would only be measurable by enhancing the detection method so it can clearly be distinguished from background noise. To achieve this, PBMCs from one donor were co-cultured with PBMCs from another donor to activate alloreactive T cells, enabling their transformation into effector T cells and subsequent expansion. Different approaches were tested. Co-culturing for seven days allowed the alloreactive T cells enough time for clonal expansion and transformation into effector T cells (priming). The primed effector T cells would then be re-challenged with HLA mismatched PBMCs. Our findings showed that a period of just two days for re-challenging is enough and even beneficial because alloreactive recognition of primed effector cells is straightforward and efficient. Nonetheless, challenges with this assay frequently occur due to the nature of alloreactive recognition. Sometimes, priming of the effector cells fails to generate effector cells that are reactive to the presented set

of HLA or gives rise to non-alloreactive effector cells. Experiments with Epstein-Barr virus (EBV)-generated B-cell lymphoblastoid cell line (B-LCL) (data not shown) only allowed for the generation of EBV-reactive effector cells.

In contrast, more extended periods of re-challenging give rise to slower, unspecific activation processes as well. During priming, the cells did not benefit from supplemented adjuvants boosting T-cell activation and proliferation, as the activation and proliferation levels were no longer distinguishable from the controls. Controls included T cells with a disabled TCR to eliminate antigen-dependent stimuli, effector T cells cultured independently, and effector T cells primed against autologous PBMCs to account for unspecific activation during re-challenging.

Our findings demonstrated the central role of co-culturing with minimal interleukin supplementation to sustain the culture. This allowed for endogenous activation due to antigen recognition being the most essential stimulus for cell survival and proliferation. While donor-based variability was evident in activation levels, the pooled analysis involving six biological replicates proved that the experimental conditions we assessed were suitable for measuring alloreactivity. It should be noted that although we have tested the limits of this assay by using a minimal concentration of cytokine and two rounds of stimulation, not all well-known markers for T-cell activation produced significant results.

In summary, a working protocol was developed for an assay (Fig. 4.3.a) that detects alloreactivity. However, it should be noted that this assay often requires several biological replicates to account for donor variability.

Our mixed lymphocyte detection assay effectively detected alloreactivity in HLA-mismatched co-cultures. HLA class I is one of the main drivers of alloreactivity and has to be matched carefully to prevent graft rejection in clinical settings. Therefore, HLA class I-deficient cells are expected to generate a weaker alloreactive response. We demonstrated that HLA class I-deficient $CD3^+$ T cells do not activate primed alloreactive effectors any more than autologous HLA-identical targets. It is important to note that these experiments were conducted in HLA class II-intact cells, and HLA-DR disparity is also one of the main drivers of alloreactivity.

In summary, our mixed lymphocyte assay shows potential for detecting alloreactivity in HLA-mismatched co-cultures. Additionally, our findings confirm that HLA class I edited targets are less alloreactive.

It should be noted, however, that it is not advised to rely solely on an *in vitro* assay that has been pushed so far to its limits, such as this one, to detect such a subtle construct like alloreactivity. Results should always be confirmed in at least a second assay or an *in vivo* model that mimics the human immune system more closely.

5.3 NK cells recognize cells that lack self HLA class I molecules

According to the 'missing self' hypothesis, NK cells recognize and eliminate cells that lack HLA class I molecules as one of their crucial functions [43]. This poses a major challenge in generating universal cells for adoptive cell therapy. While HLA class I-

deficient cells evade T-cell-induced rejection, they provoke NK-cell recognition. This recognition triggers degranulation in NK cells, a cellular process that can be observed via staining of lysosomal-associated membrane protein-1 (LAMP-1 or CD107a) [80]. The phenomenon is not limited to missing-self situations; NK cells also exhibit degranulation in response to cancer cells. Moreover, it can be manually induced through unspecific activation of transcription factors nuclear factor kappa B (NF-κB) and nuclear factor of activated T cells (NFAT) to induce NK-cell degranulation in a nonspecific manner. Therefore, we used the K562 cancer cell line and PMA/Ionomycin as stimulants to establish a positive control for NK-cell degranulation. Effector NK cells were obtained from randomly selected healthy donors and isolated from fresh PBMCs through FACS. This was done to ensure the availability of unprimed, not yet activated, and cell-culture inexperienced NK cells for the assay. This approach allows for creating a scenario akin to immediate adoptive transfer.

Our observations suggest that NK cells demonstrate the anticipated degranulation in response to HLA class I-deficient cells *in vitro*, aligning with the "missing-self" hypothesis. The activation level appears to be nearly comparable to the response observed with the K562 cancer cell line. These findings may imply that HLA class I-deficient cells are not only susceptible but may face rejection mediated by NK cells following adoptive transfer. This is in line with previously published findings, but it should be discussed that although clear degranulation of NK cells was observed, these findings may only indicate susceptibility to NK cell-mediated rejection. It is important to keep in mind that an *in vitro* assay cannot completely predict behavior in a more complex *in vivo* allogeneic mismatch situation. In summary, the knock-out of HLA class I seems to render T cells resistant to recognition through alloreactive T cells. However, it also renders the HLA class I-deficient cells vulnerable to NK-cell-dependent rejection due to the "missing-self" mechanism. This calls for a more strategically advanced engineering of cells for adoptive cell therapy.

5.4 Intrinsic *in vitro* and *in vivo* functionality of HLA-deficient T cells

Surprisingly, little is known about the functionality of HLA class I and class II-deficient T cells. HLA plays a crucial role in the process of antigen presentation and recognition of target cells, as well as in T-cell activation and recruitment of helper cells. Therefore, it is unclear whether the absence of HLA molecules affects how T cells can fulfill their functions, such as cytokine release, elimination of target cells, and antigen recognition. The question is not only whether HLA editing affects T-cell function but rather whether it is possible to generate hypoimmunogenic HLA-edited T cells that function almost physiologically.

It has already been proven that replacement of the TCR is possible without altering physiological cellular behavior [68, 79]. Given this, it was only natural to adopt this protocol [67] and published functional assays to establish not only a benchmark but also a robust way of precisely controlling T-cell activation. Before conducting the func-

tional assessment, we had to demonstrate that orthotopic TCR replacement is possible in combination with HLA editing in a single simultaneous editing step. Orthotopic TCR replacement involves two simultaneous knock-out events and one homology-directed repair (HDR)-mediated knock-in. HLA editing would require additional delivery of at least two (HLA class I and II knock-out) and up to six (HLA reduction) additional CRISPR guides.

We demonstrated that this complex multisite CRISPR/Cas9 editing robustly generated HLA-edited and TCR-replaced cells for further functional analysis or adoptive transfer (Fig. 4.5). However, we experienced variance in editing efficacies and challenges obtaining a pure target population by FACS, especially for HLA class II-deficient cells (see 5.1).

Our findings indicate no observable change in T-cell effector functionality induced by HLA editing. Both HLA class I-deficient and HLA class II-deficient $CD8^+$ T cells responded to different concentrations of antigen with the same sensitivity as physiological T cells (edited to replace TCR) and released the same levels of the cytokines IFNγ and TNFα, indicating no alteration in the T-cell-effector functions of antigen recognition and cytokine release.

The remaining pillar of T-cell functionality, cytotoxicity, was also assessed via real-time-cell analysis. Again, HLA-edited effector T cells showed no difference in the speed of recognition and killing, as well as in the efficacy of eliminating target cells. The *in vitro* assays only used sorted $CD8^+$ effector T cells. It should be noted that the presence of other lymphocyte subsets, mainly $CD4^+$ helper T cells, may affect the effector function of HLA-edited cells. Although cytotoxicity assessment via xCELLigence real-time cell analysis is generally conducted over at least 48 hours, this is still a relatively short period of time, and no conclusions can be drawn about the long-term effectiveness of HLA-edited T cells.

In summary, we have presented evidence that the *in vitro* effector functionality of HLA-deficient T cells is not altered. This finding supports the exploration of broadly applicable donor cells for adoptive cell therapy through HLA engineering.

Determining *in vivo* functionality of T cells is equally important, as adoptively transferred T cells encounter target cells in a living organism rather than in artificial *in vitro* culture dishes. Using a mouse strain transgenic for human HLA-A*02:01 and a genetically altered murine CMV that expresses a human NLV peptide, the mice become infected in a syngeneic manner. As a result, the human NLV epitope is expressed and presented on human HLA-A*02:01 molecules, enabling *in vivo* antigen display and syngeneic T cell responses for transferred primary human T cells. The functionality of T cells is not influenced by graft rejection due to the absence of immune cells other than the transferred cells. We demonstrated that a mixture of HLA class I knock-out and HLA wild-type T cells equipped with an NLV-epitope-recognizing TCR managed to maintain the ratio between cells with and without HLA class I knock-out. This data suggests that there was neither positive nor negative selection for HLA class I knock-out. Therefore, this implies that the *in vivo* behavior of HLA class I knockout and HLA wild-type cells was the same. The ratio of wild-type and knock-out T cells was maintained, indicating the same rate of proliferation due to the same level of activation in both conditions.

This provides evidence of preserved T-cell-effector function of antigen recognition. This experiment assesses both the efficacy of antigen recognition and the ability of T cells to migrate and navigate efficiently through the organism to properly recognize the antigen.

HLA class I-edited T cells demonstrate excellent *in vitro* behavior, and their physiological T-cell-effector function seems to remain unaltered. Furthermore, editing does not appear to influence *in vivo* T-cell-effector function. This further supports the point that achieving broadly applicable and almost universally applicable donor cells for adoptive therapy can be accomplished through HLA engineering. Although the known limitations demonstrated here call for a more strategically advanced approach for HLA engineering beyond the simple disruption of HLA.

5.5 HLA engineering for generation of broadly applicable donor cells for adoptive cell therapy

Threats of rejection, either through alloreactive T cells in case of an HLA-mismatched transfer or through "missing self"-recognizing NK cells in case of HLA-disrupted donor cells, make it essential to develop more sophisticated approaches for HLA engineering. Our aim is to preserve the cell's physiology as much as possible while striving for nearly universal multi-compatible donor cells. HLA class I alleles will be selectively knocked out to generate multi-compatible donor cells, retaining recipient-matching HLA alleles on the cell's surface for physiological antigen presentation. Leaving some HLA alleles unedited serves as a safety measure for scenarios such as the engineered T cell undergoing malignant transformation or infection. HLA class II alleles will be knocked out to ensure full HLA matching with the remaining molecules. HLA reduction can be used to eliminate mismatched HLA class I molecules between donor and recipient or to create an off-the-shelf library of HLA-reduced primary T cells presenting a single HLA allele or pseudo-haplotypes. Calculations based on the German Bone Marrow registry [78] reveal that the ten most common HLA class I alleles are shared by 80 % of the European Caucasian (EURCAU) population (Fig. 5.1.a). Moreover, around 20 donors with pseudo-homozygous HLA class I haplotypes (where the second allele is eliminated through genetic engineering) would also be sufficient to match about two-thirds of the German population, assuming HLA class II elimination (Fig. 5.1.b). This suggests that donor compatibility may be increased and that selectively knocking out individual HLA alleles could lead to the generation of multi-compatible donor cells.

Single HLA alleles have already been targeted in pluripotent stem cells and a library of supposedly HLA-allele-specific CRISPR guides has been published [52]. We demonstrated that a randomly selected proposed HLA-B*08-selective guide from the published database applied to one of our HLA-B*08$^+$ donors effectively eliminated HLA-B*08 while maintaining the general expression of HLA class I (Fig. 4.8). These findings enabled us to strategically select supposedly single HLA-allele-specific guides from the library for an HLA-A*02:01$^+$ A*03:01$^+$ B*44:03$^+$ B*51:01$^+$ C*15:02$^+$ C*16:01$^+$ donor. We presented evidence that it is possible to decrease HLA class I to any combination of remaining HLA molecules, or even none, by simultaneously delivering up to six guides for each

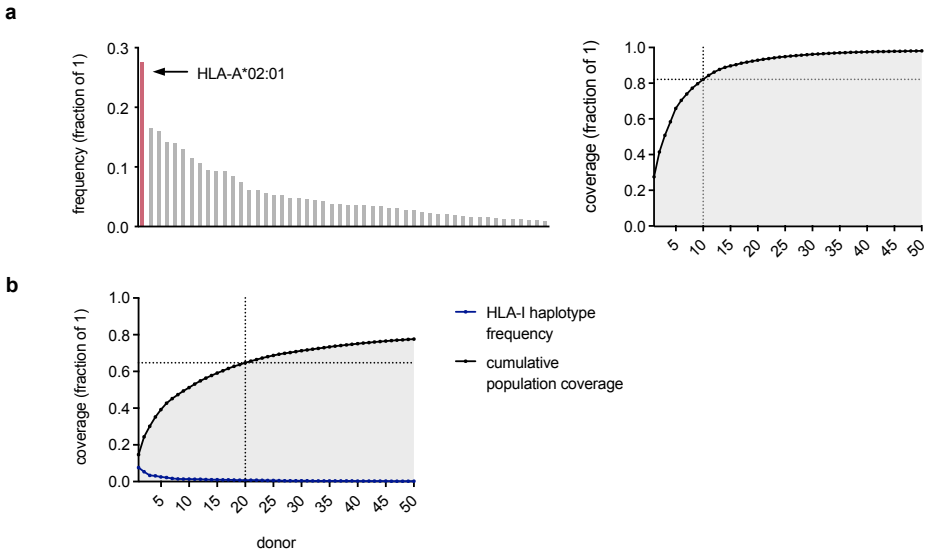

Figure 5.1: Demographics of HLA class I alleles. **a**, 50 most frequent HLA class I alleles of European Caucasian population in descending order, with HLA-A*02:01 shown in red (left panel); cumulative coverage of 50 most frequent HLA class I alleles (area under the curve in grey), dashed line indicates cumulative frequency of most common ten HLA class I alleles (right panel), data retrieved from [81]. **b**, 50 most frequent homozygous HLA class I haplotypes of European Caucasian population in descending order shown in blue; cumulative coverage of 50 most frequent homozygous HLA class I haplotypes (area under the curve in grey), dashed line indicates cumulative frequency of most common 20 HLA class I haplotypes (right). This figure was reprinted with permission from [78].

targeted allele. In many cases, CRISPR guides that are selective for multiple alleles can be used to achieve the necessary knock-out with fewer guides. Most of the guides in the published database target more than one allele. In the rare instance that a guide for each single allele is required, we demonstrated that knock-out is robustly achievable with up to six individual guides. As a result, this approach can generate T cells lacking the canonical HLA class I and every possible combination of residual HLA class I molecules. However, identifying successfully edited cells remains challenging due to the availability of HLA allele-specific antibodies. The lack of monoclonal antibodies for other individual HLA molecules may limit the broad applicability of HLA reduction as a strategy. Further investigation is needed to determine if additional steps are necessary for cell sorting in clinical settings to optimize the HLA reduction process.

Exemplary, for our donor, we demonstrated the feasibility of defining populations with distinct expression patterns of remaining HLA class I molecules for purity sort via FACS. This was possible due to commercially available flow-cytometric antibodies for HLA-BC (recognizing any HLA-B or HLA-C molecule), HLA-A*03, and HLA-A*02. An alternative sorting strategy could involve the expression level of β2m, as it correlates with the remaining HLA class I alleles. It also has to be discussed whether *in vitro* sorting and expansion would be necessary or if transferring cells directly after editing is feasible. A thorough investigation of this is essential since rejection processes can activate the endogenous immune system and cause severe adverse effects, such as cytokine storms seen in clinical aCD19-CAR T cell transfers. The selection of successfully edited cells is a crucial step in determining this approach's feasibility.

We demonstrated that sort-purified T cells reduced to a single matching HLA class I molecule do not trigger a response from alloreactive T cells *in vitro*. This suggests that HLA-reduced cells can successfully evade T-cell-mediated rejection. Moreover, single-allele-matching HLA-reduced cells do not elicit an NK cell response either. This could be attributed to preserving non-canonical HLA class I expression, such as HLA-E. Additionally, residual HLA-E expression in HLA-reduced T cells is detectable via flow cytometry. Interestingly, canonical HLA class I-deficient cells also failed to elicit NK-cell degranulation.

Moreover, HLA class I-deficient T cells exhibit lower levels of HLA-E expression than unedited cells. This decrease can be attributed to the role of HLA-E in presenting signal peptides from both canonical and non-canonical HLA class I molecules [82]. Additionally, a correlation between HLA-E and canonical HLA class I expression levels in unedited cells was observed. Specifically, T cells that retain only HLA-A*02:01 expression of the canonical HLA class I molecules demonstrate higher levels of HLA-E expression compared to T cells that are completely deficient in canonical HLA class I (Fig. 4.11.c). This suggests that preserving at least one canonical HLA molecule may be sufficient to evade NK-cell-dependent rejection. However, further investigation is necessary to provide a more definitive answer.

This data indicates resistance to both T cell and NK cell-mediated rejection for HLA-reduced donor cells, providing a significant advantage over HLA knock-out T cells.

Despite *in vitro* data suggesting resistance to rejection, we aimed to challenge a human immune system with transferred allogeneic yet through HLA-reduction compatible

T cells. While *in vitro* assays offer the advantage of being highly controlled and allowing the investigation of single factors in rejection, the human immune system is a complex interplay of various immune cells and their differentiated subsets. Thus, we opted for a humanized mouse model. In this model, NSG-SGM3 mice are reconstituted with a human immune system from HSPCs, which includes $CD4^+$ and $CD8^+$ T cells, $CD19^+$ B cells and also NK cells. Using a clinical grade aCD19-CAR we ensured constant activation through the endogenous B cell population, closely mimicking established clinical adoptive cell therapy. While this model and its implementation have limitations (e.g., absence of tumor, low number of transferred aCD19-CAR cells), the goal was not to assess the efficacy of CRISPR/Cas9-mediated aCD19-CAR knock-in T cells, but rather to evaluate the resistance of recipient-compatible HLA-reduced T cells. The combination of endogenous B cells and transferred aCD19-CAR T cells allowed us to measure the clearance of endogenous B cells as the primary outcome.

Allogenous—to a single recipient-compatible HLA molecule reduced—CAR T cells performed significantly better than allogenous HLA-mismatched CAR T cells. This data indicates no improved functionality of HLA-reduced CAR T cells in the context of the data already shown, showing that the absence of HLA class I does not affect T cell functionality. Still, somewhat less alloreactive rejection leads to less hindered functionality and, therefore, observable improvements. Additional flow-cytometric data confirms that the CAR inserted in the endogenous *TRAC* locus is subject to physiological downregulation upon successfully activating the effector T cell. This demonstrates the need for marker domains such as EGFRt to be part of the CAR construct for CAR T cell identification. These findings are all the more significant because they were not measured over a short period of time but also monitored for long-term persistence over 11 days. Numbers of recovered $CD8^+$ T cells suggest lesser rejection of HLA class I-deficient and even better performance of HLA-reduced cells, also supporting our hypothesis, yet not statistically significant.

It is worth noting that there may not be enough evidence to definitively argue that HLA-reduced T cells exhibit enhanced functionality and prolonged persistence *in vivo*, possibly due to their evasion of NK cell-mediated recognition. Conducting further experiments that deprive NK cells becomes crucial to establish a conclusive connection between HLA reduction, improved cell functionality, and extended persistence *in vivo*.

In summary, the *in vivo* data confirms our *in vitro* findings and strongly suggests that HLA-reduced donor cells have advantages in clinical therapeutic settings.

In contrast, HLA-deficient T cells exhibit robust activation of NK cells recognizing "missing self" *in vitro*. Various strategies have been proposed to address the issue of NK cell-dependent rejection. One approach involves the re-expression of non-canonical HLA molecules, such as HLA-E. HLA-E serves as a ligand for the inhibitory NK cell receptor CD94/NKG2A, thereby inhibiting cytotoxic activity. Re-expression of HLA-E in HLA class I-deficient *B2M* KO cells typically involves reintroducing a fusion gene composed of the *B2M* gene fused with a copy of the HLA-E gene as a single-chain construct. However, this further complicates editing and the generation of clinic-ready T-cell products. Either two simultaneous knock-ins of the HLA-E single-chain construct and an antigen receptor (a new TCR or a CAR) need to be performed, which is not

yet reported to be technically successful, or consecutive knock-ins, which could stress the cells and impact their fitness, functionality, and effector phenotype. Reintroducing a fusion gene into the genome further alters the cell's physiology. We demonstrated that CRISPR/Cas9-mediated HDR knock-in of a single-chain HLA-E construct is generally feasible but results in supra-physiological protein expression (Fig. 4.15.d). It is important to mention that NK cells can recognize malignantly transformed cells through a defective HLA-E ligand binding. Reintroducing constant supra-physiological HLA-E expression may pose a safety concern in case of the malignant transformation of transferred cells.

In essence, strategies to further engineer cells to circumvent the side effects of universally compatible donor cells diverge from the cell's physiology, raise safety concerns, and raise questions regarding potential impacts on T cell functionality.

To summarize, CRISPR/Cas9-mediated reduction of available HLA molecules allows the generation of broadly applicable donor cells suitable for adoptive cell therapy. These HLA-reduced cells maintain a physiological expression of the remaining HLA molecules, ensuring their antigen-presenting function even in cases of infection or malignant transformation. It is worth noting that this approach claims to address safety concerns without resorting to additional genetic modification.

Furthermore, the finding that HLA-reduced cells exhibit resistance to both T-cell and NK-cell-mediated rejection adds to the potential suitability of these cells for adoptive T-cell therapy. The findings indicate that allogeneic HLA-reduced CAR T cells have enhanced potency *in vivo*, suggesting resistance to host immune rejection and resulting in improved efficacy and prolonged persistence. This approach offers a promising opportunity to establish a bank of off-the-shelf, multi-compatible donor cells for adoptive cell therapy. Further research, particularly in diverse clinical scenarios, is necessary to confirm the feasibility, safety, and practicality of implementing this approach on a broader scale.

6 Conclusion

In this work, we have demonstrated the potential of CRISPR/Cas9-mediated HLA engineering to make an impact in the field of adoptive cell therapy. By selectively knocking out HLA class I alleles in combination with an HLA class I KO, we have demonstrated the feasibility of generating multi-compatible donor cells while preserving T cell physiology and canonical HLA class I expression as closely as possible. This HLA-reduction strategy, rather than a complete HLA class I KO, addresses the critical challenge of rejection, whether from alloreactive T cells or "missing-self" recognition by NK cells. This challenge is still one of the main factors for using only patient-derived T cells in adoptive cell therapy. Furthermore, this strategy enhances safety against the engineered cells' potential malignant transformation or infection by retaining intact endogenous HLA class I molecules.

The resistance to both T cell and NK cell-mediated rejection, as confirmed by both *in vitro* and *in vivo*, promises substantial advantages in clinical applications. This renders allogeneic donor-derived engineered cells compatible and more potent in functional potency by potential long-term persistence. Currently, our data suggest that HLA-reduced allogeneic CAR T cells exhibit enhanced functionality in a preclinical *in vivo* model that closely emulates the actual *in vivo* conditions in patients.

The high level of personalization continues to pose a major challenge in making adoptive cell therapies accessible to a wide range of patients. As of now, the emphasis lies on CAR- or TCR-engineered T cells for adoptive therapy. Yet, allogeneic donor cells are not accessible, and a tedious effort has to be made to engineer patient-derived T cells. Our approach aims to establish a library of multi-compatible donor cells in an 'off-the-shelf' manner. The use of donor-derived cells instead of patient-derived cells can decrease costs and manufacturing times while increasing accessibility to a wider range of patients. This approach enables the manufacture of a more standardized, viable, and defined pharmaceutical product. Additionally, this treatment does not only address a single instance of a disease but also allows for the potential of repeated dosing, administering multiple TCR-engineered or CAR T cells targeting different antigens, resulting in a more advanced treatment strategy.

Further investigation into the behavior of engineered cells within a complex immune microenvironment is crucial, particularly as clinical applications move forward. This includes evaluating long-term responses and persistence, potential interactions with other immune cells, and any unforeseen immune-related complications. Furthermore, refining methods for identifying successfully edited cells, especially in heterogeneous cell populations, will be crucial to ensure the purity and safety of therapeutic cell products.

In conclusion, HLA reduction, as a strategic approach to generating multi-compatible donor cells, has the potential to provide patients with more potent and durable treatments than ever before.

References

[1] K. Murphy and C. Weaver. *Janeway's Immunobiology*. Norton Company, Incorporated, W. W., 2016. ISBN: 978-0-8153-4551-0.

[2] C. Janeway, A. Rudensky, S. Rath, and D. Murphy. It is easier for a camel to pass the needle's eye. *Current Biology*, 2(1):26–28, jan 1992. doi:10.1016/0960-9822(92)90419-b.

[3] A. D. Waldman, J. M. Fritz, and M. J. Lenardo. A guide to cancer immunotherapy: from t cell basic science to clinical practice. *Nature Reviews Immunology*, 20(11):651–668, may 2020. doi:10.1038/s41577-020-0306-5.

[4] J. Gong, A. Chehrazi-Raffle, S. Reddi, and R. Salgia. Development of PD-1 and PD-l1 inhibitors as a form of cancer immunotherapy: a comprehensive review of registration trials and future considerations. *Journal for ImmunoTherapy of Cancer*, 6(1), jan 2018. doi:10.1186/s40425-018-0316-z.

[5] P. B. M. R E Billingham, L Brent. Quantitative studies on tissue transplantation immunity. II. the origin, strength and duration of actively and adoptively acquired immunity. *Proceedings of the Royal Society of London. Series B - Biological Sciences*, 143(910):58–80, dec 1954. doi:10.1098/rspb.1954.0054.

[6] P. L. Weiden, N. Flournoy, E. D. Thomas, R. Prentice, A. Fefer, C. D. Buckner, and R. Storb. Antileukemic effect of graft-versus-host disease in human recipients of allogeneic-marrow grafts. *New England Journal of Medicine*, 300(19):1068–1073, may 1979. doi:10.1056/nejm197905103001902.

[7] P. L. Weiden, K. M. Sullivan, N. Flournoy, R. Storb, and E. D. T. and. Antileukemic effect of chronic graft-versus-host disease. *New England Journal of Medicine*, 304(25):1529–1533, jun 1981. doi:10.1056/nejm198106183042507.

[8] J. F. Apperley, F. R. Mauro, J. M. Goldman, W. Gregory, C. K. Arthur, J. Hows, W. Arcese, G. Papa, F. Mandelli, D. Wardle, P. Gravett, I. M. Franklin, G. Bandini, P. Ricci, S. Tura, A. Iacone, G. Torlontano, W. Heit, R. Champlin, and R. P. Gale. Bone marrow transplantation for chronic myeloid leukaemia in first chronic phase: importance of a graft-versus-leukaemia effect. *British Journal of Haematology*, 69(2):239–245, jun 1988. doi:10.1111/j.1365-2141.1988.tb07628.x.

[9] M. Horowitz, R. Gale, P. Sondel, J. Goldman, J. Kersey, H. Kolb, A. Rimm, O. Ringden, C. Rozman, and B. Speck. Graft-versus-leukemia reactions after bone marrow

transplantation. *Blood*, 75(3):555–562, feb 1990. doi:10.1182/blood.v75.3.555.555.

[10] H. Kolb, J. Mittermuller, C. Clemm, E. Holler, G. Ledderose, G. Brehm, M. Heim, and W. Wilmanns. Donor leukocyte transfusions for treatment of recurrent chronic myelogenous leukemia in marrow transplant patients. *Blood*, 76(12):2462–2465, dec 1990. doi:10.1182/blood.v76.12.2462.2462.

[11] S. R. Riddell, K. S. Watanabe, J. M. Goodrich, C. R. Li, M. E. Agha, and P. D. Greenberg. Restoration of viral immunity in immunodeficient humans by the adoptive transfer of t cell clones. *Science*, 257(5067):238–241, jul 1992. doi:10.1126/science.1352912.

[12] S. A. Rosenberg, B. S. Packard, P. M. Aebersold, D. Solomon, S. L. Topalian, S. T. Toy, P. Simon, M. T. Lotze, J. C. Yang, C. A. Seipp, C. Simpson, C. Carter, S. Bock, D. Schwartzentruber, J. P. Wei, and D. E. White. Use of tumor-infiltrating lymphocytes and interleukin-2 in the immunotherapy of patients with metastatic melanoma. *New England Journal of Medicine*, 319(25):1676–1680, dec 1988. doi:10.1056/nejm198812223192527.

[13] M. C. O'Leary, X. Lu, Y. Huang, X. Lin, I. Mahmood, D. Przepiorka, D. Gavin, S. Lee, K. Liu, B. George, W. Bryan, M. R. Theoret, and R. Pazdur. FDA approval summary: Tisagenlecleucel for treatment of patients with relapsed or refractory b-cell precursor acute lymphoblastic leukemia. *Clinical Cancer Research*, 25(4):1142–1146, feb 2019. doi:10.1158/1078-0432.ccr-18-2035.

[14] N. Zacharakis, H. Chinnasamy, M. Black, H. Xu, Y.-C. Lu, Z. Zheng, A. Pasetto, M. Langhan, T. Shelton, T. Prickett, J. Gartner, L. Jia, K. Trebska-McGowan, R. P. Somerville, P. F. Robbins, S. A. Rosenberg, S. L. Goff, and S. A. Feldman. Immune recognition of somatic mutations leading to complete durable regression in metastatic breast cancer. *Nature Medicine*, 24(6):724–730, jun 2018. doi:10.1038/s41591-018-0040-8.

[15] E. Tran, M. Ahmadzadeh, Y.-C. Lu, A. Gros, S. Turcotte, P. F. Robbins, J. J. Gartner, Z. Zheng, Y. F. Li, S. Ray, J. R. Wunderlich, R. P. Somerville, and S. A. Rosenberg. Immunogenicity of somatic mutations in human gastrointestinal cancers. *Science*, 350(6266):1387–1390, oct 2015. doi:10.1126/science.aad1253.

[16] F. L. Pietersma, S. van Dorp, M. C. Minnema, J. Kuball, E. Meijer, R. Schuurman, and D. van Baarle. Influence of donor cytomegalovirus (CMV) status on severity of viral reactivation after allogeneic stem cell transplantation in CMV-seropositive recipients. *Clinical Infectious Diseases*, 52(7):e144–e148, mar 2011. doi:10.1093/cid/cir002.

[17] E. A. Walter, P. D. Greenberg, M. J. Gilbert, R. J. Finch, K. S. Watanabe, E. D. Thomas, and S. R. Riddell. Reconstitution of cellular immunity against cytomegalovirus in recipients of allogeneic bone marrow by transfer of t-cell clones

from the donor. *New England Journal of Medicine*, 333(16):1038–1044, oct 1995. doi:10.1056/nejm199510193331603.

[18] M. Uhlin, J. Gertow, M. Uzunel, M. Okas, S. Berglund, E. Watz, M. Brune, P. Ljungman, M. Maeurer, and J. Mattsson. Rapid salvage treatment with virus-specific t cells for therapy-resistant disease. *Clinical Infectious Diseases*, 55(8):1064–1073, jul 2012. doi:10.1093/cid/cis625.

[19] M. Neuenhahn, J. Albrecht, M. Odendahl, F. Schlott, G. Dössinger, M. Schiemann, S. Lakshmipathi, K. Martin, D. Bunjes, S. Harsdorf, E. M. Weissinger, H. Menzel, M. Verbeek, L. Uharek, N. Kröger, E. Wagner, G. Kobbe, T. Schroeder, M. Schmitt, G. Held, W. Herr, L. Germeroth, H. Bonig, T. Tonn, H. Einsele, D. H. Busch, and G. U. Grigoleit. Transfer of minimally manipulated CMV-specific t cells from stem cell or third-party donors to treat CMV infection after allo-HSCT. *Leukemia*, 31(10):2161–2171, jan 2017. doi:10.1038/leu.2017.16.

[20] M. Sadelain, R. Brentjens, and I. Rivière. The basic principles of chimeric antigen receptor design. *Cancer Discovery*, 3(4):388–398, apr 2013. doi:10.1158/2159-8290.cd-12-0548.

[21] Y. Kuwana, Y. Asakura, N. Utsunomiya, M. Nakanishi, Y. Arata, S. Itoh, F. Nagase, and Y. Kurosawa. Expression of chimeric receptor composed of immunoglobulin-derived v resions and t-cell receptor-derived c regions. *Biochemical and Biophysical Research Communications*, 149(3):960–968, dec 1987. doi:10.1016/0006-291x(87)90502-x.

[22] M. C. Gong, J.-B. Latouche, A. Krause, W. D. Heston, N. H. Bander, and M. Sadelain. Cancer patient t cells genetically targeted to prostate-specific membrane antigen specifically lyse prostate cancer cells and release cytokines in response to prostate-specific membrane antigen. *Neoplasia*, 1(2):123–127, jun 1999. doi:10.1038/sj.neo.7900018.

[23] D. J. Lenschow, T. L. Walunas, and J. A. Bluestone. CD28/b7 SYSTEM OF t CELL COSTIMULATION. *Annual Review of Immunology*, 14(1):233–258, apr 1996. doi:10.1146/annurev.immunol.14.1.233.

[24] B. Savoldo, C. A. Ramos, E. Liu, M. P. Mims, M. J. Keating, G. Carrum, R. T. Kamble, C. M. Bollard, A. P. Gee, Z. Mei, H. Liu, B. Grilley, C. M. Rooney, H. E. Heslop, M. K. Brenner, and G. Dotti. CD28 costimulation improves expansion and persistence of chimeric antigen receptor–modified t cells in lymphoma patients. *Journal of Clinical Investigation*, 121(5):1822–1826, may 2011. doi:10.1172/jci46110.

[25] K. Dhatchinamoorthy, J. D. Colbert, and K. L. Rock. Cancer immune evasion through loss of MHC class i antigen presentation. *Frontiers in Immunology*, 12, mar 2021. doi:10.3389/fimmu.2021.636568.

[26] M. L. Davila, I. Riviere, X. Wang, S. Bartido, J. Park, K. Curran, S. S. Chung, J. Stefanski, O. Borquez-Ojeda, M. Olszewska, J. Qu, T. Wasielewska, Q. He, M. Fink, H. Shinglot, M. Youssif, M. Satter, Y. Wang, J. Hosey, H. Quintanilla, E. Halton, Y. Bernal, D. C. G. Bouhassira, M. E. Arcila, M. Gonen, G. J. Roboz, P. Maslak, D. Douer, M. G. Frattini, S. Giralt, M. Sadelain, and R. Brentjens. Efficacy and toxicity management of 19-28z CAR t cell therapy in b cell acute lymphoblastic leukemia. *Science Translational Medicine*, 6(224), feb 2014. doi:10.1126/scitranslmed.3008226.

[27] S. L. Maude, N. Frey, P. A. Shaw, R. Aplenc, D. M. Barrett, N. J. Bunin, A. Chew, V. E. Gonzalez, Z. Zheng, S. F. Lacey, Y. D. Mahnke, J. J. Melenhorst, S. R. Rheingold, A. Shen, D. T. Teachey, B. L. Levine, C. H. June, D. L. Porter, and S. A. Grupp. Chimeric antigen receptor t cells for sustained remissions in leukemia. *New England Journal of Medicine*, 371(16):1507–1517, oct 2014. doi:10.1056/nejmoa1407222.

[28] D. W. Lee, J. N. Kochenderfer, M. Stetler-Stevenson, Y. K. Cui, C. Delbrook, S. A. Feldman, T. J. Fry, R. Orentas, M. Sabatino, N. N. Shah, S. M. Steinberg, D. Stroncek, N. Tschernia, C. Yuan, H. Zhang, L. Zhang, S. A. Rosenberg, A. S. Wayne, and C. L. Mackall. T cells expressing CD19 chimeric antigen receptors for acute lymphoblastic leukaemia in children and young adults: a phase 1 dose-escalation trial. *The Lancet*, 385(9967):517–528, feb 2015. doi:10.1016/s0140-6736(14)61403-3.

[29] K. Newick, S. O'Brien, E. Moon, and S. M. Albelda. CAR t cell therapy for solid tumors. *Annual Review of Medicine*, 68(1):139–152, jan 2017. doi:10.1146/annurev-med-062315-120245.

[30] J. Eyquem, J. Mansilla-Soto, T. Giavridis, S. J. C. van der Stegen, M. Hamieh, K. M. Cunanan, A. Odak, M. Gönen, and M. Sadelain. Targeting a CAR to the TRAC locus with CRISPR/cas9 enhances tumour rejection. *Nature*, 543(7643):113–117, feb 2017. doi:10.1038/nature21405.

[31] I. Hernandez, V. Prasad, and W. F. Gellad. Total costs of chimeric antigen receptor ti-/icell immunotherapy. *JAMA Oncology*, 4(7):994, jul 2018. doi:10.1001/jamaoncol.2018.0977.

[32] P. Vormittag, R. Gunn, S. Ghorashian, and F. S. Veraitch. A guide to manufacturing CAR t cell therapies. *Current Opinion in Biotechnology*, 53:164–181, oct 2018. doi:10.1016/j.copbio.2018.01.025.

[33] C. H. June, R. S. O'Connor, O. U. Kawalekar, S. Ghassemi, and M. C. Milone. CAR t cell immunotherapy for human cancer. *Science*, 359(6382):1361–1365, mar 2018. doi:10.1126/science.aar6711.

[34] J. A. Fraietta, K. A. Beckwith, P. R. Patel, M. Ruella, Z. Zheng, D. M. Barrett, S. F. Lacey, J. J. Melenhorst, S. E. McGettigan, D. R. Cook, C. Zhang, J. Xu, P. Do, J. Hulitt, S. B. Kudchodkar, A. P. Cogdill, S. Gill, D. L. Porter, J. A.

Woyach, M. Long, A. J. Johnson, K. Maddocks, N. Muthusamy, B. L. Levine, C. H. June, J. C. Byrd, and M. V. Maus. Ibrutinib enhances chimeric antigen receptor t-cell engraftment and efficacy in leukemia. *Blood*, 127(9):1117–1127, mar 2016. doi:10.1182/blood-2015-11-679134.

[35] N. Singh, J. Perazzelli, S. A. Grupp, and D. M. Barrett. Early memory phenotypes drive t cell proliferation in patients with pediatric malignancies. *Science Translational Medicine*, 8(320), jan 2016. doi:10.1126/scitranslmed.aad5222.

[36] C. Aparicio, C. Acebal, and M. González-Vallinas. Current approaches to develop "off-the-shelf" chimeric antigen receptor (CAR)-t cells for cancer treatment: a systematic review. *Experimental Hematology &amp Oncology*, 12(1), aug 2023. doi:10.1186/s40164-023-00435-w.

[37] M. A. Morgan, H. Büning, M. Sauer, and A. Schambach. Use of cell and genome modification technologies to generate improved "off-the-shelf" CAR t and CAR NK cells. *Frontiers in Immunology*, 11, aug 2020. doi:10.3389/fimmu.2020.01965.

[38] Y. Kagoya, T. Guo, B. Yeung, K. Saso, M. Anczurowski, C.-H. Wang, K. Murata, K. Sugata, H. Saijo, Y. Matsunaga, Y. Ohashi, M. O. Butler, and N. Hirano. Genetic ablation of HLA class i, class II, and the t-cell receptor enables allogeneic t cells to be used for adoptive t-cell therapy. *Cancer Immunology Research*, 8(7):926–936, jul 2020. doi:10.1158/2326-6066.cir-18-0508.

[39] J. Lee, J. H. Sheen, O. Lim, Y. Lee, J. Ryu, D. Shin, Y. Y. Kim, and M. Kim. Abrogation of hla surface expression using crispr/cas9 genome editing: a step toward universal t cell therapy. *Scientific Reports*, 10(1), October 2020. doi:10.1038/s41598-020-74772-9.

[40] J. Ren, X. Liu, C. Fang, S. Jiang, C. H. June, and Y. Zhao. Multiplex genome editing to generate universal CAR t cells resistant to PD1 inhibition. *Clinical Cancer Research*, 23(9):2255–2266, apr 2017. doi:10.1158/1078-0432.ccr-16-1300.

[41] M. Bix, N.-S. Liao, M. Zijlstra, J. Loring, R. Jaenisch, and D. Raulet. Rejection of class i mhc-deficient haemopoietic cells by irradiated mhc-matched mice. *Nature*, 349(6307):329–331, 1991. URL: https://doi.org/10.1038/349329a0, doi:10.1038/349329a0.

[42] N.-S. Liao, M. Bix, M. Zijlstra, R. Jaenisch, and D. Raulet. Mhc class i deficiency: Susceptibility to natural killer (nk) cells and impaired nk activity. *Science*, 253(5016):199–202, July 1991. doi:10.1126/science.1853205.

[43] K. Karre. Nk cells, mhc class i molecules and the missing self. *Scand J Immunol*, 55(3):221–8, 2002. URL: https://www.ncbi.nlm.nih.gov/pubmed/11940227, doi:10.1046/j.1365-3083.2002.01053.x.

[44] T. Deuse, X. Hu, A. Gravina, D. Wang, G. Tediashvili, C. De, W. O. Thayer, A. Wahl, J. V. Garcia, H. Reichenspurner, M. M. Davis, L. L. Lanier, and S. Schrepfer. Hypoimmunogenic derivatives of induced pluripotent stem cells evade immune rejection in fully immunocompetent allogeneic recipients. *Nature Biotechnology*, 37(3):252–258, feb 2019. doi:10.1038/s41587-019-0016-3.

[45] X. Han, M. Wang, S. Duan, P. J. Franco, J. H.-R. Kenty, P. Hedrick, Y. Xia, A. Allen, L. M. R. Ferreira, J. L. Strominger, D. A. Melton, T. B. Meissner, and C. A. Cowan. Generation of hypoimmunogenic human pluripotent stem cells. *Proceedings of the National Academy of Sciences*, 116(21):10441–10446, apr 2019. doi:10.1073/pnas.1902566116.

[46] G. G. Gornalusse, R. K. Hirata, S. E. Funk, L. Riolobos, V. S. Lopes, G. Manske, D. Prunkard, A. G. Colunga, L.-A. Hanafi, D. O. Clegg, C. Turtle, and D. W. Russell. Hla-e-expressing pluripotent stem cells escape allogeneic responses and lysis by nk cells. *Nature Biotechnology*, 35(8):765–772, May 2017. doi:10.1038/nbt.3860.

[47] B. Wang, S. Iriguchi, M. Waseda, N. Ueda, T. Ueda, H. Xu, A. Minagawa, A. Ishikawa, H. Yano, T. Ishi, R. Ito, M. Goto, R. Takahashi, Y. Uemura, A. Hotta, and S. Kaneko. Generation of hypoimmunogenic t cells from genetically engineered allogeneic human induced pluripotent stem cells. *Nature Biomedical Engineering*, 5(5):429–440, May 2021. doi:10.1038/s41551-021-00730-z.

[48] L. Shi, W. Li, Y. Liu, Z. Chen, Y. Hui, P. Hao, X. Xu, S. Zhang, H. Feng, B. Zhang, S. Zhou, N. Li, L. Xiao, L. Liu, L. Ma, and X. Zhang. Generation of hypoimmunogenic human pluripotent stem cells via expression of membrane-bound and secreted β2m-hla-g fusion proteins. *Stem Cells*, 38(11):1423–1437, September 2020. doi:10.1002/stem.3269.

[49] R. Lanza, D. W. Russell, and A. Nagy. Engineering universal cells that evade immune detection. *Nature Reviews Immunology*, 19(12):723–733, August 2019. doi:10.1038/s41577-019-0200-1.

[50] F. Mo, N. Watanabe, M. K. McKenna, M. J. Hicks, M. Srinivasan, D. Gomes-Silva, E. Atilla, T. Smith, P. Ataca Atilla, R. Ma, D. Quach, H. E. Heslop, M. K. Brenner, and M. Mamonkin. Engineered off-the-shelf therapeutic t cells resist host immune rejection. *Nature Biotechnology*, 39(1):56–63, July 2020. doi:10.1038/s41587-020-0601-5.

[51] H. Torikai, A. Reik, F. Soldner, E. H. Warren, C. Yuen, Y. Zhou, D. L. Crossland, H. Huls, N. Littman, Z. Zhang, S. S. Tykodi, P. Kebriaei, D. A. Lee, J. C. Miller, E. J. Rebar, M. C. Holmes, R. Jaenisch, R. E. Champlin, P. D. Gregory, and L. J. N. Cooper. Toward eliminating hla class i expression to generate universal cells from allogeneic donors. *Blood*, 122(8):1341–1349, August 2013. doi:10.1182/blood-2013-03-478255.

[52] H. Xu, B. Wang, M. Ono, A. Kagita, K. Fujii, N. Sasakawa, T. Ueda, P. Gee, M. Nishikawa, M. Nomura, F. Kitaoka, T. Takahashi, K. Okita, Y. Yoshida, S. Kaneko, and A. Hotta. Targeted disruption of hla genes via crispr-cas9 generates ipscs with enhanced immune compatibility. *Cell Stem Cell*, 24(4):566–578 e7, 2019. URL: `https://www.ncbi.nlm.nih.gov/pubmed/30853558`, `doi:10.1016/j.stem.2019.02.005`.

[53] S. O. Ryan and B. A. Cobb. Roles for major histocompatibility complex glycosylation in immune function. *Seminars in Immunopathology*, 34(3):425–441, March 2012. `doi:10.1007/s00281-012-0309-9`.

[54] A. Kumánovics, T. Takada, and K. F. Lindahl. Genomic organization of the mammalianmhc. *Annual Review of Immunology*, 21(1):629–657, April 2003. `doi:10.1146/annurev.immunol.21.090501.080116`.

[55] D. R. Madden. The three-dimensional structure of peptide-mhc complexes. *Annual Review of Immunology*, 13(1):587–622, April 1995. `doi:10.1146/annurev.iy.13.040195.003103`.

[56] S. Medhasi and N. Chantratita. Human leukocyte antigen (hla) system: Genetics and association with bacterial and viral infections. *Journal of Immunology Research*, 2022:1–15, May 2022. `doi:10.1155/2022/9710376`.

[57] J. Klein and C. O'hUigin. The conundrum of nonclassical major histocompatibility complex genes. *Proceedings of the National Academy of Sciences*, 91(14):6251–6252, July 1994. `doi:10.1073/pnas.91.14.6251`.

[58] I. Stroynowski and K. F. Lindahl. Antigen presentation by non-classical class i molecules. *Current Opinion in Immunology*, 6(1):38–44, February 1994. `doi:10.1016/0952-7915(94)90031-0`.

[59] J. Trowsdale and A. G. Betz. Mother's little helpers: mechanisms of maternal-fetal tolerance. *Nature Immunology*, 7(3):241–246, February 2006. `doi:10.1038/ni1317`.

[60] J. P. Merrill. Successful homotransplantation of the human kidney between identical twins. *Journal of the American Medical Association*, 160(4):277, January 1956. `doi:10.1001/jama.1956.02960390027008`.

[61] B. Bradley. The role of hla matching in transplantation. *Immunology Letters*, 29(1–2):55–59, July 1991. `doi:10.1016/0165-2478(91)90199-k`.

[62] G. Opelz, T. Wujciak, B. Döhler, S. Scherer, and J. Mytilineos. Hla compatibility and organ transplant survival. collaborative transplant study. *Reviews in immunogenetics*, 1(3):334—342, 1999. URL: `http://europepmc.org/abstract/MED/11256424`.

[63] J.-M. Tiercy, G. Nicoloso, J. Passweg, U. Schanz, R. Seger, Y. Chalandon, D. Heim, T. Güngör, P. Schneider, R. Schwabe, and A. Gratwohl. The probability of identifying a 10/10 hla allele-matched unrelated donor is highly predictable. *Bone Marrow Transplantation*, 40(6):515–522, July 2007. doi:10.1038/sj.bmt.1705787.

[64] R. L. Dawkins, F. T. Christiansen, P. H. Kay, M. Garlepp, J. Mccluskey, P. N. Hollingsworth, and P. J. Zilko. Disease associations with complotypes, supratypes and haplotypes. *Immunological Reviews*, 70(1):5–22, February 1983. doi:10.1111/j.1600-065x.1983.tb00707.x.

[65] C. Taylor, S. Peacock, A. Chaudhry, J. Bradley, and E. Bolton. Generating an ipsc bank for hla-matched tissue transplantation based on known donor and recipient hla types. *Cell Stem Cell*, 11(2):147–152, August 2012. doi:10.1016/j.stem.2012.07.014.

[66] L. Chicaybam, A. L. Sodre, B. A. Curzio, and M. H. Bonamino. An efficient low cost method for gene transfer to t lymphocytes. *PLoS ONE*, 8(3):e60298, mar 2013. doi:10.1371/journal.pone.0060298.

[67] C. Moosmann, T. R. Müller, D. H. Busch, and K. Schober. Orthotopic t-cell receptor replacement in primary human t cells using CRISPR-cas9-mediated homology-directed repair. *STAR Protocols*, 3(1):101031, mar 2022. doi:10.1016/j.xpro.2021.101031.

[68] K. Schober, T. R. Muller, F. Gokmen, S. Grassmann, M. Effenberger, M. Poltorak, C. Stemberger, K. Schumann, T. L. Roth, A. Marson, and D. H. Busch. Orthotopic replacement of t-cell receptor alpha- and beta-chains with preservation of near-physiological t-cell function. *Nat Biomed Eng*, 2019. URL: https://www.ncbi.nlm.nih.gov/pubmed/31182835, doi:10.1038/s41551-019-0409-0.

[69] C. J. Cohen, Y. F. Li, M. El-Gamil, P. F. Robbins, S. A. Rosenberg, and R. A. Morgan. Enhanced antitumor activity of t cells engineered to express t-cell receptors with a second disulfide bond. *Cancer Research*, 67(8):3898–3903, apr 2007. doi:10.1158/0008-5472.can-06-3986.

[70] A. Skerra and T. G. Schmidt. [18] use of the strep- tag and streptavidin for detection and purification of recombinant proteins. In *Methods in Enzymology*, pages 271–304. Elsevier, 2000. doi:10.1016/s0076-6879(00)26060-6.

[71] L. Liu, D. Sommermeyer, A. Cabanov, P. Kosasih, T. Hill, and S. R. Riddell. Inclusion of strep-tag II in design of antigen receptors for t-cell immunotherapy. *Nature Biotechnology*, 34(4):430–434, feb 2016. doi:10.1038/nbt.3461.

[72] X. Wang, W.-C. Chang, C. W. Wong, D. Colcher, M. Sherman, J. R. Ostberg, S. J. Forman, S. R. Riddell, and M. C. Jensen. A transgene-encoded cell surface polypeptide for selection, in vivo tracking, and ablation of engineered cells. *Blood*, 118(5):1255–1263, aug 2011. doi:10.1182/blood-2011-02-337360.

[73] P. J. Paszkiewicz, S. P. Fräßle, S. Srivastava, D. Sommermeyer, M. Hudecek, I. Drexler, M. Sadelain, L. Liu, M. C. Jensen, S. R. Riddell, and D. H. Busch. Targeted antibody-mediated depletion of murine CD19 CAR t cells permanently reverses b cell aplasia. *Journal of Clinical Investigation*, 126(11):4262–4272, oct 2016. doi:10.1172/jci84813.

[74] M. Crew. Genes encoding single chain human leuk10.1093/bioinformatics/btw561, November 2004. U.S. Patent No. US 2004/0225112 A1.

[75] E. K. Brinkman, T. Chen, M. Amendola, and B. van Steensel. Easy quantitative assessment of genome editing by sequence trace decomposition. *Nucleic Acids Research*, 42(22):e168–e168, oct 2014. doi:10.1093/nar/gku936.

[76] D. Conant, T. Hsiau, N. Rossi, J. Oki, T. Maures, K. Waite, J. Yang, S. Joshi, R. Kelso, K. Holden, B. L. Enzmann, and R. Stoner. Inference of CRISPR edits from sanger trace data. *The CRISPR Journal*, 5(1):123–130, feb 2022. doi:10.1089/crispr.2021.0113.

[77] X. Liu and N. Quan. Immune cell isolation from mouse femur bone marrow. *BIO-PROTOCOL*, 5(20), 2015. doi:10.21769/bioprotoc.1631.

[78] P. M. Winterhalter, L. Warmuth, P. Hilgendorf, J. M. Schuetz, S. Dötsch, T. Tonn, L. Cicin-Sain, D. H. Busch, and K. Schober. HLA reduction of human T cells facilitates generation of immunologically multi-compatible cellular products. *Blood Advances*, April 2024. doi:10.1182/bloodadvances.2023011496.

[79] T. R. Müller, S. Jarosch, M. Hammel, J. Leube, S. Grassmann, B. Bernard, M. Effenberger, I. Andrä, M. Z. Chaudhry, T. Käuferle, A. Malo, L. Cicin-Sain, P. Steinberger, T. Feuchtinger, U. Protzer, K. Schumann, M. Neuenhahn, K. Schober, and D. H. Busch. Targeted t cell receptor gene editing provides predictable t cell product function for immunotherapy. *Cell Reports Medicine*, 2(8):100374, August 2021. doi:10.1016/j.xcrm.2021.100374.

[80] G. Alter, J. M. Malenfant, and M. Altfeld. CD107a as a functional marker for the identification of natural killer cell activity. *Journal of Immunological Methods*, 294(1-2):15–22, nov 2004. doi:10.1016/j.jim.2004.08.008.

[81] M. Effenberger, A. Stengl, K. Schober, M. Gerget, M. Kampick, T. R. Müller, D. Schumacher, J. Helma, H. Leonhardt, and D. H. Busch. Flexamers: A double tag for universal generation of versatile peptide-mhc multimers. *The Journal of Immunology*, 202(7):2164–2171, April 2019. doi:10.4049/jimmunol.1801435.

[82] N. Lee, D. R. Goodlett, A. Ishitani, H. Marquardt, and D. E. Geraghty. Hla-e surface expression depends on binding of tap-dependent peptides derived from certain hla class i signal sequences. *The Journal of Immunology*, 160(10):4951–4960, May 1998. doi:10.4049/jimmunol.160.10.4951.

Tools and Resources

The following table acknowledges all functional uses of AI-based tools throughout the writing process of this thesis.

AI-based Tool	**Forms of Use**	**Affected Work**	**Comments**
DeepL Translator	Translation of text passages	Zusammen-fassung	
ChatGPT Version 3.5 (OpenAI)	Generation of text suggestions	Entire work	Prompt was ”Please list me suggestions on how to enhance the clarity of the following paragraph and list me suggestions on how to improve flow of reading.”
ChatGPT Version 3.5 (OpenAI)	Proofreading	Entire work	Prompt was ”Please correct my grammar.”
Grammarly Desktop Version 1.47.2.0	Proofreading	Entire work	

A Publications

Parts of this thesis have already been published or are submitted for publication.

First-author publications

- **Winterhalter PM***, Warmuth L*, Hilgendorf P, Schütz JM, Dötsch S, Busch DH, Schober K. *HLA reduction of primary human T cells facilitates generation of broadly applicable cellular products.* Blood Advances, April 2024. doi:10.1182/bloodadvances.2023011496. *contributed equally

B Acknowledgements

This is probably the most important part. Even though the writing part can be a bit lonely, these past five years on this journey have been great, thanks to some wonderful companions. There are numerous individuals to whom I owe gratitude for crossing paths with me.

First of all, I would like to thank my Doktorvater Prof. Dr. Dirk Busch, for entrusting me with the opportunity to contribute to and to validate my capabilities on this project. I am truly thankful for his ongoing support, valuable feedback, and that spark of competitiveness that caught on with me.

My sincere gratitude extends to Dr. Kilian Schober, who supervised my thesis work as my mentor. Initially, he guided me as an experienced postdoc in the Busch lab, and even as he transitioned to becoming the group leader of his own lab in Erlangen, his exceptional support continued unwaveringly. His challenging approach and high expectations served as the catalyst that this work needed, pushing me to learn and grow.

Next, I would like to thank Füsun Gökmen and Monika Hammel for helping me to take my first steps in the lab and eventually run with it. Monika, in particular, became a reliable source of support, always available to lend her wealth of expertise. Special thanks are owed to Inge Hensel and Andrea Werner, for their extensive help with the mouse work. Thanks are due to Anna Hochholzer, Franziska Graml, Laura Valentiner and Noomen Hamed for their contributions in maintaining the smooth operation and collegial atmosphere of our lab. A special acknowledgment goes to the team at the cell sorting facility–Immanuel Andrä, Matthias Schiemann, Corinne Angerpointer, Lynette Henkel, Dharshini Raju, and Susi Dürr–for their tireless hours in cell sorting and addressing various technical challenges.

Furthermore, I would like to express thanks to our veterinarians, animal caretakers, and, most importantly, the 280 mice that played a crucial role in the unavoidable yet essential aspects of this research.

Many thanks are due to Linda Warmuth and Philipp Hilgendorf, whose experimental help enabled our paper to fly.

Working in research is far from ordinary; it involves long hours and shared sorrows that forge companionship and even friendships. My heartfelt gratitude goes to the exceptional individuals in the Busch lab, including Simone Weber, Sarah Dötsch, Jack Barton, Adrian Straub, Mortimer Svec, Linda Warmuth, Sebastian Jarosch, Anna Purcarea, Jan Köhlen, Thomas Müller, Elvira D'Ippolito and associated member Andreas Wanisch. Special recognition is reserved for Karolin Wagner, Julius Schütz and Laura Mateyka, whose friendship extended beyond working hours.

But no scientific progress would have been possible without my strong network of friends and family. Thank you to all my friends for your friendship throughout this journey. Many, many thanks to my parents, Janine and Jürgen, who did not only provide my generous funding, but unconditionally supported every decision I made, even when they clearly did not like it, and allowed me to become the person I am today. I extend the same gratitude to my sister Sophie, who did not only show care by joining me for an internship in the lab, but also provided surprisingly valuable experimental assistance. Finally, to my partner in crime, Theresa. I am truly grateful to have met you along the way. For all your emotional support, your occasional kicks in the ass to get me moving on this project, and creating the circumstances for its completion.

It has been a hell of a ride, and I am really glad I bought the ticket.